Aston, Eoghan (2023) ***Quantifying and assessing coral reef structural complexity and its role in ecological processes and dynamics using photogrammetry.*** **PhD Thesis, James Cook University.**

Quantifying and assessing coral reef structural complexity and its role in ecological processes and dynamics using photogrammetry

Eoghan Aston

A thesis submitted for the degree of Doctor of Philosophy at James Cook University, Australia in 2023

College of Science and Engineering

IN LOVING MEMORY OF

John Brian Woodward O.B.E

“*Mighty oaks from little acorns grow*”

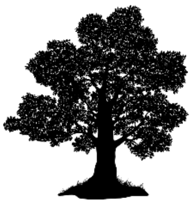

Contributions of others

The work presented in this thesis is a result of collaborations primarily with my supervisors, Dr Stephanie Duce, Dr Renata Ferrari and Professor Andrew Hoey. I was responsible for the conceptualisation of ideas and study design, with valued input from all advisors to refine ideas. I was an active part of data collection throughout and was assisted by many able hands under the Australian Institute of Marine Science's (AIMS) Ecological Intelligence for Reef Restoration and Adaptation Program (EcoRRAP), a subprogram of the Reef Restoration and Adaptation Program, a partnership between the Australian Government's Reef Trust and the Great Barrier Reef Foundation. I was responsible for the development of python scripts throughout the project, as well as the statistical modelling, interpretation of results and all writing. All supervisors contributed to providing editorial and intellectual feedback.

Some python scripts (**chapter 2 & 4**) were co-developed with Januar Harianto, who provided valuable technical expertise. Processing of photogrammetry models were shared between myself, Dr. Renata Ferrari, Dr. Sophie Gordon and Marine Lechene. The extraction of complexity metrics from large-scale habitat reconstructions (**chapters 4 & 5**) was facilitated by a custom-coded tool provided by Dr. William Figueira. The original scripts were written by Dr. Will Figueira, Dr. Mitch Bryson and Ryan Krensel.

Funding

I was supported by a postgraduate scholarship from James Cook University to cover the cost of tuition fees and three years of stipend payments. **Chapter 2** was funded by a combination of the Director of National Parks - Australia, who generously funded fieldwork costs to gather the necessary data, along with partial funding from the Hunter Research Project Support Grant, awarded in 2020. The Orpheus Island Morris Family Trust grant funded fieldwork for **chapter 3**. All other funding for fieldwork and data processing (**chapter 2**, **4** and **5**) was provided by the Australian Institute of Marine Science project EcoRRAP.

Publications

Chapter 3 was published on 07 Apr 2022:

Aston, E.A., Duce, S.D., Hoey, A.S. and Ferrari, R. A protocol for extracting structural metrics from 3D reconstructions of corals (2022) *Frontiers in Marine Science,* **11,** e3894395.

Chapter 2 has been submitted to *The ISPRS Journal of Photogrammetry and Remote Sensing* with co-authorship from *E.A. Aston, R. Ferrari, S. Duce, S. Gordon and A.S Hoey.*

Chapters 4 & 5 are in preparation for submission to Ecography and Coral Reefs, respectively.

Acknowledgements

I have had the good fortune to be advised by a panel of experts for the past four years, each of whom have provided a different aspect of expertise to my PhD, from the technical side, to not getting trapped in my many rabbit holes, to learning when to give myself a break. Andy was the first to take a chance on me back in 2018, providing me with many valuable opportunities to work amongst other PhD candidates at JCU before applying for my own. Since then, the lessons in navigating a doctoral degree that he has taught have helped me to finish almost on time, no mean feat considering the wild ride of the past few years. Steph accepted me as a primary supervisor knowing next to nothing about me, and always seems to know the right thing to say on those not-so-rare occasions when panic is my immediate reaction to some unwanted news. Rena, the technical guidance and your willingness to step up to the plate and help look after my project when circumstances necessitated it will never be forgotten. I am forever in debt to all three of you.

The AIMS team at EcoRRAP have been a wonderful group to work alongside for the past few years. I have the good fortune of being able to say I was involved in this fantastic project from day-one (even if from the other side of the world), and the memories of being in the field amongst such capable yet welcoming scientists will always stay with me. Soph, Marine, Mariana, Sam, Tiny, as well as everyone else who has collected data as part of EcoRRAP have my sincerest thanks – so many capable hands working together to beat the huge volume of data into submission has taught me the value of teamwork and collaboration within science, a lesson that I'm sure will form my approach to science for as long as I continue.

I have made some friends along the way, without whom, I probably wouldn't be putting the final touches to a PhD thesis. In particular, Katie and Debs, office pals from day one, have always been happy to bounce ideas off, make half-hearted attempts to steer me away from procrastination, and tell me my coffee is the best they've ever tasted. Eric and Erika, later additions but have all very much filled the same supportive roles that we all so desperately need.

I would like to say a final thanks to my family and friends. My stepfather John, who sadly passed away during September 2020 will forever be my inspiration and the person I look up to. My whole family have always been supportive in many different ways. Additionally, Kyle and Robin gave me a home when I needed it after returning to Australia, along with little Myah, who brightened up every one of my mornings. A huge thanks has to go to Ben the mechanical doctor and the rest of the boys for keeping me sane between office sessions with some fantastic times on the golf course. I'd also like to say a final and heartfelt thankyou to my girlfriend, Georgie. Over the past year, she has been my biggest fan, supporter and voice of reason on the days I've needed it most. Without her, I'm not sure whether I'd have made the finish line.

Abstract

The quantification of the structural traits of coral reefs permits a detailed understanding of natural processes in both benthic and animal communities. Recently, 3D photogrammetry (the generation of three-dimensional reconstructions using a series of overlapping still images) has begun to supplant manual, analogue *in situ* methods of structural complexity quantification thanks to its relative ease-of-use, high precision/accuracy, and the lack of reliance on expert knowledge in the field. Although a variety of ecologically useful habitat descriptors have arisen, there remain many aspects of photogrammetry, from interrogation of methodological procedures to ecological interpretation of the resultant metrics, that are as yet understudied. Thus, the overall aim of my thesis was to advance knowledge in how photogrammetry is conducted both in the field and during processing of the reconstructions, and to use this information to conduct broad-scale ecological investigations into how complexity varies among locations and how this affects fish communities. Specifically, my objectives were to: (1) Investigate the importance of key decisions during data collection and processing during the photogrammetry workflow to make recommendations to enhance the validity of comparing metrics from different reconstructions; (2) Design and implement a workflow to streamline the repeatable processing of models and extraction of a suite of ecologically relevant structural complexity metrics, using the resultant data to demonstrate the function of important complexity metrics; (3) Use the principals of repeatable routines to generate and investigate a spatially expansive dataset with which to make far-reaching comparisons of reef structure at spatial scales ranging from habitats within reefs to entire regions of the Great Barrier Reef and Torres Strait; and (4) Pair the wide-scale, high resolution structural complexity data with surveys of small-bodied fish communities to further elucidate fish-habitat relationships in the context of different trophic groups and their varying relationships with different aspects of complexity.

Chapter 2 examines the effects of some key choices that can be made when designing photogrammetry studies including equipment choices, study design and in-software processing protocols. I investigated the effect of image density (number of images per unit area) and resolution (a combination of sensor resolution and software quality settings) on the resultant reconstructions. Both image density and resolution were found to have varying effects on the resolution and surface area of resultant reconstructions. Model resolution (the average size of the faces making up the model) improved with increasing image density, model resolution and decreased flying elevation in a predictable manner. An increase of one step in the software quality settings, analogous to a four-fold

increase in image resolution, resulted in an increased rugosity value of ~15-20% over otherwise identical models. However, contrary to expectation, increasing image density, which resulted in improvements in reconstruction resolution, had no effect on the resultant surface area (i.e., rugosity), despite the smaller average face size. My findings highlight the importance of robust data collection and modelling procedures as well as the importance of reporting on the specifications of the equipment, the field protocols and the processing routines used to enhance the shareability and/or comparability of photogrammetric models. The results also serve as a guideline for those looking to use photogrammetry in their research.

Chapter 3 builds on the results of **chapter 2** by developing an automated, freely available processing protocol in the form of a downloadable python script designed to streamline both the reconstructions of models and the subsequent extraction of a suite of ecologically relevant complexity metrics. Using a training dataset of 69 corals at the colony scale, models were constructed using the most popular photogrammetry software package among ecologists (Agisoft Metashape Pro v1.7.2). A second tool, requiring only the installation of python and no coding knowledge, extracts a suite of 12 ecologically useful complexity metrics. The removal of user-choices from the processing pipeline and metrics extraction process is designed to enhance the validity of comparisons made between models. To test this, I explored the relationships between colony size (i.e., maximum diameter), morphotaxa and novel complexity metrics in some thematic analyses. Using the high-resolution dataset, I found that even with the relatively small sample size presented, the combination of growth morphology, genus-level taxonomic identity, and colony diameter, explained up to 95% of the shelter provisioning capability of corals. These results demonstrate the utility of automated routines to produce datasets in which models can be compared accurately and precisely. Furthermore, with more replicates using a robust data-generation process, it is possible that reliable two to three-dimensional conversion parameters may be uncovered that serve as a satisfactory proxy when only simple measurements are available as part of an in-water workflow.

Chapter 4 applies the lessons learned in the preceding chapters to explore an unprecedentedly large dataset spanning the latitude of the Great Barrier Reef and Torres Strait, Australia. A total of 330 reef plots, each measuring 72m^2 area were mapped for a total of 23,760m^2 of reef area across two depths, four habitats and 12 reefs that covered both inshore and offshore localities. Using a rigorously processed set of models, building on the routines designed in **chapter 3**, I explored spatial gradients in two key structural complexity metrics, rugosity and fractal dimension, across scales from habitats to geographic regions of the Great Barrier Reef system. Unexpectedly, no patterns in either metric of structural complexity were identified in broad-scale changes in both latitude and shelf position. Instead, the most reliable environmental gradients that resulted in differences in rugosity and fractal dimension were at the habitat level, with pronounced decreases in complexity as a result of increases in wave exposure. This pattern was consistent regardless of broad geographical region. Fractal dimension differed mainly with depth, and it was found that the most complex and highly fractal locations tended to be shallow reef slopes in sheltered locations. The results suggest that there are predictable patterns in complexity across habitats and depths, and that exposure to prevailing incoming wave energy is a major determinant of the level of complexity across the Great Barrier Reef, perhaps even more influential than shelf location and latitude. This dataset sets a precedent for using photogrammetry-derived reconstructions to make broad geographical scale comparisons in reef structural complexity whilst acting as a modern-day baseline to which future trajectories in complexity can be compared.

Chapter 5 furthers the efforts of **chapter 4** by pairing the Great Barrier Reef-wide dataset of complexity metrics with concurrent fish surveys. I explored how the community of small-bodied fish with small home ranges were affected by overall structural complexity (rugosity) and the tendency for complexity to be provided by relatively fine-scale or coarse-scale features (fractal dimension). First, I examined the entire assemblage of these small-bodied fish to determine whether structural complexity affected their overall abundance and diversity. Fish were then grouped in to feeding guilds (trophic groupings) to examine whether the different behaviours that tend to be exhibited based on foraging strategy led to different relationships with these two aspects of structural complexity. Both rugosity and fractal dimension positively influenced overall abundance and diversity. The relationship between complexity metrics and abundance of fish varied in both direction and strength according to group identity. The results suggest that different fish groups have varying relationships with structural complexity in line with their behavioural traits. Groups comprised of species with small body sizes that tend to engage in gregarious behaviours had a higher affinity for plots with high levels of fine-scale complexity, reflecting need for many individuals to be able to hide in small refugia simultaneously. Contrarily, fish with a slightly larger average body size that are less likely to be found in aggregations, tended to respond positively to rugosity but negatively to fractal dimension, suggesting a preference for refugia generated at scales larger than the inter-branch spacing of colony branches (or similar size).

Overall, my research highlights some key considerations to be made moving forwards when implementing photogrammetry studies and explores spatial gradients in reef structural complexity and its effects on concurrent animal communities in novel ways. This contributes to the rapidly evolving field of 3D spatial ecology by demonstrating some of the barriers to reconstruction comparability that may result from different processes both in the field and during the reconstruction pipeline, as well as

ways to overcome these. Importantly it provides guidelines to fostering best practises to ensure that the outputs can be explored reliably, and sound ecological conclusions can be drawn using the resultant data. These principals are demonstrated effectively through the comparison of reconstructions paired with fish surveys at sites spanning the latitude of the Great Barrier Reef and Torres Strait. The rigorous generation of high-resolution complexity metrics can provide a nuanced understanding of how reef structure varies spatially and how it affects concurrent animal communities. Given the ongoing threats to coral reef health and the potential for structural reorganisation/degradation globally, this thesis highlights how 3D spatial ecology can benefit from using more rigorous processing routines and considering complexity gradients in a multi-scale approach. The results and implications thereof can help to promote enhanced understanding of the distribution and functioning of habitats with various levels of complexity, to aid stewardship of tropical coral reefs in a time of change and uncertainty.

Table of Contents

Chapter 1 General Introduction 6
1.1 Structural complexity in natural systems 6
1.2 Structural complexity on coral reefs 7
1.3 Threats to structural complexity in coral reef systems 8
1.4 Evolution of methods to measure structural complexity in aquatic systems 9
1.5 3D Photogrammetry: overview and applications 10
1.6 Knowledge gaps underwater photogrammetry 12
1.7 Thesis overview 14
Chapter 2 Combined effects of image density and quality on the resolution and metrics of underwater photogrammetry reconstructions 16
2.1 Introduction 16
2.2 Methods 19
2.3 Results 25
2.4 Discussion 29
2.5 Conclusions 32
Chapter 3 A protocol for extracting structural metrics from 3D reconstructions of corals 35
3.1 Introduction 35
3.2 Methods 37
3.3 Results 47
3.4 Discussion 52
3.5 Conclusions 55
Chapter 4 Consistent spatial patterns in structural complexity with wave exposure across the Great Barrier Reef and Torres Strait 56
4.1 Introduction 56
4.2 Methods 58
4.3 Results 66
4.4 Discussion 70
4.5 Conclusions 73
Chapter 5 Three-dimensional rugosity and fractal dimension of habitats influence the abundance and diversity of small-bodied reef fish assemblages across broad spatial scales on the Great Barrier Reef 74
5.1 Introduction 74
5.2 Methods 76
5.3 Results 80
5.4 Discussion 88

Chapter 6 General Discussion 93
6.1 Significance and ecological interpretations of this thesis 93
6.1.1 Methodological advancements in photogrammetry 93
6.1.2 Ecological implications of the thesis 95
6.2 Future research directions 100
6.3 Final thoughts 102
7. Bibliography 103
8. Supplementary Materials 121

Contents of figures and tables

Figure 2.1 | Visual conceptualisation (stylised) of the effects of reductions in image density and image resolution on model resolution and rugosity of 3D habitat reconstructions. Focal object is a coral colony measuring ~1m in diameter at the native model resolution (5mm) in panel (A), before being serially depleted to progressively coarser resolutions (B-D). Note that for model resolution, the thicker end indicates larger face sizes and thus, "coarser" resolutions. 18

Figure 2.2 | Field and office workflows used at both spatial extents considered in this study. A more detailed description of processing steps is presented in Table 2.1. 21

Figure 2.3 | (A) Change in 3D reconstruction effective resolution with increasing image density and quality across the entire sample. Bayesian model outputs showing the simultaneous effects of image density and quality on both model resolution and rugosity of the small (B,C) and large (D,E) spatial extent plots. Note that for graphs indicating model resolution changes, a negative slope denotes an improvement (i.e. smaller faces making up the mesh). Note also that "high" image resolution (green) indicates reconstructions processed on a medium quality setting in Agisoft Metashape. 27

Figure 2.4 | Coarsest to finest model resolutions achieved in the small (A) and large (B) spatial extent reconstructions. The triangles represent the faces making up reconstructions. Note that the relative scaling of the triangles is correct in each panel (but not between panels). Blue triangles indicate that the models were processed using lower image resolution (0.63mpix), green indicates higher image resolution (2.5mpix). Note that the numbers on triangles represent the area of the triangle and not the lengths of the sides. 28

Figure 2.5| Conceptual diagram indicating processing choices that have directional effects on model resolution. Shaded arrows between stages indicate processing 'paths' that can lead to high (black), intermediate (grey) or low (white) resolution models. Note that it is not possible to achieve the highest resolutions over large spatial extents with a standard desktop computer, and that the high overlap needed for small extent models to be complete prevents low resolutions. Also note that model rugosity is not included here due to differential effects of image resolution and density. 33

Figure 3.1| In situ examples of the seven distinct modelled morphotaxa. Note the galvanised scale bars present in several panels used to scale the reconstructions. 39

Figure 3.2| (A) Scaling of absolute spatial refuge with increasing colony diameter across all morphotaxa**.** (B) Plotted posteriors from log-log linear model of absolute spatial refuge (mean centred) from the interaction model containing colony diameter as a predictor for each of the seven coral morphotaxa as well as intercept (α) and slope (β) estimates. Shaded regions are 95% highest density probability distribution. **(C)** Posterior predictions for intercept α and β parameters in the model. Straight line slope parameters indicate the existence of power-law relationships, with steeper slopes corresponding to higher power-scaling. Points indicate means, thick bars are 50% credible intervals, thin blue lines are 95% credible intervals. Numerical values off all model coefficients including posterior uncertainty are included in Table S3.1.. 49

Figure 3.3 | (A) Plotted posteriors from linear model of shelter size factor from the interaction model containing colony diameter as a predictor for each of the seven morphotaxa. Shaded regions are 95% highest density probability intervals and solid lines are mean slopes of the mean from the posterior probability distribution. (B) Posterior predictions for intercept (α) and slope (β) parameters in the same model. Circles indicate means, thick blue bars are 50% credible intervals, thin blue line are 95% credible intervals. All model coefficients including posterior uncertainty are available numerically in Table S3.3. 52

Figure 4.1| Map of the Queensland coast, eastern Australia, showing the location of the twelve study reefs. Note that the Keppel Islands cluster (yellow) was comprised of five separate reefs (Miall, Middle, Halfway, Great Keppel and North Keppel), each with a single site, due to low coral cover in exposed and moderately exposed reef slopes. (Inset) Example of study design at Davies Reef reflective of prevailing incoming wave energy exposure: Exposed slope (red dots), moderately exposed slope (yellow dot), sheltered slope (green dots) and lagoon (blue dots) sites. 60

Figure 4.2| (A) Area of interest and total area of benthos imaged by divers during photo acquisition. (B) Swimming pattern of divers used during data capture, showing the five longways and five sideways passes of the total imaged area. 62

Figure 4.3| Increasing surface rugosity and surface fractality because of the inclusion of features of different size. The inclusion of large and relatively smooth features leads to higher rugosity but does not increase fractality much, since these features are well-preserved as the mesh is smoothed to a lower resolution. The inclusion of both small, fine scale features as well as large features simultaneously increase rugosity (i.e., 3D surface area) whilst also increasing fractality................... 63

Figure 4.4|Rugosity measurements across all habitats and reefs (shallow sites) across the entire sample. Plots are arranged in order of descending latitude and are colour coded according to region. Habitat classes are denoted by the following acronyms: SS = sheltered slope, MES = moderately exposed slope, ES = exposed slope, Lagoon habitats were generally within the same range of incoming wave energy as sheltered slopes. 66

Figure 4.5| Model-fitted rugosity values (A) and fractal dimension (B) across all shallow sites within each of the reef sectors considered in this study. 67

Figure 4.6| Rugosity across different habitats for all shallow sites within each habitat (n =231). Circles indicate the average estimated mean for each group, black bars indicate 95% confidence intervals. Coloured points represent overlaid raw data points representing complexity metrics in each plot. 68

Figure 4.7|Comparisons of both rugosity (A) and fractal dimension (B) among sites and habitat zones with adjacent deep and shallow sites (6 reefs, 18 sites, 196 plots). 69

Figure 5.1| Map of the Queensland coast showing the location of the study reefs. (Inset) Example of study design reflective of prevailing incoming wave energy exposure: Exposed slope (red dots), moderately exposed slope (yellow dots) and sheltered slope (green dots). 77

Figure 5.2 | Partial Dependency plots showing the influence of each of the five predictor variables on overall small-bodied fish abundance (left column) and Shannon-wiener diversity (right column). Percentages under each panel represent the relative influence of each variable, whilst percentages at the top of columns represent overall variance explained by the model. Note that panels are not necessarily in order of most to least influential variables and the different scales on panels. Region codes: I = Inshore, O = Offshore, N = Northern, C = Central, S = Southern, TS = Torres Strait. Habitat zone codes: SS = Sheltered slope, MES = Moderately exposed slope, ES = Exposed slope 82

Figure 5.3 | Three-dimensional interaction plots from BRT models showing the combined effects of structural complexity metrics on fitted values of small-bodied fish abundance (A) and diversity (B) across all plots in all regions. Darker shades indicate higher fitted values (I.e., greater abundance or diversity).. 83

Figure 5.4 | Influence of predictor variables in each BRT model relative to the overall variance explained by the model for each trophic group.. 85

Figure 5.5 | Partial dependency plots showing effects of categorical variables on the abundance of each of the five trophic groups, across all sampling locations. Percentages are the relative influence of each variable for that model and are not reflective of absolute values of variance explained. Region codes: I = Inshore, O = Offshore, N = Northern, C = Central, S = Southern, TS = Torres Strait. 86

Figure 5.6 | Partial dependency plots showing the effects of (A) rugosity and (B) fractal dimension on the abundance of individual fish trophic groups across the sample, taken from each BRT model. Note that the percentage of variance explained by these complexity metrics varied between models (See Fig. 5.3).. 88

Chapter 1 General Introduction

1.1 Structural complexity in natural systems

Structural complexity is a major determinant of the functioning of ecosystems, including temperate and tropical forests, arid savannahs, kelp forests and tropical coral reefs (MacArthur 1958; Graham and Nash 2013). Structural complexity increases the availability and diversity of microhabitats, thereby moderating biotic interactions, (MacArthur 1958) and in many cases increasing the provision of food (González-Rivero et al. 2017; Oakley-Cogan et al. 2020), whilst also reducing otherwise harsh environmental conditions to tolerable levels (Tokeshi and Arakaki 2012). The importance of structural complexity in generating habitat diversity and supporting diverse communities was first noted as early as the 1950s (MacArthur 1958; MacArthur and MacArthur 1961), where structurally complex patches of forest were observed to be home to a greater number of bird species. Whilst the increase in faunal diversity, abundance or biomass does not always equate precisely to increasing gradients of structural complexity (Risk 1972; Komyakova et al. 2013), the general propensity for complex environments to support more abundant and diverse animal communities has been well studied by ecologists (Tews et al. 2004; Graham and Nash 2013).

Positive relationships between structural complexity and faunal abundance/biodiversity are not ubiquitous (Fukunaga et al. 2020b), since the benefits offered by different environmental attributes are not the same for every species. For example, the size of individuals has implications for how they interact with their surroundings; animals with a smaller body size use spaces that their predators cannot access (Rogers et al. 2018b). In addition, the relative success and behaviour of predators and prey differ according to the habitat arrangement; trade-offs in foraging capability and the ability to detect and evade/predate, influence the behaviour of, and may shape the distributions of animals in both terrestrial (Gigliotti et al. 2020, 2021) and aquatic systems (Nunes et al. 2015; Quadros et al. 2019). Prey for example, may be more risk averse where complexity is high and visual acuity is low (Quadros et al. 2019). In this context, it appears that the importance of structure may depend on its scale relative to specific organisms. Since complexity is often generated in large part by biogenic structures i.e., ecosystem engineers (Tokeshi and Arakaki 2012), which are inherently subject to change over time due to growth, competition, and external disturbances, animals' relationships with their surroundings are somewhat plastic.

1.2 Structural complexity on coral reefs

Coral reefs exemplify the importance of structural complexity in natural systems. Corals themselves are the cornerstones of tropical reefs as autogenic ecosystem engineers which, through the production of a calcium carbonate skeleton, provide the structural complexity for the thousands of species they support (Wild et al. 2011), from small cryptobenthic species (Dalben and Floeter 2012) and invertebrates of a range of sizes (Fuchs 2013), to large, commercially important roving fish (Kerry and Bellwood 2015). The natural range of corals is relatively narrowly constrained by a combination of specific temperature, light, depth, wave energy and substrate requirements, and they cover less than 0.1% of the ocean floor (Spalding and Brown 2015). Nevertheless they provide food security for in excess of half a billion people worldwide (Cruz-Trinidad et al. 2014).

Mechanisms by which coral reef structural complexity support abundance or diversity of associated animal communities are varied. Corals are food for some species (Pratchett 2005; Graham et al. 2009) and providers of space for both small- (Noonan et al. 2012) and large-bodied individuals (Kerry and Bellwood 2015) alike, whilst simultaneously reducing water movement and allowing fish with varying locomotive capabilities to reduce their energy consumption (Bellwood and Wainwright 2001; Johansen et al. 2007). In addition, the attenuation of wave energy, and the coastal protection benefits this provides, extend directly to humans. The reduction of the incoming wave energy that reaches shorelines is well documented (Monismith et al. 2015), with reefs providing protection from both normal wave conditions (Harris et al. 2018; Duce et al. 2022) as well as acute disturbances such as tsunamis and cyclones/hurricanes (Kunkel et al. 2006). When compared with other coastal ecosystems, the friction that structurally complex coral reefs exert to break waves and reduce water movement results in highly efficient wave attenuation over short distances, making reefs one of the most important coastal defences supporting coastal human populations (Ferrario et al. 2014; Monismith et al. 2015; Carlot et al. 2022).

The refuge spaces generated by complex structures on coral reefs are of particular importance (Rogers et al. 2018a; Urbina-barreto et al. 2020). It is intuitive that higher levels of complexity may yield benefits by providing shelter for prey and the role of structural complexity in mediating predator versus prey success during encounters has been studied in experimental scenarios (Nunes et al. 2015). The trade-offs between prey being able to forage effectively in low-complexity environments (Rilov et al. 2007) where they can see well but are relatively exposed (George et al. 2021) versus high complexity environments with abundant places to hide (Quadros et al. 2019) modifies the behaviour of both predators and prey. Perceptions of safety have also been found to vary according to fish body size

(Chan et al. 2018). Fish-complexity relationships may therefore be affected by not only species identity and the level of complexity, but also by life history stage and foraging behaviour. For these reasons, high complexity does not ubiquitously benefit predatory/prey or small/large species (Almany 2004; Rilov et al. 2007).

At spatial extents covering reef patches larger than a few square meters, observational studies have indicated that there is generally a positive relationship between the availability of appropriately sized refugia for fishes and their abundance (Rogers et al. 2014), but also that this relationship varies according to body size and life history strategies of particular individuals/species (Alvarez-Filip et al. 2011b; Fukunaga et al. 2020b; Helder et al. 2022). Whether the relationship between structural complexity and the abundance of fish is positive, neutral or negative appears to be dependent on a mixture of behavioural traits (e.g., solitary versus schooling) (Ferrari et al. 2017b), body-size (Alvarez-Filip et al. 2011b), foraging behaviour (Helder et al. 2022) and the scale of complexity generated by the environment relative to the needs of a particular individual/group. More research using high-resolution complexity metrics at appropriate spatial extents is required to better understand the complexities of these relationships.

1.3 Threats to structural complexity in coral reef systems

The degradation of habitats and the resultant loss of structural complexity in natural ecosystems is a major concern in the Anthropocene. This is especially true of coral reefs, since corals are autogenic habitat engineers that are disproportionately at risk from climate change due to their already relatively specific environmental requirements. It has been noted for several decades that reefs are getting flatter on average (Alvarez-Filip et al. 2009) due to an intensifying disturbance cycle from which structure-providing benthic communities struggle to recover between stress events (Hughes et al. 2017b). Primarily, elevated temperatures that lead to coral bleaching and the subsequent decay of three-dimensional structures (Hughes et al. 2019b; Morais et al. 2022), along with more frequent extreme weather events (Cheal et al. 2017) and outbreaks of crown-of-thorns starfish (De'ath et al. 2012). Combined with limited recovery times, these events negatively impact reef carbonate budgets and reduce accretion to a point where yearly structural changes are losses rather than gains (Perry et al. 2014; Januchowski-Hartley et al. 2017). In particular, the high susceptibility of reef structures such as highly branching or tabular morphotaxa (Madin and Connolly 2006) to extreme weather events threatens the productivity of reefs as these, often faster growing, structures decline in abundance. Since different fish and invertebrate taxa utilise the environment in different ways (Munday 2004), the degradation of habitats and reductions in complexity are likely to have varied effects depending on species identity and exactly in what manner the degradation occurs (Wilson et al. 2008). To accurately detect and forecast the flow on effects of coral reef habitat degradation to their dependent communities requires the measurement of structural complexity at ecologically meaningful scales and spatial extents accompanied by detailed assessments of the myriad relationships supported.

1.4 Evolution of methods to measure structural complexity in aquatic systems

The measurement of structural complexity in aquatic systems has evolved considerably since it was first noted that coral reefs are often organised into distinct zones that vary in species composition and the predominant growth morphology of benthic groups, which in turn mediates structural complexity (Goreau 1959). The first attempt at quantifying structural complexity of coral reef habitats was by Risk (1978), whereby a fine-link chain was draped over the substrate and conformed to any cracks and crevices over one linear meter, and the ratio of the length of the conformed chain to the linear distance recorded. To obtain a measurement for a meter-square quadrat, this was repeated as many as eight times. Despite providing a relatively precise metric of structural complexity, measuring substrate complexity and collecting data on fish diversity was time consuming, taking ~80 hours to collect repeat samples over a reef area of just 16m^2 (Risk 1972). However, the use of the chain-and-tape method and the resultant measure of rugosity was widely adopted and is one of the primary measures of measuring structural complexity on coral reefs to this day (Alvarez-Filip et al. 2011b; Trebilco et al. 2015; Morillo-Velarde et al. 2018). In most cases, where complexity is measured using this method, rugosity is only quantified one-dimensionally (i.e., a single transect lying within an area that is three-dimensional). Over the past four decades, numerous measures of structural complexity have been developed, adapted, streamlined and compared in an attempt to determine the most appropriate and efficient way to measure structural complexity on reefs. Some of these methods include using visual qualitative categorisations of complexity (Polunin and Roberts 1993; Wilson et al. 2007), measuring the height of the substrate at regular intervals using a field profile gauge (McCormick 1994). and measuring the contour distance using wheels of varying diameter (Richardson et al. 2017b, 2017a). Whilst these have been tailored to effectively answer specific questions, few have been widely adopted due to their highly specialised equipment requirements and limited gain in information over chain-and-tape rugosity.

1.4.1 Advancements in the field of structural complexity measurements

Computer vision has seen great advancements since the beginning of the 21st century (Green et al. 2014). Whilst traditional "analogue" measurements of complexity such as those derived from chain-and-tape rugosity provide a proxy for measuring structural complexity (Luckhurst and Luckhurst 1978), they are at best, two-dimensional representations of complex 3D systems that require extremely fine spatial resolution i.e., many repetitions in a small area (Risk 1972). Given the importance of structural complexity, the need for continuous topographic maps of the seafloor over greater areas than is possible using analogue methods was recognised (De Moustier and Matsumoto 1993). Using novel technologies to generate three-dimensional habitat maps (such as shipborne acoustics or active light-scanning methods) greatly boosted the amount of available data on surface roughness of marine systems (Kotilainen and Kaskela 2017; Zhang et al. 2017; Wedding et al. 2019). Whilst data obtained from these sources is useful for mapping large areas at moderate spatial resolutions (i.e., ~0.5 m to 10s of metres), the associated costs are extremely high, with charters of ships/aircraft generally being prohibitive to the wide-scale collection of such data by most research groups. Further, although the need for multi-scale measures of habitat complexity (i.e., from single coral colonies to general profiles over hundreds of meters) has long been recognised (Purkis et al. 2008), the relatively coarse resolution from the aforementioned methods prohibits the measurement of complexity at scales relative to many species of fish (i.e., sub-centimetre to centimetres).

1.5 3D Photogrammetry: overview and applications

Photogrammetry is a "passive" light-based sampling technique, in that active light-sources such as those used in LIDAR or laser scans are not required. Using this method, a specialised software package searches successive pairs of overlapping images for common 'features', which are slowly built up into a network of points in three-dimensional space. The resultant point matrix is joined together to form a mesh of interconnected triangular faces, forming a 3D reconstruction that can be accurately scaled and measured in numerous ways. The reconstruction resolution (the distance between neighbouring vertices/face intersections) can be on the order of centimetres or even millimetres (Marre et al. 2019; Million et al. 2021), which is only surpassed by methods that are higher in cost and/or not applicable *in situ* such as computerised tomography (CT) scans or laser scans (Groves et al. 2018; Zawada et al. 2019a).

Whilst the concept of using computer vision to turn still images into 3D reconstructions has existed for some time (Fryer 1983), the technique was not widely used until at least 2015, when commercially available software packages streamlined the process and sufficient computing power became accessible enough for researchers to consider the method viable (Burns et al. 2015; Micheletti et al. 2015). Subsequently, a large portion of the literature has concentrated on developing workflows (Bayley and Mogg 2020), assessing accuracy and precision (both in absolute terms and in comparison with earlier methods) (Bythell et al. 2001a; Figueira et al. 2015; Bryson et al. 2017; Ferrari et al. 2017a; Raoult et al. 2017), and the effect of different equipment specifications on the quality of the resultant models (Marre et al. 2019). While work remains to be done in this space, the use of photogrammetry has realised the potential to increase our understanding of the structural intricacies of coral reefs by enabling robust measurements of complexity to be derived from the resultant three-dimensional models.

Besides the accuracy and resolution increases provided by photogrammetry, one of the greatest advantages of three-dimensional habitat reconstructions is the diversity of structural complexity metrics that can be extracted from the models. The diversity of metrics allows 3D reconstructions to provide more insight into how the structure of the environment relates to its functioning, and how community organisation influences this. Further, the resultant surface measurements and structural complexity metrics can be used to track changes over time comprehensively, whether this relates to degradation or recovery following disturbance (Fukunaga et al. 2022). A multitude of primary metrics (direct measurements) and secondary derivations (calculations involving two or more primary metrics) have been proposed and implemented to disentangle how structural complexity varies through space and time in different ways. At small spatial scales covering single coral colonies, photogrammetry permits the measurement of features including 3D surface area and volume and derivatives (Doszpot et al. 2019), interstitial space (Urbina-barreto et al. 2020), height (Agudo-Adriani et al. 2016), width and planar area (House et al. 2018). With the exception of basic two-dimensional attributes such as width, the measurement of detailed attributes previously was time-consuming and inaccurate, and most methods required the sacrifice of the colony, preventing the measurement of 3D growth. For example, wrapping a coral's surface in foil or using wax dipping to measure surface area or by forcing modelling clay into interstitial spaces to measure interstitial volume were proposed methods (Naumann et al. 2009; Veal et al. 2010; Hesterberg et al. 2017) that have not been used *en masse*. Using photogrammetry on the other hand has in recent times allowed for the repeated measurement of corals over time to measure detailed surface metrics and measure growth accurately without any disturbance (Ferrari et al. 2017a; Million et al. 2021). However, despite the aforementioned metrics and methods with which to extract them, there remain several gaps in knowledge at the coral colony scale regarding which metrics are the most ecologically relevant to use, and how they perform on of different growth morphologies of corals.

At broader spatial scales, photogrammetry has been used to develop multiscale metrics that quantify the structural attributes of reefscapes in far greater detail than was previously possible (Bayley et al. 2019). As a series of interconnected faces, each with their own area and orientation, the calculation of many metrics of complexity that relate to reefscape functioning in different ways is possible. Primary metrics notably include a three-dimensional extension of rugosity (Young et al. 2017; Bayley et al. 2019), vertical relief (the vertical distance between the highest and lowest points in a mesh) (Helder et al. 2022), slope and surface area (Yuval et al. 2021), among many others. Secondary derivatives of metrics are appropriate to address specific questions and tend to be more complex and computationally more challenging than direct measurements of structural attributes, and some are only appropriate at certain spatial scales (i.e., not all colony-level metrics can be applied to larger areas and vice versa). These include: fractal dimension, which is aimed at measuring whether complexity in a particular reconstruction is generated by comparatively small or large feature sizes (Torres-Pulliza et al. 2020); curvature (or slope of slope), which measures the rate of change in slopes in various directions (Fukunaga and Burns 2020). Such secondary metrics are difficult to conceptualise but can be related to the ecological functionality of reefs and are only possible to calculate from fully three-dimensional habitat maps built using the appropriate methodologies. Certainly, such metrics have been used to relate reef structure to the community composition and/or abundance and diversity of both the benthic (Fukunaga et al. 2020a; Urbina-barreto et al. 2020) and fish communities (Ferrari et al. 2017b; Fukunaga et al. 2020b; Helder et al. 2022), with greater explanatory power than was established using the chain-and-tape or other earlier methods. Whilst these studies show promise, further work is required to integrate high resolution 3D models with environmental drivers and populations of fish to determine spatial gradients in structural complexity, and how this affects the inhabitant assemblages of animals.

1.6 Knowledge gaps underwater photogrammetry

As a non-invasive and relatively easy to use tool, photogrammetry can be used to tackle some of the greatest problems facing contemporary ecologists. Given the speed with which reefscapes have the potential to change under intense disturbance, the use of technologies that are comprehensive, non-invasive, and repeatable over time is critical for adequate monitoring and management. A variety of useful metrics of complexity are increasingly being used to assess variation in both benthic (Osuka et al. 2018; Carlot et al. 2020; Fukunaga et al. 2020a) and fish communities at a variety of scales (Jankowski et al. 2015; Agudo-Adriani et al. 2019; Urbina-barreto et al. 2021; Helder et al. 2022), offering great potential to understand how environmental perturbations are likely to affect different components of reef ecosystems. Hitherto, most photogrammetric surveys are somewhat constrained in their spatial scale, generally focussing on single patches of the same reef or reefs in the same locality (Agudo-Adriani et al. 2019; Castaño et al. 2021). Some efforts have been made to quantify complexity at broader spatial scales (González-Rivero et al. 2014), but generally, large regional-scale datasets that capture the effects, not only of local-scale variation in environmental position, but also latitude and shelf position, are rare. Quantifying broad-scale variation in complexity across a wide geographic extent may provide insights into what environmental/physical conditions are most important for its creation and will be a useful avenue to guide effective stewardship. For example, past disturbances have affected different sectors of the Great Barrier Reef (GBR) differentially according to latitude and shelf position (Emslie et al. 2008; Anderson et al. 2015; Mellin et al. 2019). Indeed, geographic region is a well-known driver for differences in biotic communities (Emslie et al. 2010, 2012; Cheal et al. 2012; Hoey et al. 2013), so understanding how structural complexity varies at multiple spatial scales between and within regions would help to explain further variance in both benthic and motile assemblages.

The volume of data that it is possible to collect and process (i.e., turn raw images into 3D reconstructions) is ever increasing due to the constantly lowering cost, improving ease of use and increase in power of computing systems (Bayley and Mogg 2020). This opens opportunities for collaboration and data sharing between groups globally that will allow broad-scale questions to be addressed. However, despite photogrammetry's widespread adoption/uptake and the "new era in spatial ecology" that this represents (D'Urban Jackson et al. 2020), there are still barriers to its widespread implementation concerning the repeatability of data acquisition and processing protocols (Rossi et al. 2021). There are many options available to researchers that will influence some aspect of the reconstruction, including camera system choice (Mosbrucker et al. 2017), in-water data collection protocols (Marre et al. 2019), software choice (Forsmoo et al. 2019), and even the settings used in-software during processing. Whilst this is by no means an insurmountable barrier that nullifies results obtained using photogrammetry, further research is required to quantify the sources of variation that may arise due to human decisions versus the natural variation that ecologists are looking to understand. Better understanding the nature of methodological variations will allow datasets from different groups globally to be compared and yield more powerful results. Indeed, several guidelines have been published to this end, and the integration of photogrammetry into many monitoring programs has been discussed (González-Rivero et al. 2014; Palma et al. 2017; Fukunaga et al. 2019). Yet, whilst these guidelines offer an entry-point for new users of photogrammetry, little attempt has been made to quantify exactly how different data collection and processing protocols affect the final reconstructions (but see Marre et al. 2019).

In summary, photogrammetry is likely to continue to increase in popularity into the future due to the many possibilities and benefits that the method has in comparison with existing methods. In this context, my PhD thesis proposes new and informative ways in which to make the best use of photogrammetry, from data collection and processing, to using reconstructions to give new insights into the ecological analyses that are possible with the resultant outputs.

1.7 Thesis overview

The overall aim of this thesis is to advance our capability to use photogrammetry from both a methodological and an ecological perspective by developing and implementing routines to build 3D reconstructions, extract relevant structural complexity metrics, and use them to draw ecologically meaningful conclusions. This aim is achieved in four distinct objectives, each relating to a specific chapter.

The first two objectives relate to advancing the methodology of photogrammetry to facilitate the generation of comparable outputs, specifically to:

1) Determine the extent to which the choices of users during the photogrammetry process, both in the field and during processing, affect the comparability of the outputs generated by the reconstructions (chapter 2).
2) Develop and implement a methodology to easily build replicable reconstructions of corals and extract a suite of ecologically relevant structural complexity metrics (chapter 3).

The second two objectives further the use of photogrammetry in an ecological context by using a spatially expansive dataset generated using repeatable routines to explore spatial variation in structural complexity and assess how this affects fish communities. Specifically, the aims were to:

3) Use highly accurate and high-resolution 3D models from locales spanning a wide geographic range to assess possible environmental determinants of structural complexity (chapter 4).
4) Determine the extent to which structural complexity metrics influence the regional and local-scale distribution of small bodied, site attached fish species (chapter 5).

Chapter 2 explores issues with repeatability in photogrammetry and presents a comparison of the influence of image density and in-software quality settings, two parameters that may vary considerably depending on equipment choices/constraints, as well as how these affect the robustness of structural complexity metrics extracted from the resultant reconstructions. **Chapter 3** presents a two-part methodology to serially generate models of coral colonies and extract a suite of 11 different structural complexity metrics that are repeatable and save users time by removing the need to interface directly with software. The ecological utility is explored via analyses which predict the shelter provisioning capability of several different coral morphotaxa and how this changes with colony size. **Chapter 4** presents a broad-scale spatial comparison of high-resolution structural complexity patches across the Great Barrier Reef and Torres Strait to determine whether there are patterns in ecologically relevant aspects of structural complexity at both the intra-reef scale and across the whole region. Predictive models estimating overall complexity (rugosity) and feature size distributions (fractal dimension) with depth, habitat exposure to wave energy and regions are presented and discussed. **Chapter 5** aims at enhancing our understanding of the relationship between the structural complexity of reefs and their inhabitant fish communities. The same broad spatial-scale dataset used for chapter 4 is combined with surveys of small, site attached fish to investigate how two ecologically useful metrics of structural complexity (rugosity and fractal dimension) influence the diversity and abundance of these fish.

Chapter 2 Combined effects of image density and quality on the resolution and metrics of underwater photogrammetry reconstructions

2.1 Introduction

The physical three-dimensional (3D) structure of natural environments is a key predictor of ecological communities and functioning across both terrestrial (MacArthur 1958; Franklin and Pelt 2004; Connell et al. 2010) and aquatic environments (Graham and Nash 2013; Ferrari et al. 2017a; Rees et al. 2018). The presence of diverse structure generates microhabitats and allows for a greater per unit area occupation of a given space by animals, since the space and refuge needs of a greater diversity/richness of animals can be met (Mac Nally et al. 2001). Additionally, predator-prey interactions are regulated by the shelter spaces provided by complexity-generating features, increasing the survivability of prey species in some cases, and increasing the success of predators in others (Hixon and Menge 1991; Sass et al. 2006; Wasserman et al. 2016; Quadros et al. 2019; Gigliotti et al. 2020). The importance of structural complexity is broadly applicable to all ecosystems (Calders et al. 2020), but it is particularly crucial in underwater environments, since the higher drag exerted by water compared to air necessitates the shelter provided by structure to reduce harsh environmental conditions to tolerable levels (Tokeshi and Arakaki 2012; Pygas et al. 2020). However, it is increasingly recognised that the relationship between structural complexity and the inhabitant fauna of reefs is highly nuanced, with specific groups of fish and other animals reacting differentially to changes in complexity. For example, structural complexity can benefit or inhibit abundance of similar species at different life stages due to shifts in vulnerabilities to different types of predation, highlighting that the positive correlation between faunal abundance and structural complexity is not always ubiquitous (Almany 2004).

Remotely sensed habitat maps that can be collected over relatively broad spatial extents using field-based methods are being used to assess the biophysical characteristics of environments (Kerr and Ostrovsky 2003). Ecologists increasingly are using photogrammetry, a series of still images stitched together to make virtual three-dimensional terrain reconstructions to create habitat maps from which surface structures can be empirically measured. This method has been used in terrestrial ecology for modelling forest canopy structures across both wide and fine extents (Cunliffe et al. 2016; Iglhaut et al. 2019; Calders et al. 2020) and has been applied to the marine realm at spatial scales from single individual coral colonies to large patches of reefs (Agudo-Adriani et al. 2016; Storlazzi et al. 2016; Casella et al. 2017; Bayley et al. 2019).

Ecologists can extract many metrics from three-dimensional reconstructions that characterise different elements of structural complexity, including the slope of the terrain, surface roughness, shelter capacity and how good the field of view is from different perspectives, among others (Aben et al. 2017; González-Rivero et al. 2017; Zawada et al. 2019a, 2019b; Urbina-barreto et al. 2020; Fukunaga and Burns 2020). The most often reported with respect to habitat structural complexity and one of the earliest metrics measured *in situ* is rugosity (Risk 1972), the length of contoured distance between two fixed points divided by its linear distance, thus resulting in a metric based on two-dimensional features. In three-dimensional ecology, rugosity refers to the surface area of a 3D object area divided by its 2D planar area. Higher rugosity indicates higher complexity and has been recognised as a key ecological indicator of coral reef biodiversity and health trajectory (Alvarez-Filip et al. 2011b; Nash et al. 2013; Ferrari et al. 2016a; Bayley and Mogg 2020). Yet, regardless of the metric used to answer a particular question, most of these are tied to the model's resolution (analogous to the chain link size if measured in 2D). In photogrammetry, resolution refers to the face size of the polygons making up the models, with finer resolutions expected to result in a higher estimated surface area and therefore rugosity. Despite the increasing popularity of photogrammetry amongst ecologists, very little regard has been given to the resolution of models (Fukunaga and Burns 2020; Urbina-barreto et al. 2020; Million et al. 2021), potentially hindering comparability between studies.

In spite of the rapid increase in the use of photogrammetry among different scientific disciplines, little consideration has been given to the potential effects of user decisions during gathering and processing of photogrammetric data to generate 3D reconstructions of habitats (Tinkham and Swayze 2021). Analog to when remote sensing was rapidly adopted in landscape ecology, this will likely result in disparate photogrammetric workflows and datasets that are not standardised. It is essential to understand which aspects of variation in 3D measurements may be attributed to 'real' spatial and temporal variation, versus those introduced by differences in data collection and processing approaches (i.e., artificial variation). Two key user choices that have strong potential to influence 3D measurements include image density (number/m^2) and the resolution of individual images. Whilst it is assumed that higher image densities and resolutions will improve model resolution (Fig. 2.1), and that these lead to increased model surface areas and therefore rugosity (Young et al. 2017), the specifics of these relationships are yet unknown. Similarly, using chains with different link sizes to measure linear rugosity produces large effects on structural metrics, which is not problematic if this is specified and accounted for. Given the high volume of studies linking 3D habitat reconstructions to infer ecologically important conclusions (González-Rivero et al. 2017; Ventura et al. 2018; Carlot et al. 2020; Ferrari et al. 2021), and the lack of consideration of sources of variation of model resolution and surface measurements, it is important to establish to what extent various parameters may influence these, so that comparability between studies is not confounded moving forwards.

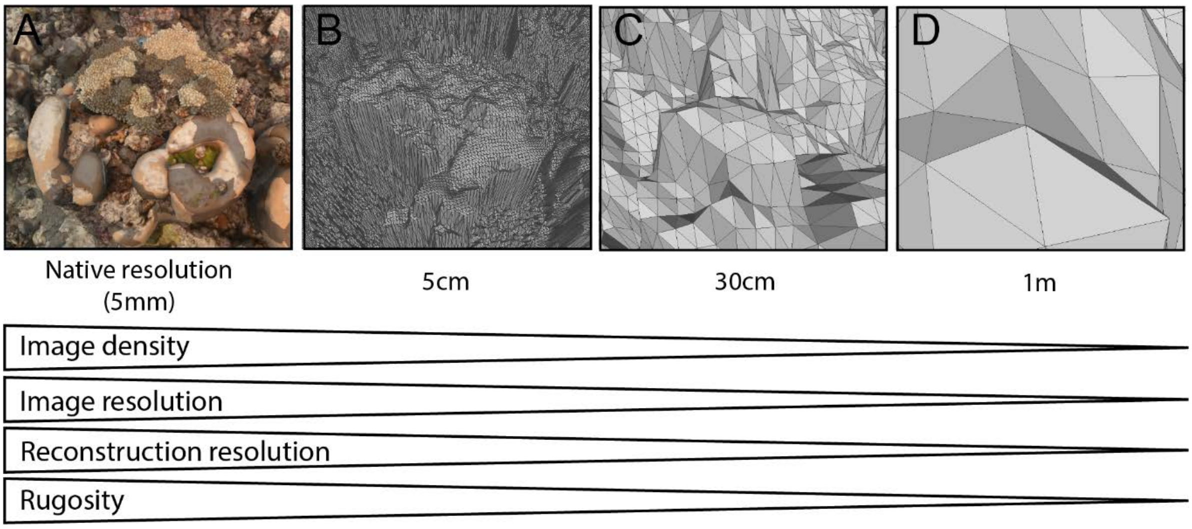

Figure 2.1 | Visual conceptualisation (stylised) of the effects of reductions in image density and image resolution on model resolution and rugosity of 3D habitat reconstructions. Focal object is a coral colony measuring ~1m in diameter at the native model resolution (5mm) in panel (A), before being serially depleted to progressively coarser resolutions (B-D). Note that for model resolution, the thicker end indicates larger face sizes and thus, "coarser" resolutions.

The use of photogrammetry for aquatic applications is particularly challenging for several reasons. First, the need to house high-quality cameras inside waterproof housings leads to an additional optical element being introduced (Menna et al. 2016a; She et al. 2022), which can be problematic for image-matching algorithms due to the distortion of images. Second, the lower light level (compared to when in air) darkens images, so it is more challenging to obtain good-quality data. However, despite the associated challenges, photogrammetry is becoming more popular since it represents the best available methodology to visualise and quantify the structure of aquatic environments (Storlazzi et al. 2016; Bayley et al. 2019; D'Urban Jackson et al. 2020; Urbina-barreto et al. 2020). Amongst marine ecosystems, coral reefs are complex environments that can be challenging to reconstruct effectively (Figueira et al. 2015; Bryson et al. 2017), although they exist primarily in shallow-water, well-lit environments, which are well suited to photogrammetry. Further, coral reefs are under threat globally due to direct anthropogenic effects and climate change (Hughes et al. 2018), with large-scale declines in complexity characterising these ecosystems in recent times (Alvarez-Filip et al. 2011a; Graham and Nash 2013; Newman et al. 2015) so it is critical to understand the limitations of the methods used to study them.

The aim of this study was to assess how model resolution and derived measurements are affected by user choices made during the photogrammetry workflow. Specifically, I assessed the effect of image density (7-816 images/m^2) and image resolution (2.5 and 0.63 megapixels) on the resolution and rugosity measurements of photogrammetric 3D reconstructions. The chosen combinations of image densities and resolutions were reflective of what were considered 'real-world' scenarios, tailored to answering questions at different spatial scales (1-2 square meters of reef and large, 72m^2 patches of reef) using nine coral reef patches. I then compared the resolution and rugosity measurements of the resultant models to assess the extent to which the choices that were made affected the quality of the resultant reconstructions. My results have important implications for mission-planning and user choices during data processing, and for the comparison of 3D metrics between studies with contrasting workflows. Lastly, this study provides recommendations to future users of photogrammetry on image density and quality settings that are most appropriate to construct complete models and achieve a specific desired model resolution depending on the spatial scale of measurement, and the ecological questions being asked. This information is also vital for workflow design due to its implications for determining required computing power and time to process photogrammetry datasets (D'Urban Jackson et al. 2020). While coral reef ecology is used as an example, the results of these comparisons are applicable to any underwater photogrammetry workflow and dataset, across many disciplines such as underwater archaeology or conservation.

2.2 Methods

Study sites

Photogrammetry surveys of coral reef habitat were conducted at two locations (Heron Island and Orpheus Island) on the Great Barrier Reef, Queensland, Australia. All survey sites were selected for their high coral cover and complexity, since highly complex features are the most challenging to reconstruct in high detail (Guo et al. 2016). Each location was positioned in shallow water (2-9 m depth) and vertical visibility was >5 m during all photogrammetry surveys. Surveying was conducted with some cloud cover to ensure caustics were not present and to avoid disruption of image-matching algorithms. Data were gathered from across nine plots in total at two different spatial scales: four of these were 'small' plots of 1-2 m^2 and five were 'large' plots of 72 m^2 (12 x 6 m). Each of these plots were in different geographical locations, separated by at least 10 metres of linear distance.

Data capture and photogrammetry equipment

High-quality DSLR camera systems (Nikon D850) paired with underwater housings (Nauticam housings, 8-inch dome ports) were used to obtain the highest possible quality images and thus the highest quality reconstructions. While it has been shown that action cameras (e.g., GoPro) can be used to make adequate reconstructions of complex underwater structures (Raoult et al. 2016), this study aimed to test the thresholds of photogrammetry and the influence of fine-scale variation in resolution and 3D metrics, so a high-resolution camera arrangement was selected. Camera arrangements varied slightly between small- and large-scale imaging techniques to best meet the imaging requirements of each scale (Fig. 2.2). The imaging swim pattern consisted of several passes over the area of interest capturing nadiral and oblique imagery, using a mow-the-lawn pattern (Fig. 2.S1) for large and orbital pattern for small plots. Since distortion tends to occur on the outer edges of models, a 1 m buffer was captured around the desired area to ensure that the modelled area of interest was of high quality. Camera settings were chosen depending on lighting and in-water visibility: shutter speed minimum 1/500, f-stop value minimum 5.6, ISO maximum 5000. Where poor lighting and visibility prevented adequate images with these settings, data collection was postponed until these requirements could be met.

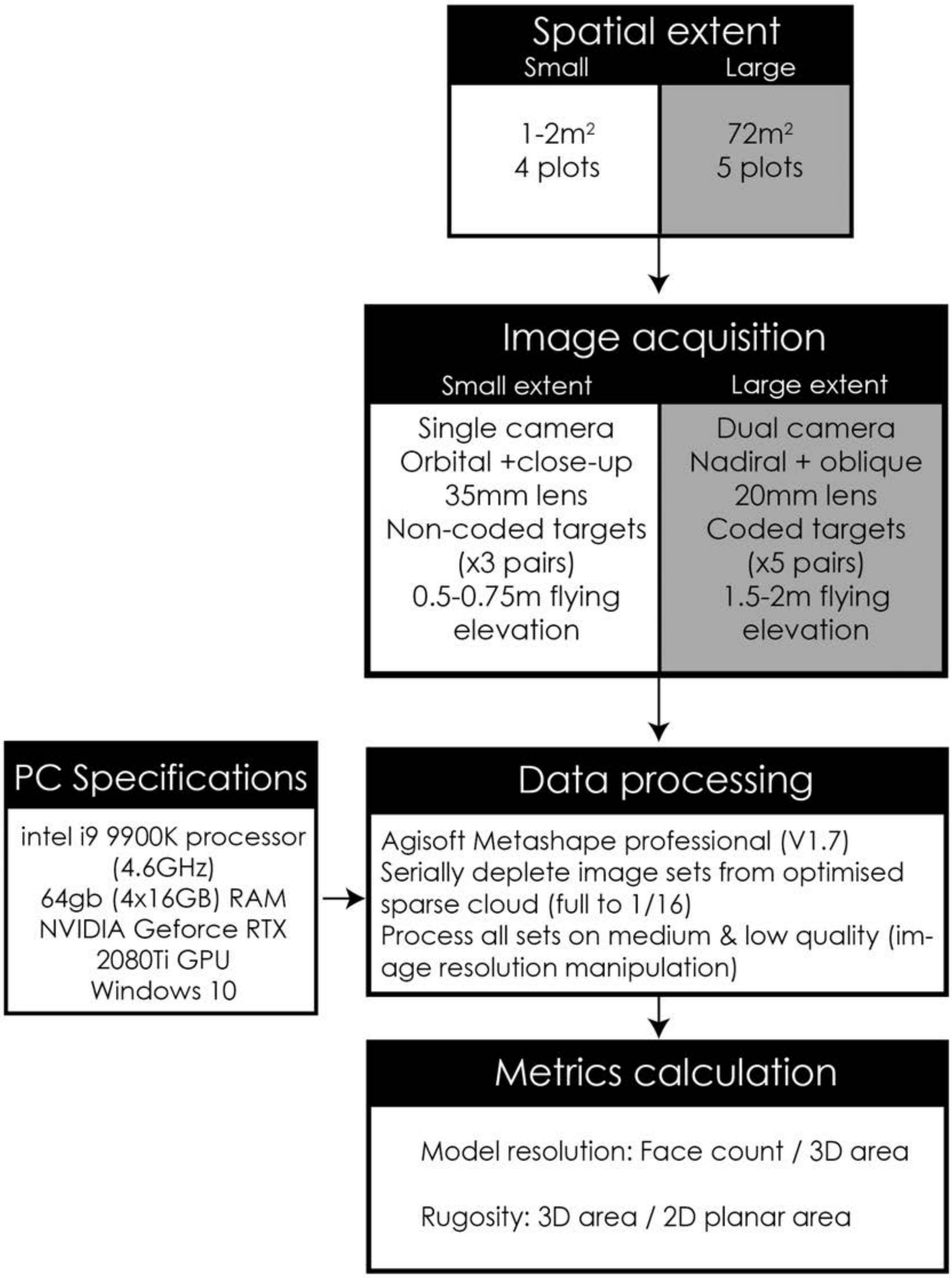

Figure 2.2 | Field and office workflows used at both spatial extents considered in this study. A more detailed description of processing steps is presented in Table 2.1.

Data processing

Models were generated using Agisoft Metashape Professional (Version 1.7) using a high-quality desktop PC (Fig. 2.2). The detailed workflow procedures for model generation within Metashape are described in Table 2.1. I filtered the sparse cloud for poor points to improve the accuracy of the estimation of camera locations, ensuring the reconstruction geometry was as close as possible to being true-to-life (Bayley and Mogg 2020). This was implemented via a custom-coded python script to ensure user choices could not influence its effectiveness.

TABLE 2.1 | Processing workflow used in the generation of each model.

STEP NAME	Details
PRE-PROCESS IMAGES	Estimate image quality and disable images with score <0.5.
DETECT MARKERS AND CHECK MARKERS *	Detect targets in each chunk in the project and remove poorly or incorrectly identified targets based on the number of projections. I used a tolerance value of 30, and used Agisoft's coded target system to print paired markers at pre-set distances apart. Manually check that all markers have at least 10 projections and error of < 2 pix.
ALIGN PHOTOS	"High" quality used for all plots and all scales. An a priori minimum of 80% photo alignment was used. Below this, plots were discarded (n = 0 in this instance).
ADD SCALE BARS AND CHECK MEASUREMENT ERROR	Added scale bars between paired targets and entered distance between them. Error (m) was checked to ensure it was below 0.001 m (1mm). If this was not met, markers were checked again, and high reprojection error detections were removed more aggressively.
CLEAN SPARSE CLOUD/OPTIMISE CAMERAS	Reduce Root Mean Square and Maximum reprojection error via a 3-iteration removal of low-quality points based on three separate criteria: reprojection error, projection accuracy and reconstruction uncertainty. Optimise cameras was performed after each step., followed by camera network optimisation after each removal of poor points. The worst 5% of points were removed for each criteria, and this was repeated 3 times. In total, 53% of the total sparse cloud points were removed.
DUPLICATE CHUNK/REMOVE IMAGES	Prepare chunks for testing by duplicating 8 times. For each duplicated chunk, I removed photographs at regular intervals so that progressively less were retained. Remaining photos ranged from full sets to 1/16 images retained.
BUILD DENSE POINT CLOUD	Medium and Low quality settings used for each chunk (to manipulate image resolution). Each step down in quality downscales the image by a factor of 4.
BUILD MESH	Face count: High Source data: Dense cloud
EXPORT REPORTS	Generate pdf report for each chunk to extract metrics later.

Final models were reconstructed from duplicates of a single optimised sparse cloud for each plot, ensuring any differences in models could be ascribed purely to variation in the parameters of interest. To test the effect of photograph density on model resolution and rugosity measurements, images were removed at regular intervals from the photoset, down to a minimum of 1/16 the original number. Similarly, to test the effect of image resolution on model resolution and rugosity measurements, image resolution was depleted using the in-software dense cloud quality settings (Table 2.2). Agisoft Metashape supports in-software downscaling of the images used to build reconstructions, which is often necessary given the high volume of data contained in high-megapixel images. Each successive downscaling step reduces the image in both the x and y dimensions by 2 times, resulting in a quarter of the megapixels remaining. In total, each of the 9 plots were processed 18 times, for a total of 162 models. After removal of poor-quality models, 156 meshes with continuous surfaces remained for statistical analyses.

Original image sets each numbered above 2000, and the number of images used to reconstruct models varied from 81-2588 due to serial depletion. Over the two spatial extents, the photograph density varied from 2.1 – 816/m^2. Given the size of the original images (45.4 megapixels), processing was repeated at medium and low-quality dense cloud settings (Table 2.3). Using a high-quality desktop with 64GB of random-access memory (RAM), it was found that when more than ~2600 images were used to build dense clouds using medium quality settings, the computer was unable to process the data. I attempted to use high-quality settings (11.43Mpix images), however processing could not be completed with more than approximately 300 photographs, so I opted to omit this as a possibility given that most users would not currently have access to computers with this capability. Thus, I capped the data sets to a maximum of 2600 images per plot, processed on medium quality (hereafter referred to as "high resolution images"). It should be noted that those with more powerful computing systems may not see the memory footprint as a project constraint, and that those with less capable systems will need to bear these limitations in mind.

Table 2.2 | Conversion parameter between megapixel counts of original photographs and the photographs used by metashape to make reconstructions at various quality settings used for dense cloud construction. This table includes the image sizes used in this study, as well as other original image sizes for reference. Note that for this study, the two settings used to build models were medium and low since models failed to process on a desktop PC with a 64gb of RAM. *Asterisks (*) indicate settings used in this study.*

Original/Ultra high-quality resolution (Mpix)	High quality resolution (Mpix) – 1:2 scaling	Medium quality resolution (Mpix) - 1:4 scaling	Low quality resolution (Mpix) – 1:8 scaling
45.4 (this study)	11.43	2.84*	0.71*
40 (High quality DSLR)	10	2.5	0.63
30 (typical DSLR resolutions)	7.5	1.88	0.47
20 (action cameras)	5	1.25	0.31
10 (older action cameras/off the shelf digital cameras)	2.5	0.63	0.16

Model effective resolution and rugosity calculations

I assessed the effects of variation in photograph density and resolution (*i.e.* quality settings) by comparing final model effective resolution and rugosity measurements among all of the 3D reconstructions. Effective model resolution (R_{eff}; herein simply resolution) and rugosity (*Ru)*, a unified, dimensionless measure of complexity to standardise for variations in spatial extent of the models, were calculated as:

$$R_{eff} = \frac{1}{n_{faces} \div A_{3D}}$$

$$Ru = A_{3D} \div A_{2D}$$

where A is equal to area, measured in m^2. Note that it does not matter the unit used, only that these are the same for both the three- and two-dimensional measurements. For model resolution, as n_{faces} increases, the resolution of the model becomes finer (i.e. better) as the average face size decreases (Fig. 2.1). Rugosity was chosen as the complexity metric since it is ecologically informative and is the most popular measure of terrain complexity across marine ecology (Pygas et al. 2020).

Statistical analyses

All data were analysed in R version 4.0.1 (R Core Team, 2022) using the '*brms*' package to fit the models (Burkner 2017). All graphics were produced using the package *'ggplot2'* (Wickham 2016). To determine the effects of image density and resolution on the model resolution and the derived rugosity measurements, a series of Bayesian linear mixed effects models were developed. Posteriors were generated via a No-U-Turn sampling (NUTS) run for 5000 iterations (excluding the first 1000 warmup samples) from each of the three chains and a thinning rate of 5. All chains were found to be well mixed (assessed using trace and trace-rank plots) and converged on a stable posterior. DHARMa residuals revealed no goodness of fit issues or departures from assumptions of normality nor homogeneity of variance. The predictive capability of the regression models were excellent ($R^2 = 97\%$ for small and large-scale models).

Initial data exploration suggested that it was appropriate to separate the data into their respective spatial extents, thus, a total of four models were fitted to the data. The first two models tested the effect of photograph density (continuous fixed effect) on model resolution (Model 1), and on the rugosity of the resultant meshes (Model 2), of the small (1-2m^2) spatial extent plots. This process was then repeated for the large (72m^2) spatial extent plots (Model 3 & Model 4). Across all models, the two image resolution settings (medium and low dense cloud quality) were included as a fixed effect, and project ID (i.e., the physical plot) was included as a random effect (random intercepts), to encompass any of the natural variation that may occur in either model resolution or rugosity as a result of either natural variation in complexity or any untested sources of variation (e.g., small variations in flying elevation between plots). This approach also accounted for the non-independent nature of extracting data from resampled versions of the same plots. An interaction term between number of images and image resolution was included in each model to determine whether the effect of adding more photographs on the resolution and surface measurements differed, conditional on whether the quality settings were medium or low.

2.3 Results

Effects of image density and resolution on model resolution

Overall, model resolution improved (i.e. the value became smaller) with increasing image density and image resolution (Fig. 2.3A). Of the two spatial extents, the smaller, 1-2 m^2 areas were typified by much finer effective model resolutions, which was on average fourteen times finer than the large-scale plots across the whole sample. This was due to a combination of the higher image densities (at the extremes this was greater for the smaller extents compared to the larger extents by a factor of over one hundred) and the fact that these were imaged with a lower flying elevation (i.e., the camera was much closer to the benthos for the small plots). Image density and resolution were good predictors of model resolution (conditional bayes R^2=0.959), with increased image density and resolution both improving model resolution. The interaction between image density and resolution indicated that the effect of increasing image density produced a greater increase in model resolution when using lower image resolutions (i.e. low dense cloud quality setting), compared to when using higher image resolutions (Fig. 2.3B;3D). Across the entire range of photograph densities, the higher image resolution yielded an improvement in the resolution of the models by a factor of approximately three for the small-scale plots and four for the large-scale plots. Because of this, resolutions of models began to converge towards the high end of photograph densities, regardless of the input image resolution. The per-image improvement in model resolution was greater for low-resolution images (0.28mm^2 with each additional photograph per square meter) compared with high resolution images (0.09 per mm^2 for each additional photograph), highlighting the complimentary effects of the density and resolution of input images. These trends were mirrored in the small-scale plots, although model resolution improvements due to both image density and resolution were of smaller magnitude, presumably because the extremely high overlap needed to build a complete model with such a low flying elevation secured a fine model resolution, even at the lower end of image densities and resolution. Small extent models built with low resolution images, the per-photograph improvement was again greater (0.0017m^2/image) than for those built with high resolution images (0.0005m^2/image).

The finest model resolution achieved in this study was an average face size of 0.14 mm^2, achieved using image resolution of 2.5mpix, an image density of 816 images/m^2, and a flying elevation of 0.75 m (Fig. 2.3A). At the 72 m^2 spatial scale, the finest model resolution that was able to be achieved was 2.47 mm^2 (Fig. 2.4B). This resolution was obtained using an image density of 36 images/m^2 (Fig. 2.4), an image resolution of 2.5mpix and a flying elevation of 2m. Despite these extremely fine resolutions, model resolution was also relatively fine under the low-density, low image resolution scenario. At the large spatial extent, even with the fewest images (7 images/m^2) and lowest image resolution (0.63mpix), model resolution was still 34mm^2 average face size, enough to resolve fine-scale features in models. At the small spatial extent, the coarsest model resolution was still 1.4mm^2, since image overlap was still very high at 100 images/m^2.

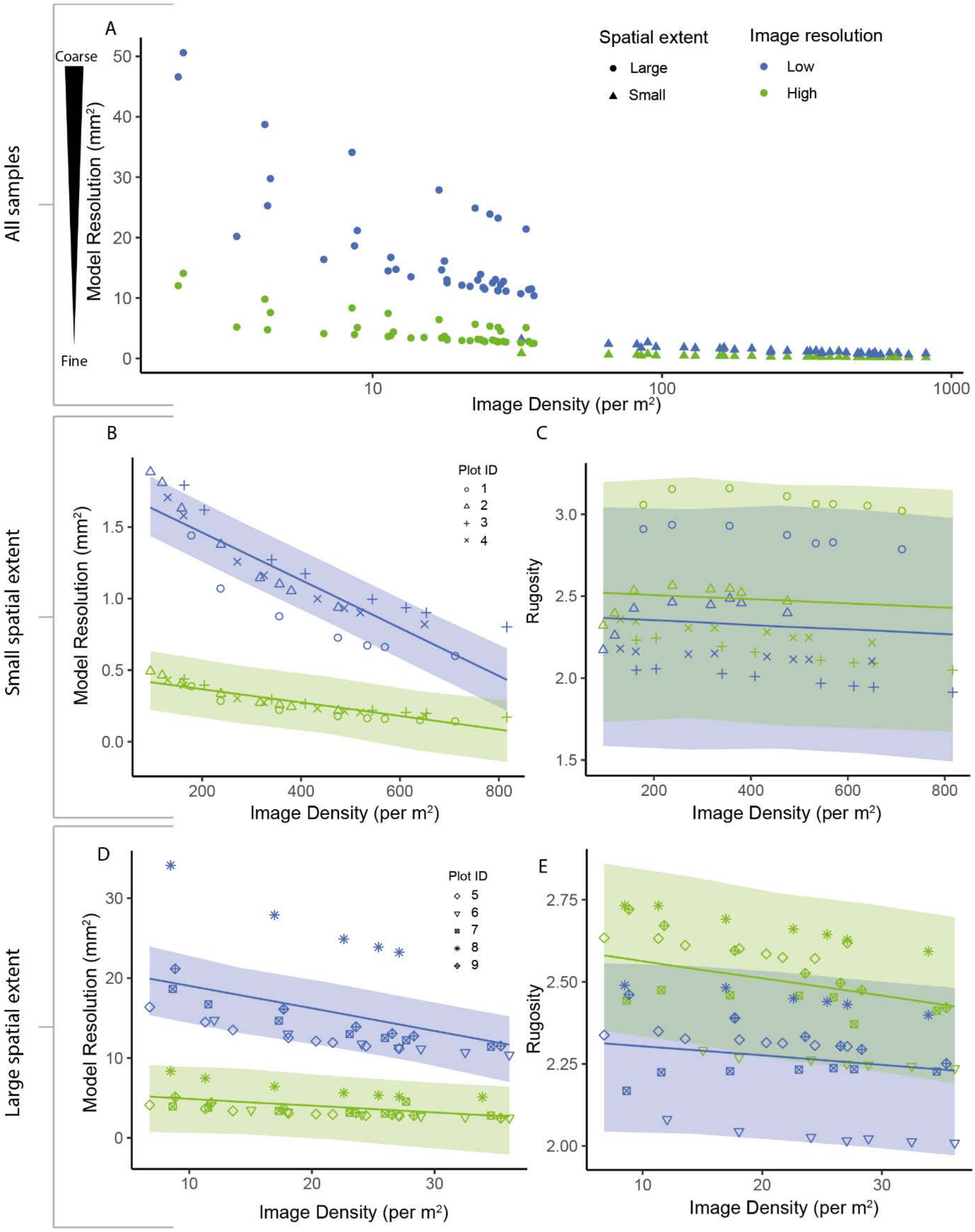

Figure 2.3 | (A) Change in 3D reconstruction effective resolution with increasing image density and quality across the entire sample. Bayesian model outputs showing the simultaneous effects of image density and quality on both model resolution and rugosity of the small (B,C) and large (D,E) spatial extent plots. Note that for graphs indicating model resolution changes, a negative slope denotes an improvement (i.e. smaller faces making up the mesh). Note also that "high" image resolution (green) indicates reconstructions processed on a medium quality setting in Agisoft Metashape.

Model completeness also varied towards the low end of image densities at both spatial scales (Fig. S2.2; S2.3), with large holes appearing in the reconstructions below a certain threshold. It was found that approximately 100 images/m^2 at the small and 5 images/m^2 at the large spatial scale were required to avoid this and generate full reconstructions with no holes. Important to note however is that equipment setups varied slightly between the two spatial extents. For the small-extent plots, a 35mm rather than a 20mm wide angle lens was used, shrinking the footprint of each image and necessitating a higher density of images to secure sufficient overlap between images.

Effects of image density and resolution on model surface measurements

Image Resolution

Regardless of the spatial scale, estimates of rugosity (which changes with differences in surface area) showed a strong positive relationship with image resolution. The difference in estimated rugosity between models using images with higher versus lower resolution remained consistent across the range of image densities examined, with near-identical regression slopes for the reconstructions, indicated by the lack of an interaction between image density and resolution in the model (Tables S2.3; S2.4; Fig. 2.3C; 3E). Regardless of the image density used in a reconstruction, rugosity was on average 6.3% higher when using higher compared with lower image resolution (i.e. medium vs low dense cloud quality). These differences were slightly larger for the large spatial-extent plots. Reconstructions using higher image resolution were on average 0.29 rugosity units higher than those built with lower image resolution (Fig. 2.3E), a consistent difference of 12.3% across the whole range of image densities.

Image Density

In contrast to image resolution, rugosity was largely insensitive to increases in image density across all plots (Fig. 2.3C;3E). For the small-scale plots, each additional photograph per square meter of benthos yielded a decrease in rugosity of 0.00015 and 0.00013 units, for models built using low and high image resolution, respectively (Fig. 2.3C, Table S2.4). Over the entire range of the image densities used (95-816 m^{-2}), the average difference in rugosity was just 0.1 units or 4.3%, despite an increase in image density of over 700 images/m^2. Large-area plots appeared to follow the same trend, though the effects of image density appeared to be slightly stronger at this spatial extent (Fig. 2.3E; Table S2.4), and the effect of photograph density was marginally different depending on the image resolution used. Over the range of image densities used, the per-image decrease in rugosity units was 0.0028 and 0.0053 for low and higher image resolutions, respectively. Over the whole range of image densities (7 - 36 images/m^2), this accounted for a reduction in rugosity measurements of 0.081 (3.5%) and 0.153 (5.8%), respectively.

Table 2.3 | Overview of the relevant model parameters leading to coarsest and finest model resolutions achieved in this study. Ground sample distance (GSD) of the images are calculated as a sample-level average at each spatial extent, and are calculated using an in-air reference.

Spatial Scale	Average flying elevation (m)	No. photos / density m^{-2} (min)	No. photos / density m^{-2} (max)	Dense cloud quality	Image resolution (mpix) / GSD (mm/pix)	Model resolution (coarsest, mm^2)	Model resolution (finest, mm^2)
Small 1-2m^2	0.5-1m	285 / 95	2073 / 816	**Medium**	2.5 / 0.35	0.49	0.14
				Low	0.63 / 0.70	1.88	0.63
Large 72m^2	1.5-2m	446 / 6.8	2588 / 36.1	**Medium**	2.5 / 1.15	8.35	2.48
				Low	0.63 / 3.04	34.11	10.38

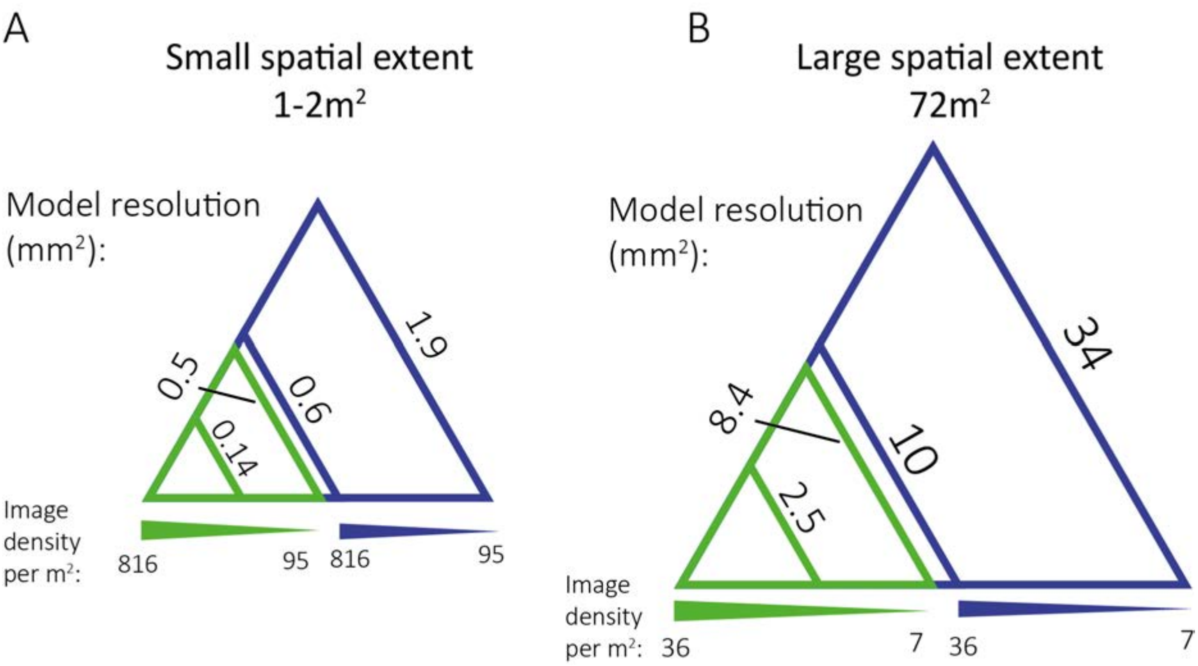

Figure 2.4 | Coarsest to finest model resolutions achieved in the small (A) and large (B) spatial extent reconstructions. The triangles represent the faces making up reconstructions. Note that the relative scaling of the triangles is correct in each panel (but not between panels). Blue triangles indicate that the models were processed using lower image resolution (0.63mpix), green indicates higher image resolution (2.5mpix). Note that the numbers on triangles represent the area of the triangle and not the lengths of the sides.

2.4 Discussion

The resolution and surface measurements of 3D reconstructions of habitats are important within the fields of spatial and landscape ecology and conservation (Graham and Nash 2013), yet the portion of their variation that is attributable to human choices during data collection and processing is rarely considered. A portion of the literature has dealt rather exhaustively with the effect of different equipment configurations, such as camera system choice (Guo et al. 2016), flat vs domed lenses and their effects in underwater environments (Menna et al. 2016a; She et al. 2022), camera orientation (Marre et al. 2019) and even the choice of software used to make reconstructions (Burns and Delparte 2017; Forsmoo et al. 2019). Most of these studies are aimed at accuracy assessment or the closeness of measurements to reality, assessed by comparing a photogrammetry estimation of dimensions to some other baseline. To the best of my knowledge, there are no published guidelines on the combined effects of image density and resolution on resulting reconstruction resolution or, importantly, derived complexity metrics for close-range photogrammetry aquatic datasets. Where model resolution is considered (Marre et al. 2019), variation in the measured surfaces of the models (i.e., rugosity) has not been considered in the literature.

Here it was shown that increasing the image density and resolution to build 3D reconstructions leads to systematically finer model resolutions, as expected (Table 3). The greatest improvements in resolution were achieved when increasing image density for lower input image resolutions. Surprisingly, these improvements in model resolution did not consistently translate to increases in rugosity, which were relatively insensitive to changes in image density. Rugosity did increase with higher image resolution, but not with higher image density. In other words, a researcher wanting to capture the finest level of rugosity should use high resolution images; but does not need to collect excessive high image densities, as the benefit of higher image density quickly dies off once enough images are collected to ensure enough image overlap to achieve model completeness.

At small spatial scales where the camera lens is close to the object of interest, it was shown that excessively high resolution and image densities yield relatively little benefit to model quality. Even when using the lowest image densities tested in this study, and lowest image resolutions, model resolution was still on the order of under 2 mm^2 average face size. Therefore, unless specific ultra-fine resolutions are required, such high-resolution images and image densities may be superfluous. For example, tracking fine-scale growth in small or highly complex morphologies of coral may benefit from high model resolution more so than when the purpose is to measure growth of larger or simpler coral morphs (e.g. Ferrari et al. 2017a; Million et al. 2021b).

Previous studies have used photogrammetry to measure temporal changes to examine the effect of disturbances and subsequent recovery on structural complexity (Burns et al. 2016; Fukunaga et al. 2022; Yuval et al. 2022). The results of this study indicate that image resolution (a product of sensor resolution and in-software quality settings), but not image density (i.e. the number of images used to make a reconstruction in a given area), represents a potential confounding factor when making temporal comparisons if the same processing protocols are not followed with each survey or if equipment changes. Others have pointed to the necessity of maintaining consistency over repeat samples in the workflow to avoid issues with repeatability (Skarlatos et al. 2018; Nocerino et al. 2020), yet even in studies that discuss methods for temporal change monitoring, image resolution is sometimes overlooked entirely (Nocerino et al. 2020; Yuval et al. 2021). The magnitude of change in rugosity (up to 20%) as a result solely of alterations of the input image resolution (which was manipulated by varying the dense cloud quality settings between low and medium in this study) underlines the importance in considering everything from camera system choice to in-software quality settings when designing their photogrammetric surveys, especially when conducting repeat surveys or comparing photogrammetric data across studies.

It was found that whilst model resolution became finer with increasing image density, this had very little effect on surface measurements in the resultant mesh, which was unexpected. The area-resolution relationship would hypothesise that as the resolution of measurement of a surface increases, so does the estimation of that surface's length or area, because more lines/faces are "packed in" to the same 2D space (Knudby and LeDrew 2007; Young et al. 2017). In this study, regardless of whether the spatial scale was on the order of 1-2 m^2 or $72m^2$, rugosity measurements remained stable over the entire range of image densities (Fig. 2.2). It is not clear why this was the case, since it is counter-intuitive that as more images were added and model resolution became progressively finer, rugosity remained largely unchanged. Thus, the benefits of excessive image densities beyond what are required to reconstruct a complete model appear to be questionable. This is encouraging for several reasons. First, it suggests that the operational methodology for photogrammetric data gathering should tend towards taking fewer photos, saving on data storage space, time in the water, and streamlining the model reconstruction process, without sacrificing any detail. Second, models that have been reconstructed using different image densities should be comparable in terms of surface measurements, if the images used were of the same resolution (with image resolution being a product of the camera's sensor size in megapixels and the in-software quality settings, whilst being modified by flying elevation).

Researchers using photogrammetry are constrained by the bounds of their camera systems (Mosbrucker et al. 2017) as well as their computer hardware and software (Marre et al. 2019). Data must be processed and used within a timely manner for research to be effective, and this task must be manageable in a relatively streamlined process for photogrammetry to remain a practical alternative to other methods of complexity assessment. Research has pointed to the importance of establishing permanent in-water networks of ground control points to properly assess accuracy of photogrammetry reconstructions (Skarlatos et al. 2018; Nocerino et al. 2020), but this is sometimes impractical. Given the need to be pragmatic, it is important to establish how much variation is a result of differences in the reconstructed surfaces versus those caused by human choices, to ensure comparisons between studies and between individual reconstructions are appropriate. The source of most variability in any photogrammetry study (terrestrial or aquatic) is likely to be a combination of the number of images collected per unit area (density), and the resolution of the images (a combination of sensor size and the quality settings used in-software). It is encouraging that surface measurements were stable regardless of the number of photographs used to make reconstructions, since this suggests as long as adequate surface coverage is achieved to make a complete model (i.e. free of holes), models made using photographs of similar resolutions are comparable and variations in surface measurements can be reasonably attributed to natural variability in complexity rather than human decision-making. Overall, it is important that researchers balance the input information depending on their spatial extent of interest, camera systems, and desired model resolutions (Fig. 2.5) to ensure that data gathering meets the needs of the ecological questions being asked, whilst keeping data collection and processing as efficient as possible.

The main limitations of this study, and indeed with photogrammetry as a tool in ecology, is the necessity to make trade-offs between spatial expanse of the reconstruction and detail that can be captured within models. The RAM (random access memory) of a computer defines the maximum data volume that can be used for a reconstruction, with additional images and increases in resolution both consuming some of this capacity. Maximising both simultaneously would be desirable, but as of now there appear to be some clear limits on what is possible, and these are calculable according to the camera and processing equipment available. In this study, even when using a desktop PC with relatively high specifications (64GB RAM), even when images were downscaled to 11.4Mpix (High quality settings), the use of more than 300 images resulted in a failure to process the large-area plots, since the volume of data was too high for the PC. Original image sets necessarily numbered several thousand, highlighting that image densities must be as low as 4 per square meter of reef to meet the Agisoft recommendation of 12Mpix images, which here led to holes within the reconstruction due to insufficient coverage (Fig. S2.3). The effects of using different image resolutions and flying elevations should therefore be the subject of further study. The optimal way of doing so would most likely be to use 3D printed objects resembling corals with known dimensions and surface areas to ascertain the extent to which different combinations of image resolutions and densities lead to measurement deviations from the real object. Whereas this study is aimed squarely at quantifying how different approaches to photogrammetry may affect comparability of results and foster good practises and reporting, the experimental approach mentioned above may be equally useful in determining exactly how well reconstructed surfaces represent real surfaces.

2.5 Conclusions

Ecologists are increasingly turning to photogrammetry to construct high quality habitat reconstructions with which ecological relationships can be described and importantly, quantified. Whilst a good portion of literature deals with the accuracy, repeatability and precision of photogrammetry (e.g., Figueira et al. 2015; Bryson et al. 2017), there are still knowledge gaps that should be filled prior to interpreting 3D reconstructions. Furthermore, the recent influx of aquatic photogrammetric datasets in marine ecology, will soon lead to the comparison of datasets, guidelines on which metrics are best suited for comparison and how to standardise them are urgently needed. This study is an important step towards fully quantifying the magnitude of user-based variation in photogrammetry reconstructions, as well as defining what the expected model resolutions might be given the practical and budgetary constraints that are often faced (Fig. 2.5). The specifics of the technological process that lead to photogrammetry-based reconstructions of submerged structures can have large effects on the dimensions of the resultant surface models. In particular, image resolution, which is affected strongly by camera system choice and in-software quality settings, can lead to substantial variation in rugosity estimates. These should always be considered as an integral part of study design since the specifics of how data is gathered and processed should be tailored with the research questions and requirements in mind. Researchers should be aware that in-software choices can have effects on the resolution of input images, which in-turn can influence the surface measurements that are used to make ecological inferences. Reporting image resolutions at the stage of processing is key to determining how comparable different 3D reconstructions may be, which is likely to become especially important in the future as more photogrammetry studies are conducted and more 3D data is published.

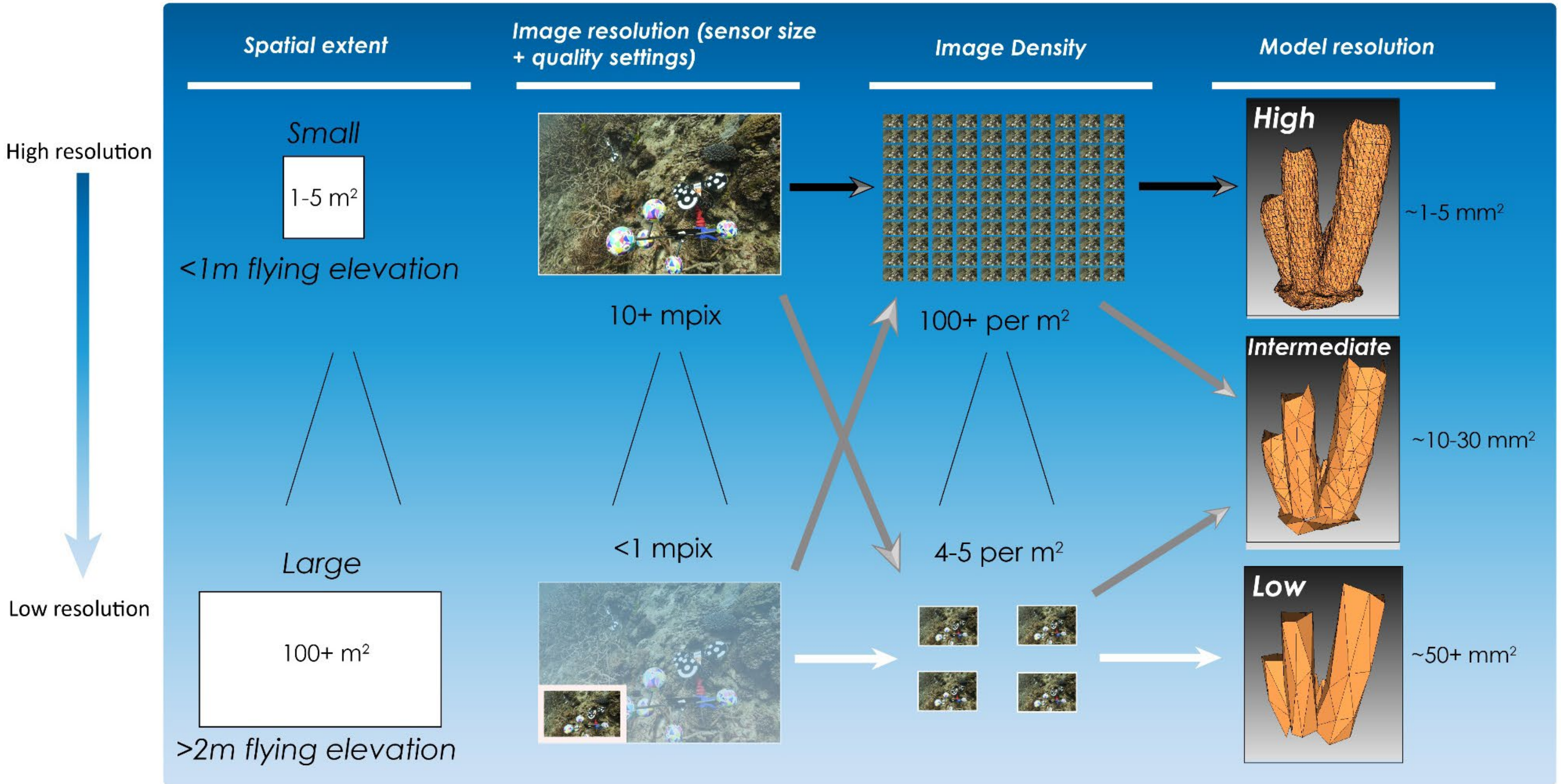

Figure 2.5| Conceptual diagram indicating processing choices that have directional effects on model resolution. Shaded arrows between stages indicate processing 'paths' that can lead to high (black), intermediate (grey) or low (white) resolution models. Note that it is not possible to achieve the highest resolutions over large spatial extents with a standard desktop computer, and that the high overlap needed for small extent models to be complete prevents low resolutions. Also note that model rugosity is not included here due to differential effects of image resolution and density.

1

Chapter 3 A protocol for extracting structural metrics from 3D reconstructions of corals

This chapter has been published as: **Aston, E.A**., Duce, S., Hoey, A.S. and Ferrari, R., 2022. A protocol for extracting structural metrics from 3D reconstructions of corals. *Frontiers in Marine Science*, *9*, p.854395.

3.1 Introduction

Structural complexity is an important component in the functioning of ecosystems, with the abundance and diversity of species generally being positively related to structural complexity of the habitat, especially at low levels of complexity (MacArthur 1958). The presence of structure creates protected environments that moderate environmental conditions and creates a wide breadth of ecological niches for animals to exploit (Bruno et al. 2003; Alvarez-Filip et al. 2011b; Tokeshi and Arakaki 2012). As the abundance and diversity of complex physical structures in an ecosystem increases, so does the ability of that ecosystem to support animals with different microhabitat needs (Willis et al. 2005). Whilst the effects of structural complexity are often confounded by differences in the taxonomic composition of habitat-forming organisms, its importance transcends any particular ecosystem and is applicable in almost every natural habitat, from terrestrial coniferous forests (Franklin and Pelt 2004) and savannahs (Gigliotti et al. 2020) to freshwater rivers (Warfe and Barmuta 2006) and coral reefs (Graham and Nash 2013).

On coral reefs, one of the world's most biodiverse ecosystems, the importance of structural complexity has long been recognised (Risk 1972; Vine 1974). The availability of complex structure provides refugia from predators (Ménard et al. 2012; Rogers et al. 2014; González-Rivero et al. 2017), reduces competition for habitat space through the formation of diverse and abundant ecological niches or microhabitats (Graham and Nash 2013) and increases the surface area available for foraging (Vine 1974). Whilst the abundance, density and spatial arrangement of habitat-providing structures are important in shaping fish communities (Pygas et al. 2020), the structural characteristics of individual coral colonies can also play an important role for many small-bodied, site-attached fishes (Quadros et al. 2019). For example, structurally complex colonies are good providers of habitat because they generally supply a large amount of physical refugia from larger bodied predators (Hixon and Beets 1993; Noonan et al. 2012). As such, fish-habitat relationships vary according to the species of coral and fish, and also change over time according to colony growth and/or erosion (Graham and Nash 2013; Ferrari et al. 2017b). The physical structure provided by individual coral colonies has been related to differences among coral species and/or growth forms (Komyakova et al. 2013; Richardson et al. 2017a; Urbina-barreto et al. 2020), among colony sizes (Noonan et al. 2012; Agudo-Adriani et al. 2016; Urbina-barreto et al. 2020), and with environmental setting (Todd 2008; Ow and Todd 2010; Doszpot et al. 2019). Despite the importance of the structural complexity of coral colonies, accurately quantifying the physical structure of individual colonies is challenging.

At the scale of individual coral colonies, technical limitations have led to simplified measurements of structural complexity, including the manual measurement of the space between colony branches (Noonan et al. 2012), measurements of colony morphometrics such as height and diameter (Harborne et al. 2011, 2012), as well as estimates of surface area from foil-wrapping or wax-dipping branches (Veal et al. 2010). However, these methods are generally imprecise, cannot be easily repeated *in situ,* and often damage the colonies (Naumann et al. 2009; Ferrari et al. 2016b). Recent advances in computer vision and processing have allowed the full dimensionality of objects to be recorded and analysed through 3D reconstructions of high-resolution imagery (i.e., close-range photogrammetry; Lavy et al. 2015, Bayley & Mogg 2020), which is becoming popular among ecologists.

Underwater close-range photogrammetry offers enormous potential to investigate the physical structure of coral colonies, however there is a need to explore and develop new, ecologically relevant metrics that can be compared among and within coral taxa. The process of analysing reconstructed objects is now readily accessible and the structure of coral colonies can be analysed in numerous ways (Figueira et al. 2015; Ferrari et al. 2016b). Several metrics offer valuable insights into the structure of colonies including 3D surface area, colony volume, and a variety of ratios, including surface area to volume ratio, and colony rugosity (a ratio of the 3D to 2D surface area) (Bythell et al. 2001a; Agudo-Adriani et al. 2016; Ferrari et al. 2016b; Doszpot et al. 2019; Zawada et al. 2019a). However, metrics that focus on the delivery of an ecological function, such as shelter provisioning, are somewhat rare (but see Madin et al. 2016, Urbina-barreto et al. 2020). Given the rapidly changing ecological composition of global reef communities due to the combined effects of climate change (Hughes et al. 2017b, 2018; Richardson et al. 2018; Dietzel et al. 2021) and local anthropogenic stressors (Cheal et al. 2017; Suchley and Alvarez-Filip 2018), metrics that reflect the ecological functions of corals are required (Madin et al. 2016; Doszpot et al. 2019; Streit et al. 2019). Progress has been made to this end recently, as ecologists are exploring the structural traits of coral colonies in more detail. Quantification of the shelter provisioning capability and size structure of available refuge spaces have been discussed in specific types of coral (Urbina-barreto et al. 2020), as well as how this metric changes over time with coral growth (Million et al. 2021). Underwater close-range photogrammetric reconstructions have also revealed complex, non-linear relationships between simple coral growth measurements, such as linear extension rates, and higher order traits, such as shelter provisioning (Million et al. 2021).

Several aspects of the process of underwater photogrammetry have been assessed to date, including the effects of various parameters such as photograph density and resolution (Marre et al. 2019), camera systems (Guo et al. 2016), lenses and housings (Menna et al. 2016b, 2016a), water turbidity (Bryson et al. 2017) and flying elevation (Marre et al. 2019). Whilst it is of critical importance to understand how models may be affected by user-decisions, comparability between studies could and should be improved by the adoption of standardised workflow procedures. Given that there exist multiple studies based on photogrammetry and deriving estimates of complexity from corals (Agudo-Adriani et al. 2016; Reichert et al. 2016; Doszpot et al. 2019; Vivian et al. 2019; Million et al. 2021), there is great incentive to adopt reproducible methods via the use of standardised workflows at key parts in the processing pipeline. This applies both to the reconstruction of coral models (Lange and Perry 2020) and the extraction of structural complexity metrics.

The aim of this study is to ensure repeatability among users by using python scripts to serially process 3D reconstructions of coral colonies and extract a suite of three-dimensional complexity metrics. Following manual isolation of colonies from the surrounding benthos in the models, I developed a second python script that automatically extracts a suite of three-dimensional structural complexity metrics from each model, saving time and increasing repeatability among users. To investigate the utility of these metrics as ecological indicators, I compared two of these key metrics among 69 colonies of varying size and morphotaxa using Bayesian linear regression models.

3.2 Methods

Data collection and classification of corals

Images of 69 colonies were collected from seven reefs on the Great Barrier Reef (GBR) and in the Coral Sea during February 2020 (GBR: Hickson, and Tiger Reefs; Coral Sea: Saumarez, Cato, Wreck, Frederick, and Marion Reefs). The imaged colonies were located at depths between 3 to 13m in sheltered, back reef environments on each reef. Colonies with partial mortality, disease or algal overgrowth were avoided, as this may have affected structural characteristics.

Given the difficulties in identifying coral colonies to species in the field, I used morphotaxa to allow relevant comparisons. Individual colonies from each of the following seven morphotaxa were haphazardly selected and imaged: corymbose *Acropora,* digitate *Acropora,* tabular *Acropora,* branching *Isopora,* branching *Pocillopora,* branching *Porites* and 'massive' corals (Fig. 3.1). Massive and submassive corals from different genera (mainly *Porites* and *Favia*) were aggregated into a single category (i.e., 'massive' corals) due to their structurally comparable morphologies and because none of the massive coral colonies imaged had overhangs contributing to their refuge space. To classify coral morphology, I followed the CATAMI scheme (Althaus et al. 2015), which includes visual guides to broad-level morphologies.

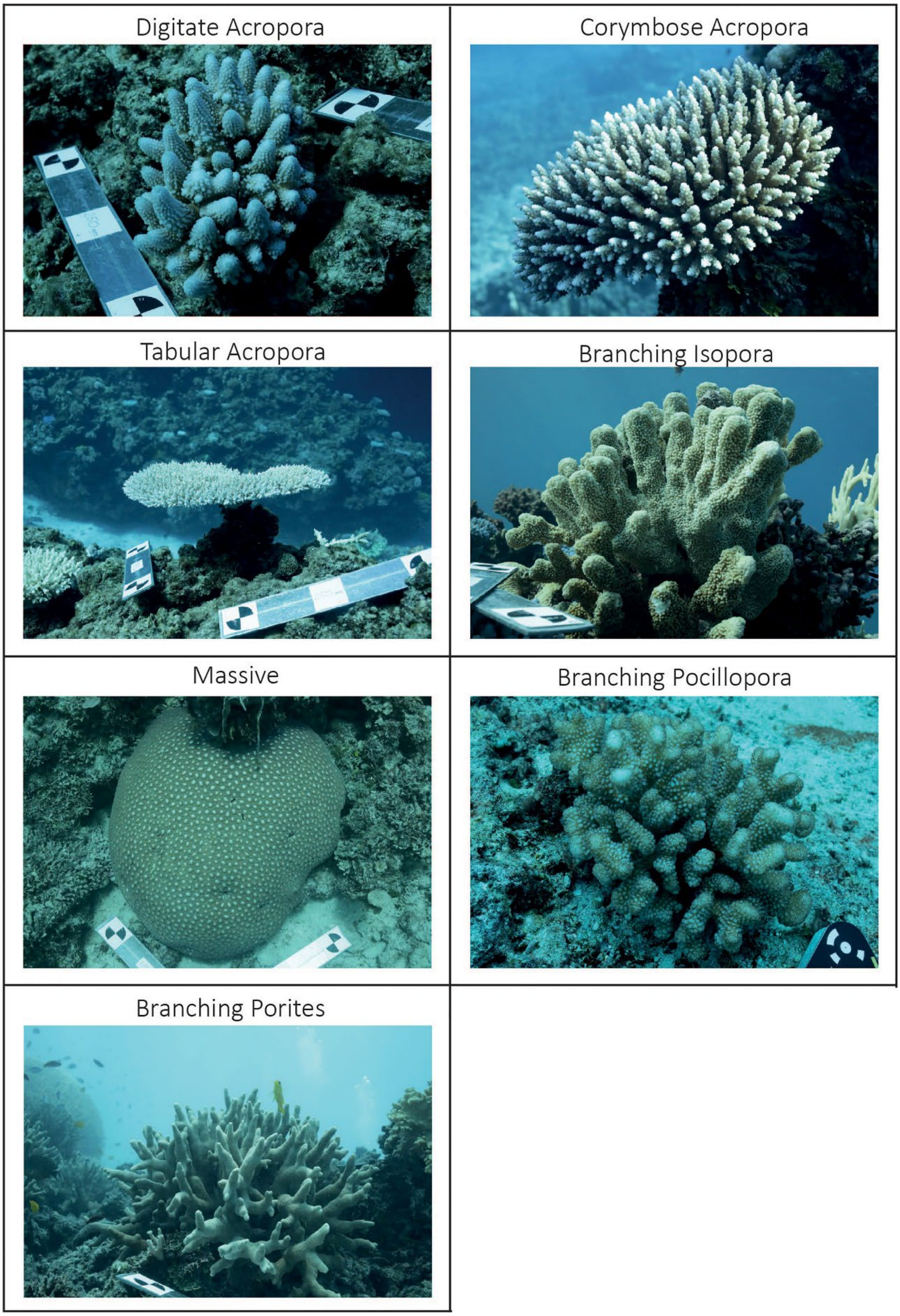

Figure 3.1| *In* situ examples of the seven distinct modelled morphotaxa. Note the galvanised scale bars present in several panels used to scale the reconstructions.

Field and laboratory equipment

Camera system choice has been shown to play an important role in the quality of the final model (Marre et al. 2019). Resultant models from different camera/computer systems can be of comparable quality, however these should always be reported since the resolution (i.e., the smallest resolvable details) can be affected. All images used in this study were taken using a Canon 5D MK IV body (Canon USA Inc.) Ikelite housing (Ikelite Underwater Systems), fitted with an 8” dry lock dome port. A Canon 35mm f/2 IS USM prime lens was used to minimise perspective distortion in photographs while a dome port was chosen to reduce barrel distortion near the edges of images (Menna et al. 2018). Each photograph was a 30.2 Megapixel JPEG image. Relevant PC system specifications were as follows: Intel Core i9 9900K 3.6GHz CPU, 64GB RAM, 1x NVIDIA GeForce RTX 2080Ti Graphics card. High resolution 3D models are possible using cheaper, more compact cameras and off-the-shelf laptops (Lange and Perry 2020). However, changes in model resolution and processing times associated with different cameras and processing settings affect surface measurements and may hinder comparisons if not given appropriate consideration. At the colony scale, flying elevation is low (i.e., the sensor is very close to the object of interest), so sufficient overlap is likely to result in comparable model qualities regardless of sensor size (see Menna et al. 2016, Marre et al. 2019 for discussions of camera systems and flying elevation).

Agisoft recommends the use of coded targets for model scaling purposes. There were mounted in pairs (12-bit, printed on waterproof paper) on to two galvanised steel bars at known measured distances apart, ready for automatic detection by the software.

Data collection protocols

The two scale bars were first placed adjacent to the coral colony prior to taking images and were included in a minimum of 20 photographs per colony. For each colony, 100-250 images (depending on colony size and morphotaxa) were taken. The goal was to collect a set of overlapping images taken from multiple angles such that the entire colony was imaged (Bythell et al. 2001a; Million et al. 2021). Observers used an orbital swimming motion – three to four 360 degree passes around the colony at different heights. Imaging for a colony generally took 3-5 minutes (based on 100-250 images plus time before for testing camera settings). It is not critical that swimming motion is identical to generate comparable data, only that the entire colony is imaged with sufficient overlap to resolve all required details in the resultant model.

Camera settings were chosen based on local light conditions, but aperture was fixed at f/10 to ensure the entire colony was in focus during imaging.

Model reconstructions and extraction of structural complexity metrics

A variety of paid and free options are available to generate structure from motion models. The choice of software has been shown to lead to differences in the measured characteristics, affecting repeatability and potentially comparability between model data from different studies (Forsmoo et al. 2019). Agisoft Metashape (formerly Photoscan) is the most popular choice of software among ecologists for generating coral reconstructions (Agisoft LLC, St. Petersburg, Russia). 3D models were constructed using Agisoft Metashape Professional Ver 1.7. Total processing time for models varied; massive morphologies with ~150 images per colony took approximately 10-20 minutes to process, whereas larger and complex colonies with image sets numbering over 200 required several hours of processing. Steps for model generation have been discussed extensively, including error reduction, photograph selection, model scaling and accuracy metrics (Green et al. 2014; Forsmoo et al. 2019; Lange and Perry 2020).

A single python script to reconstruct colonies using the same processing workflow is available (https://github.com/E-Aston/CoralGeometry). This script comes with detailed instructions and is interactive within Metashape, designed to be run from within the graphical user interface using the “Run Script” command. These instructions are also provided as supplementary material. For the use of this script, no knowledge or installation of python is required, only installation of Metashape Professional. On execution of the script, a series of dialogue boxes prompt users to input the settings to be used in serial processing of the models, including the quality threshold for the disabling of photographs, photo alignment accuracy, and dense cloud quality. The settings used to reconstruct the colonies used in this study are provided below (Table 3.1), and strongly recommend that others use the same settings when following this reconstruction protocol, since processing settings affect model resolution and thus final measured characteristics.

Following the reconstruction of models, some manual preparation is needed for metrics extraction. Given the *in-situ* nature of the data collection, some of the benthos to which corals are attached is also reconstructed and needs to be removed manually. This includes “isolating”, i.e., removing any benthos from the reconstruction using metashape such that they are ready for automatic metric extraction (Table 3.1). The only measure of colony geometry to be extracted from metashape is planar area, which is automatically calculated using a top-down view upon generation of the model report (Table 3.1; Step 9).

Table 3.1 | Beginning to end of reconstruction pipeline in Metashape. These settings were the same for each model in the dataset. Within the workflow steps, (M) refers to manual steps needed to be performed by the user, (A) refers to steps automated using the python script.

Workflow Step	Details
1. Remove low-quality images (A)	Disable photos with quality score <0.5
2. Detect markers (A)	Tolerance value is set to 30 by default
3. Align Photos (A)	High Accuracy, generic preselection, Key Point Limit: 40,000 Tie Point Limit: 4,000
4. Clean Sparse cloud and optimise cameras (A)	Three-step automatic iterative process to remove the worst tie points based on reprojection error, reconstruction uncertainty and projection accuracy. Recommended setting: 95 (removes the worst 5% of points at each step in the process).
5. Build Dense Cloud (A)	Quality: Medium Depth filtering: Mild Calculate point colours
6. Build Mesh (A)	Source data: Dense cloud Surface type: Arbitrary (3D) Face count: High Interpolation: Enabled Calculate vertex colours: Yes
7. Build Texture (A)	Mapping mode: Generic Blending mode: Mosaic Texture size/count: 4096 x 1 Enable hole filling: Yes Enable ghosting filter: yes
8. Isolate model (M)	Free-form selection tool Select and delete all faces in the model that are not part of the reconstructed colony
9. Model scaling (M)	Manually delete incorrectly detected markers. Enter distance between targets in reference pane. Update model to apply scaling
10. Object orientation (M)	Use the navigator tool to manipulate the colony to a top-down view (perpendicular to the orientation of upwards growth)

	Generate report for model with projection set to 'current view'. Planar area is found as 'coverage area' on page 2 of the .pdf which will automatically open on generation. Metric is given in m^2
11. Export object	Export each completed isolated mesh to a single folder in preparation for metrics extraction

Extraction of structural complexity metrics

Ten further metrics of the surface geometry or structural complexity were extracted from each colony, using a custom-coded python script utilising the package *pymeshlab* (Cignoni et al. 2008), which integrates with the open source 3D software MeshLab v2016.12 (Cignoni et al. 2008). This package contains the full capability of MeshLab without the need to manually obtain surface measurements for each mesh. The script 'cleans' the mesh (i.e., removes any unwanted faces that are not attached to the colony itself, which are often still present following the export of the model), then applies a series of scripts to measure and calculate several geometric complexity metrics automatically. These higher order complexity metrics were: 3D surface area, colony volume, convex hull volume (the simplest polygon that fully encloses the colony), absolute spatial refuge (a volumetric measurement of the space generated by the interstices of each colony), surface area to volume ratio, shelter size factor (fragmentation of shelter volume), proportion occupied (the ratio of the convex hull volume occupied by the colony), colony maximum diameter and colony height. A detailed summary of these metrics is presented below as well as how each is calculated (Table 3.2), in addition to a graphical representation of metrics (Fig. S3.1).

Given a set of reconstructions in the form of .obj files (the standard output from Metashape), the code returns a .csv file populated with the value of each metric for every coral, saving up to several hours of manual calculations. The use of the metrics extraction script assumes zero knowledge of python programming on the part of the user. All that is required is installation of python and the ability to run scripts from an interpreter. Detailed instructions on how to do this are provided in supplementary materials. For further analysis, we investigated a small subset of these (diameter, absolute spatial refuge and shelter size factor), however depending on the research questions, any of the described metrics are extracted and available for analysis.

Table 3.2 | Summary of metrics calculated for each colony using a combination of Metashape and MeshLab. A graphical representation of metrics is available in Fig. S3.1.

Metric name	Description	Unit	Software	Ecological reasoning / application
Colony diameter *(D)*	Length along X axis of bounding box (the longest horizontal axis) enclosing each colony	cm	Python/Meshlab	Widely used in the literature as a basic size metric. Also used to relate to higher order complexity metrics (House et al. 2018; Urbina-barreto et al. 2020)
Height *(H)*	Length along Z-axis of bounding box enclosing each colony	cm	Python/Meshlab	Identified as important for fish abundance (Harborne et al. 2011, 2012; Agudo-Adriani et al. 2016)
Planar area (A_{2D})	Total area of reef floor occupied by each colony	cm^2	Metashape	Important metric of spatial occupancy of the reef floor by each colony. Used to calculate popular metrics such as percent cover and useful for examining how different colonies fit together within a patch of reef. Also useful for growth rates (Ferrari et al. 2016b; Dornelas et al. 2017)
3D Surface area (A_{3D})	Total surface area of colony	cm^2	Python/Meshlab	Relevant metric of potential foraging area provided to corallivores (González-Rivero et al. 2017). Also related to metabolic processes in corals such as photosynthesis (Naumann et al. 2009) Also used to measure 3D growth of colonies (Ferrari et al. 2017a)
Volume *(V)*	Total volume of colony	dm^3 (litres)	Python/Meshlab	Metric related to biomass, size and carbonate production. Also used over time to infer growth rates (Lavy et al. 2015; House et al. 2018)
Convex hull volume (V_{CH})	Volume of the simplest polygon which fully encloses the coral	dm^3 (litres)	Python/MeshLab	Intermediary step for calculating other metrics related to interstitial space generated by colonies (Doszpot et al. 2019; Urbina-barreto et al. 2020).
Absolute spatial refuge *(R)*	Volume of the total amount of space generated by each coral $(R = V_{CH} - V)$	dm^3 (litres)	Python/Meshlab	Quantifies interstitial space, with potentially important links to inhabitant fish (Urbina-barreto et al. 2020). Can potentially be used over time to track coral growth in an ecologically relevant manner (Million et al. 2021). Higher values of *R* indicate more overall shelter volume. This metric is calculated by subtracting the volume of the colony itself from the volume of its enclosing convex hull, leaving a volumetric measure of the interstitial space generated by each colony.
Surface area to volume ratio	Ratio between 3D surface area of a colony to its volume $(A_{3D} \div V)$	Ratio	Python/Meshlab	Ecologically important metric of colony surface complexity that can be used to compare corals of different morphology (Doszpot et al. 2019). Higher surface area to volume ratios indicate greater surface complexity.
Shelter size factor *(S)*	Ratio of Absolute spatial refuge *(R)* to 3D	Ratio	Python/Meshlab	Quantifies the level of fragmentation of habitat space, useful for comparing the size structure of refugia among colonies of different size and morphology (Urbina-barreto et al. 2020).

	surface area *($S = R \div A_{3D}$)*			Higher values indicate comparatively more "open" structures and larger spaces due to the higher volume of shelter space relative to colony surface area.
Proportion occupied *(ProCC)*	Ratio of colony volume to convex hull volume (*PrOcc* $=V \div V_{CH}$)	Ratio	Python/Meshlab	Quantifies compactness, a particularly useful metric for branching colonies (Doszpot et al 2019). A higher proportion occupied indicates a more compact branching structure. Also referred to as convexity (Zawada et al. 2019a).

Statistical models for methods validation

To assess the validity of the calculated complexity metrics extracted using the python script I selected two of the higher order and popularly used metrics and compared them among colonies of different size and morphotaxa. I chose absolute spatial refuge and shelter size factor. Although any of the 3D metrics presented in this study may be ecologically informative depending on the research question, quantifying the shelter capacity of corals and how this shelter is delivered (i.e. the fragmentation of the shelter) is broadly applicable for ecological purposes, including measuring the functional capacity of corals to provide habitat (Urbina-barreto et al. 2020) and tracking how this changes over time with colony growth (Million et al. 2021). It was hypothesised that due to differences in the physical structure of colonies of different morphotaxa, the rate of increase in absolute spatial refuge volume with colony size would vary among morphotaxa. It was also hypothesised that the differences in physical structure would result in variation in the size-structure of spatial refuges among colonies of different size, again with parameters specific to each morphotaxa considered.

To determine whether 3D metrics of complexity (in this case spatial refuge) could be predicted by simpler linear metrics (i.e., colony diameter) I fitted two Bayesian linear regression models using the package *'brms'* (Bürkner 2017), both using colony diameter to predict the value of a 3D complexity metric. The first was absolute spatial refuge and the second was shelter size factor. For each of these models, morphotaxa was included as a predictor, so I could also infer how the scaling relationships between these variables differed among morphotaxa. Appropriately informative Gaussian priors were used to inform the model and restrict to a reasonable outcome space (Banner et al. 2020). Assumptions about the underlying data distribution and prior predictive distributions were chosen based on visual exploration of the data following transformations as well as previous studies that have used similar data in the same way (Urbina-Barreto et al. 2020). Priors for all models were assessed visually using randomly sampled lines from the prior probability distribution (Fig. S3.2). Posterior distributions were obtained using four Markov Chain Monte Carlo (MCMC), with 20,000 iterations and a warmup period of 10,000 samples. Inferences about the strength of the relationships between variables in both models were based on 95% highest density probability intervals around means predicted from the posterior distribution of the models. Analyses were carried out using R 4.0.1 (https://r-project.org). Initial data exploration of 2D and 3D variables was carried out using a scatterplot matrix on raw data generated using the '*Ggally'* package (Fig. S3.2) (Schloerke et al. 2020, https://cran.r-project.org/package=GGally). Plotting was carried out using the package *ggplot2* (Wickham 2016). Bayesian R^2 values were obtained to assess how well the regression models fitted the data in each case.

Model 1: Absolute spatial refuge (R) vs diameter (D)

Prior predictive distributions were set using the results of regression models previously fit to this data type (Urbina-Barreto et al. 2020). The present data encompassed a similar size range of colonies; the main difference was that colonies were classified based on morphotaxa, a combination of taxonomic identity (genus) and morphology, rather than just morphology. I used log colony diameter $Dlog_i$ and an indicator variable for morphotaxa (colony ID = CID) to predict log absolute spatial refuge for each colony $Rlog_i$, with the following model structure:

$$Rlog_i \sim \text{Normal}\ (\ \mu_i\ , \sigma\ )$$
$$\mu_i = \ \alpha_{CID[i]} + \ \beta_{\text{CID}[i]} Dlog_i$$
$$\alpha_{CID} = \text{Normal}\ (-9\ , 0.5\ )$$
$$\beta_{CID} = \text{Normal}\ (\ 3\ , 0.5\ )$$
$$\sigma = \text{Exponential}\ (\ 1\ )$$

I assumed a normal distribution with mean μ_i and standard deviation σ. The prior values for the intercept α was the same for each morphotaxa, as was the slope value β, reflective of Urbina-Barreto et al. (2020). An intercept of -9 on the log scale is close to 0 on the natural scale, so scientifically this prior made sense. This subverted the need to attach uninformative priors to the slope and intercept values or to rescale the data in a way that would result in a loss of information in the posterior distribution. These priors were relaxed enough to allow data to drive any differences in the posterior predictions between morphotaxa. An exponential prior with mean 1 was assigned to the standard deviation σ, given that little was known about this parameter beforehand.

This model was compared to one without the morphotaxa variable using pareto-smoothed importance sampling leave-one-out (PSIS-LOO), to determine whether splitting colonies into morphotaxa resulted in an improved fit to the data (Yao et al. 2018).

Model 2: Shelter size factor (S) vs diameter (D)

Because shelter size factor is a new metric, I used less informative priors to allow the data to drive the model fit. I used colony diameter to predict shelter size factor for each morphotaxa. The model structure was:

$$S_i \sim \text{Normal}\ (\ \mu_i\ , \sigma\ )$$
$$\mu_i = \alpha_{\text{CID}[i]} + \beta_{\text{CID}[i]} D_i$$
$$\alpha_{\text{CID}} = \text{Normal}\ (\ 0\ , 0.5\ )$$
$$\beta_{\text{CID}} = \text{Normal}\ (\ 4\ , 2\ )$$
$$\sigma = \text{Exponential}\ (\ 1\ )$$

Where S_i is the shelter size factor of each colony i, normally distributed with mean μ_i and standard deviation σ. D_i is the diameter of each colony i and this model. The morphotaxa indicator CID was the same as the previous model. Since shelter size factor is dimensionless, I did not log-transform any of the variables for this model. The same exponential prior was assigned to the standard deviation σ as in the previous regression model. To see whether morphotaxa and colony diameter were useful predictors of shelter size factor, and to check for overfitting, models with and without morphotype were compared, again using PSIS-LOO (Yao et al. 2018).

3.3 Results

Sixty-nine colonies across the seven morphotaxa (range: 4-17 colonies per morphotaxa) were used for morphometric analysis (Table 3.3). Colonies ranged in diameter from 6.8 to 97.1 cm (mean diameter: 29.6 ± 2.0cm (s.e)) though size distribution was skewed towards smaller colony sizes with 44 of the 69 colonies being < 30cm in diameter. Measurement error was very low across the dataset, with a maximum scaling error of 0.5mm across the entire sample. Most were considerably lower and fell in the range of 0.1-0.3mm scaling error.

Table 3.3 | Summary of representation and dimensions among the seven unique morphotaxa used for colony reconstructions. Note that these are summary statistics only and were not tested statistically for between-group differences.

Morphotaxa	***n***	**Mean Diameter *(D)* (cm ± se)**	**Mean Absolute spatial refuge *(R)* (dm^3 ± se)**	**Mean Shelter size factor *(S)* (± se)**
Branching *Pocillopora*	17	27.6 ± 3.2	4.923 ± 2.559	0.85 ± 0.11
Digitate *Acropora*	16	24.2 ± 2.1	2.0129 ± 0.794	0.80 ± 0.08
Corymbose *Acropora*	13	23.2 ± 3.4	1.8682 ± 0.653	0.67 ± 0.09
Tabular *Acropora*	10	32.5 ± 4.3	3.1685 ± 1.470	0.95 ± 0.16
Massive	5	32.3 ± 6.6	0.4842 ± 0.177	0.21 ± 0.06
Branching *Isopora*	4	68.0 ± 13.2	39.758 ± 15.271	3.96 ± 0.69

Branching *Porites*	4	31.4 ± 6.4	9.940 ± 5.955	2.31 ± 0.06

Shelter size factor is a ratio of the overall spatial refugia volume to the 3D surface area of the colony and is thus unitless. Units for absolute spatial refuge are given in cubic decimetres. One cubic decimetre is equivalent to one litre.

Model 1 predictions: log-Absolute spatial refuge (R) vs log-diameter (D)

The best model for predicting absolute spatial refuge included the interaction between morphotaxa and colony diameter (PSIS-LOO model weighting = 1, Bayes $R^2 = 0.95$) (Table S3.2). Most morphotaxa appeared to fall within a somewhat similar range of increasing spatial refuge with increasing colony diameter (Fig. 3.2A, 2C; Table S3.1). For most morphotaxa, posterior credible intervals were narrow and most colonies fell near the mean prediction slope (Fig. 3.2B). The linear model determined that the scaling of absolute spatial refuge with colony diameter was broadly similar among most of the morphotaxa included in this study (95% credible intervals for the posterior estimates of slope overlapped between morphotaxa in most cases, Table S3.2), but there were some differences in the scaling relationships among morphotaxa. The exception was 'massive' corals, where the increase in spatial refuge was considerably lower than the six other morphotaxa with increasing colony diameter.

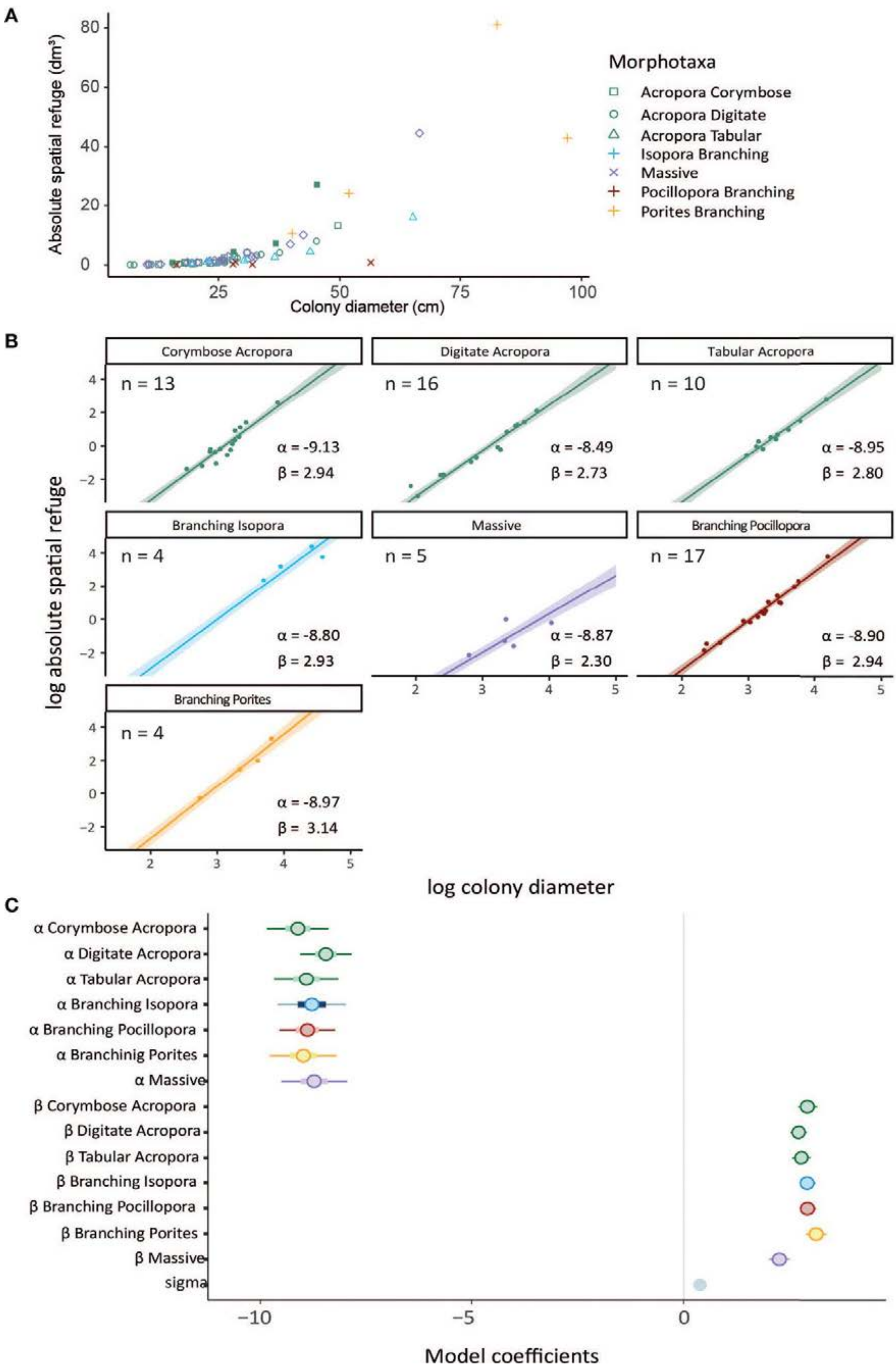

Figure 3.2| (A) Scaling of absolute spatial refuge with increasing colony diameter across all morphotaxa**.** (B) Plotted posteriors from log-log linear model of absolute spatial refuge (mean centred) from the interaction model containing colony diameter as a predictor for each of the seven coral morphotaxa as well

as intercept (α) and slope (β) estimates. Shaded regions are 95% highest density probability distribution. **(C)** Posterior predictions for intercept α and β parameters in the model. Straight line slope parameters indicate the existence of power-law relationships, with steeper slopes corresponding to higher power-scaling. Points indicate means, thick bars are 50% credible intervals, thin blue lines are 95% credible intervals. Numerical values off all model coefficients including posterior uncertainty are included in Table S3.1.

The relationships in the models indicate that there is a power-law relationship between colony diameter and spatial refuge provisioning such that as colonies grow and increase in size, the rate of increase of spatial refuge rises exponentially. Thus, subtle differences in slope gradients on the log-scale become larger when converted back to the natural scale, particularly in larger colonies (Fig. 3.2A). For example, absolute spatial refuge in digitate and corymbose *Acropora* scaled to the power of 2.73 and 2.94 respectively (maximum likelihood estimate). For a colony of diameter 25cm, the expected spatial refuge volume would be 1.34 and 1.39dm^3 (1dm^3 = 1000cm^3 or 1 litre) for digitate and corymbose *Acropora* respectively. Following the same scaling law, by the time colonies reach a diameter of 50cm, the expected values of refuge volume would be approximately 8.85dm^3 and 10.59dm^3, a difference of approximately 20%. For large colonies of diameter 75cm for example, a digitate A*cropora* colony would provide an estimated 27 dm^3 (27 litres equivalent) whilst a comparable corymbose *Acropora* colony would provide an estimated 35.5 dm^3, a comparatively large difference (36% larger). By contrast, at this large colony size, a branching *Pocillopora* colony, which was also captured well in this study, would have an expected absolute spatial refuge of 44.7dm^3, scaling at a greater rate with increasing diameter than any of the *Acropora* morphotaxa.

For 'massive' colonies, the increase in spatial refuge with increasing colony diameter was the lowest, this group consistently providing the lowest volumes of absolute spatial refuge. A colony with diameter 50cm would have an expected spatial refuge of just 1.13dm^3, or just over 1.1 litres. Whilst there was relatively little data for this morphotaxa, massive corals clearly provide the least spatial refuge among all morphologies considered in this study.

Model 2 predictions: Shelter size factor (S) vs diameter (D)

The best model was again the interaction model containing morphotaxa (PSIS-LOO model weighting = 1, Bayes R^2 =0.84) (Table S3.4). Whilst shelter size factor was predicted well by the combination of colony diameter and morphotaxa, (branching *Acropora, Pocillopora*, digitate *Acropora* and tabular *Acropora*, there were no strong differences in the rate of increase of shelter size factor with increasing colony diameter in the posterior predictive distributions (Fig. 3.4, Table S3.3), with the rate of increase estimates *(β)* overlapping in all cases. For all morphotaxa except 'Massive' corals, shelter size factor *(S)* and colony diameter *(D)* were positively correlated (Fig. 3.3). 'Massive' corals had the lowest values *of* shelter size factor across all colony sizes and a very small increase in shelter size factor with colony diameter. For branching *Isopora* and *Porites*, which respectively had high values for α and *β,* highly valid statistical inferences could not be made since the sample sizes were too low.

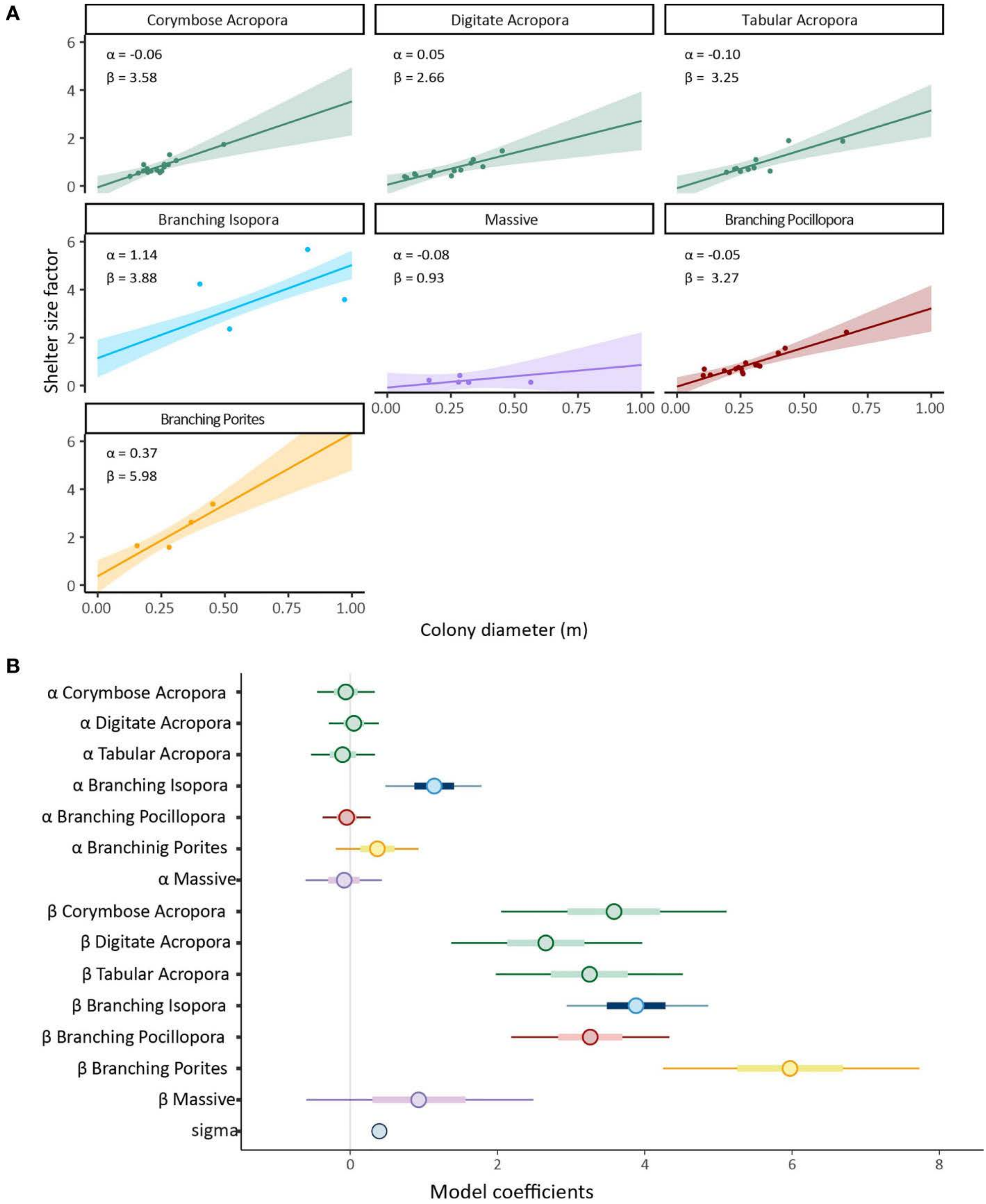

Figure 3.3 | (A) Plotted posteriors from linear model of shelter size factor from the interaction model containing colony diameter as a predictor for each of the seven morphotaxa. Shaded regions are 95% highest density probability intervals and solid lines are mean slopes of the mean from the posterior probability distribution. (B) Posterior predictions for intercept (α) and slope (β) parameters in the same model. Circles indicate means, thick blue bars are 50% credible intervals, thin blue line are 95% credible intervals. All model coefficients including posterior uncertainty are available numerically in Table S3.3.

3.4 Discussion

Metrics extraction from reconstructed 3D models

The methods developed in this study allow for the manual and automated extraction of a suite of informative structural complexity metrics from digital reconstructions of coral colonies (or other objects). Applying novel technologies to create 3D reconstructions is accessible, accurate and requires little training. Yet, there is limited guidance on how to apply these technologies for ecological studies. Much of the recent literature deals with the accuracy, precision and repeatability of the resultant models, as well as how to make the reconstructions themselves, laying a critical foundation for the broad uptake of this method (Figueira et al. 2015; Shortis 2015; Bryson et al. 2017; Raoult et al. 2017; Bayley et al. 2019; Marre et al. 2019). Ecological applications of photogrammetry, whilst rare, show that the accuracy and information-richness of resultant metrics affords more explanatory power of associated biotic communities than comparable manual methods such as chain-and-tape rugosity (Ferrari et al. 2017b; González-Rivero et al. 2017; Urbina-barreto et al. 2020; Million et al. 2021). Therefore, it is an ideal time to establish practises of transparency of processing methods as well as standardisation. These routines are designed extract metrics simply and quickly minimising manual input and decision-making on the part of the user.

Whilst I did not statistically analyse all the calculated metrics, the utility of each of these has been documented in the literature. Thus, researchers can select the most appropriate metrics for research questions from the suite provided by this code (see Table 3.3).

Establishing the ecological utility of structural metrics

The metrics presented in this study can be used to compare various aspects of reef functionality by relating aspects of the shape of colonies to their size among different categorical growth forms simultaneously. Such approaches have been shown to be effective in estimating the functional capacity of reefs at the assemblage-scale (Urbina-barreto et al. 2020), predicting higher-order traits of corals using simple morphometrics (House et al. 2018), tracking reef responses to disturbance events (Zawada et al. 2019b), and measuring functional changes associated with colony growth (Million et al. 2021).

Comparison of two metrics of refuge provisioning among the sampled colonies revealed subtle differences in spatial refuge provisioning among a range of morphotaxa (Fig. 3.3). I found that absolute spatial refuge could be predicted as a function of colony diameter and morphotaxa, despite a relatively small sample size for some coral groups. The power-law scaling relationships present among colonies are in agreement with other studies of 3D geometry at the colony scale (Dornelas et al. 2017; Urbina-barreto et al. 2020). It is promising that historical data, collected when only 2D metrics were available, may be usefully compared with modern data to document changes overtime. It also suggests that where resource and time limitations prevent the gathering and processing of comprehensive suites of 3D data, for example in small-scale community reef management or citizen science scenarios, ecologically meaningful inferences could be drawn from the measurement of colony diameter and morphotaxa alone. However, whilst there was some evidence found here for strong scaling relationships between two and three-dimensional elements of colony geometry, the dataset was relatively small, and many more colonies will be needed to solidify these relationships. Given enough data, a combination of the metrics presented here could be used as a platform to relate colony geometry not only to morphotaxa (as was the case did here) but also to environmental variables such as depth or exposure. This is arguably necessary as such variables have been shown to influence the phenotype of different coral taxa in the past (Todd 2008; Ow and Todd 2010; Doszpot et al. 2019).

Our results indicated that, contrary to Urbina-Barreto et al. (2020), tabular colonies did not provide greater volumes of spatial refuge among colonies of similar size from other morphotaxa. Further, the high surface area created by the finely branching structure of the canopy itself depresses slightly the estimate of shelter size factor. Their generation of a single, large and continuous overhanging space below the 'canopy' has been shown to be a keystone reef structure, capable of supporting high biomass of a range of sizes of fish and other biota (Kerry and Bellwood 2015). Whilst my generation of estimates for absolute spatial refuge and shelter size factor do capture in part the shaded overhang generated by tabular colonies, it is a conservative estimate of the space they generate. Depending on the growth orientation, vertical distance between the canopy and the benthos and canopy size, the refuge space generated by such morphotaxa can be considered highly variable, which should be a consideration when applying these metrics extraction routines in the future.

Future uses of structural complexity metrics

Coral reefs are undergoing substantial change due to a combination of global (Hoegh-Guldberg et al. 2007; Hughes et al. 2017a, 2017b; Williams and Graham 2019), and local stressors (Suchley and Alvarez-Filip 2018). Temperature-induced bleaching events cause differential mortality among coral taxa, with structurally complex taxa such as tabular and branching *Acropora* often being the most adversely affected (Wilson et al. 2006; Madin et al. 2014; Álvarez-Noriega et al. 2016; Hughes et al. 2019b). It is expected that as shifts in community composition occur and the relative abundance of stress-tolerant, structurally simple species such as massive and submassive corals increases, reefs may have a reduced capacity to provide shelter spaces for fishes (Karkarey et al. 2017). My hope is that others will generate data using the routines presented in this study to begin to build a repository of data containing information on many aspects of 3D colony geometry so that such contemporary questions as these can be answered effectively.

Some of the most practical future uses of the photogrammetry derived metrics presented here will be to measure colony growth and to relate aspects of their structure and size to the inhabitant fish species assemblages. Previous studies have found larger colonies support larger and more diverse fish assemblages even at these fine spatial scales, but these relationships are nuanced (Noonan et al. 2012; Agudo-Adriani et al. 2016). The use of photogrammetry scans to relate the full 3D structure of colonies to inhabitant fish is lacking (but see Agudo-Adriani et al. 2016) and establishing reliable relationships across the diverse suite of corals and fish will require large amounts of data from different study groups. Such information will be valuable to management and restoration efforts, where it is useful to know which specific combination of structural parameters leads to maximal biomass of the inhabitant fauna. Selection of coral species in restoration efforts should be tailored to include species that balance hardiness and survivorship with the ability to support fish through the provision of quality refugia (e.g. Shaish et al. 2010). There is a paucity of data across the literature on the 3D nature of growth among different colony morphotypes (but see Million et al. 2021). Reimaging the same colonies at different time points and extracting a full suite of metrics such as those in this study could provide good insights into how various elements of coral structure changes over time when paired with suitable structural complexity metrics beyond simple linear extension.

Considerations and limitations of photogrammetry-based metrics

Photogrammetry scans are, at present, the only way to obtain estimates of surface measurements of corals and the volume of generated habitat refuge at sub-centimetric resolution without disturbing/killing colonies. I was not able to compare underwater scans to control references due to the *in-situ* nature of this study, and thus could not empirically validate the accuracy of the surface measurements. However, studies validating the method using laser and/or computerised tomography (CT) scans of dead coral skeletons have found highly realistic representations (>90% similarity to laser scans) can be obtained even when scanning complex branching corals (McKinnon et al. 2011).

Most of the colonies in this study were <50cm maximum diameter, which does not capture the full range of sizes able to be obtained by all the included morphotaxa, so more data is needed these larger sized colonies. However, the larger reconstructed colonies (~1m diameter) that had associated photosets of >250 photographs were still well modelled in a few hours. The main constraint on the reliability of estimates of the generated in this study is the likely to be the complexity of the branching structures of complex colony shapes (Figueira et al. 2015). Photogrammetry scans are unable to model what is not seen by the camera lens, so occlusions caused by excessively complex/fine branching structures lead to incorrect representations of the 3D structure. The addition of more photographs overcomes this to an extent as excessive overlap between photographs leads to more detail in the surfaces of models, but as colonies become larger and more structurally complex, the model representations are susceptible to a reduction in accuracy (Bythell et al. 2001b; Figueira et al. 2015; Zawada et al. 2019a).

3.5 Conclusions

Photogrammetry is a suitable tool for assessing structural complexity at the colony scale. It is shown here the information richness and wide utility of photogrammetry by extracting 11 metrics of surface geometry and structural complexity using a single method. The semi-automated workflow presented in this study provides both new and experienced photogrammetry users with a tool to reconstruct corals at the colony scale, then extract an extensive suite of 3D structural complexity metrics. By automating processing at key steps, I aim to facilitate replicability and thus comparisons between studies, boosting the predictive power of statistical models over time and building a repository of shareable 3D data. As more studies incorporate such routines into their 3D processing workflow, the potential to uncover the nature of how structure relates to function among coral morphotaxa to aid ecological interpretation is immense.

Chapter 4 Consistent spatial patterns in structural complexity with wave exposure across the Great Barrier Reef and Torres Strait

4.1 Introduction

The importance of structural complexity in influencing the composition and functioning of ecosystems is well-established. Complex structures provide refugia from predation (Rogers et al. 2014; González-Rivero et al. 2017; Gigliotti et al. 2021), increase the diversity of microhabitats available (MacArthur 1958; Agudo-Adriani et al. 2016), increase surface area for foraging (Oakley-Cogan et al. 2020), and reduce environmental conditions such as excessive irradiance and water flow to tolerable levels for some organisms (Bruno et al. 2003). In both terrestrial and marine ecosystems, structural complexity is interlinked with biodiversity and density of associated animals (Franklin and Pelt 2004; Chong-Seng et al. 2012; Ferrari et al. 2017b; Gigliotti et al. 2020). It is also generally accepted that complex ecosystems provide more goods and services in comparison with structurally simple ones (Alvarez-Filip et al. 2009; Pittman et al. 2010; Magel et al. 2019). However, it is increasingly recognised that different components of habitat complexity influence biota in different directions, with complexity not ubiquitously benefitting all species simultaneously (Harborne et al. 2012). The ongoing loss of complexity in both terrestrial and marine systems is increasingly recognised as a major driver of declines in the abundance and richness of ecological communities (Graham 2004; Mortelliti et al. 2010; Wearn et al. 2012; Chase et al. 2020). This is particularly evident in ecosystems built by biotic habitat engineers that are being reduced by climate change and/or anthropogenic stressors, such as coral reefs (Pratchett et al. 2014). Indeed, coral reefs are one of the world's most threatened ecosystems. The effects of climate change are being compounded by local anthropogenic stressors, leading to reductions in the cover of live corals (Hughes et al. 2017b, 2018, 2019b; Magel et al. 2019) and the flattening of reef habitats (Alvarez-Filip et al. 2009; Hughes et al. 2017b).

Corals are the foundational species of coral reefs and through their structural complexity, provide both refuge and a food source for a multitude of different fish and invertebrate species (Wild et al. 2011; Emslie et al. 2014; Ferrari et al. 2017b; González-Rivero et al. 2017; Eggertsen et al. 2020). As reef complexity increases, so does the availability and diversity of refugia and microhabitats, often resulting in a positive correlation with fish biodiversity and abundance (Harborne et al. 2011; Graham and Nash 2013). Structural complexity has also been suggested to aid recovery of coral populations through the provision of microhabitats that enhance the settlement and survival of coral larvae (Yanovski and Abelson 2019). Given the importance of structural complexity in shaping other elements of the reef communities (Ferrari et al. 2016a), understanding how it varies across a range of spatial scales is a priority (Graham and Nash 2013). Whilst gradients of change in taxonomic composition and coral cover between coastal and outer-shelf environments (Jupiter et al. 2008) driven by changes in incoming wave-energy and water clarity have been documented (Emslie et al. 2010), such metrics of reef health/productivity do not always correlate reliably with indices of structural complexity (Harborne et al. 2012). For example, it has been shown that corals themselves exhibit little plasticity in morphology in response to cross-shelf gradients in wave energy across the central Great Barrier Reef (Doszpot et al. 2019).

Disturbance events such as cyclones (Adam et al. 2014), coral bleaching (Graham et al. 2006; Wilson et al. 2006; Hoogenboom et al. 2017) and crown-of-thorns starfish outbreaks (Feary et al. 2007) can also markedly impact structural complexity on coral reefs over varying timescales and spatial extents. Disturbance intensity and response differs among locations within the Great Barrier Reef (Hughes et al. 2018) and disturbance histories across these locations are not ubiquitous (Hughes et al. 2019b). With bleaching events increasing in frequency and intensity over the past decade more than at any other time in recent years, coral communities are becoming increasingly reflective of their disturbance history (Hughes et al. 2019b; Dietzel et al. 2021), with "mediocre" reefs becoming increasingly numerous (Mumby 2017). Currently, there is little understanding of spatial gradients in structural complexity at local and regional spatial scales that may exist because of gradients in environmental drivers.

Historically, comparisons of complexity over space or time have been hindered by simplistic methods, which were time-consuming and only quantified certain aspects of complexity (Storlazzi et al. 2016; Bayley et al. 2019). The methods available to measure complexity have begun to change in recent years as highly accurate and precise digital technologies such as structure-from-motion photogrammetry have increased in popularity (D'Urban Jackson et al. 2020). This technique enables the measurement of structure across a larger spatial footprint than is possible using traditional 'chain-and-tape' measurements such that benthic communities can be described in far greater detail as continuous layers (Figueira et al. 2015; Raoult et al. 2017; George et al. 2021). More nuanced aspects of complexity that deal with the scale of different features that contribute to the overall 3D surface of areas of reef mean that, in addition to simply measuring overall complexity, the relative size, density and spatial arrangement of complexity-generating elements can also be sufficiently quantified (Tokeshi and Arakaki 2012; Reichert et al. 2017; Yuval et al. 2023). However, few studies have attempted to compare the 3D complexity of reef habitats over large spatial scales (Alvarez-Filip et al. 2011a; Ferrari et al. 2018).

To adequately manage reef ecosystems through periods of unavoidable change, it is important to understand the nature of variation in structural complexity over multiple spatial scales (from intra-reef to inter-regional). Therefore, the aim of this study is to quantify how structural complexity of reefs vary across multiple habitats, depths, reefs and regions within the Great Barrier Reef and Torres Strait, Australia. I used an unprecedented dataset of high-resolution photogrammetry to compare structural complexity within and between reef habitats at 330 plots from 12 reefs spanning 1500 km of latitude along the Great Barrier Reef and Torres Strait to provide insights into the dominant mechanisms which might contribute to determining complexity. It was hypothesised that structural complexity would be influenced by cross-shelf position and latitude, reflective of potential differences in environmental conditions (Burn et al. 2018; Doszpot et al. 2019) and the marked impact this has on benthic biota (Doszpot et al. 2019). Secondly, it was hypothesised that there would be predictable gradients in structural complexity among different habitats within individual reefs, with more exposed habitats being less structurally complex than sheltered habitats due to phenotypic plasticity of coral communities (Doszpot et al. 2019) and lower coral cover caused by wave action (Storlazzi et al. 2005; Williams et al. 2013). Finally, it was predicted that there would be depth-gradients in structural complexity caused by changes in coral species and/or morphological composition (Roberts et al. 2015), which would be expected to result in peak complexity values at shallower depths (Hall and Kingsford 2021).

4.2 Methods

Study sites

Twelve reefs spanning 1500km of latitudinal change across the Great Barrier Reef and Torres Strait Islands were selected, representing both inshore and offshore locations across Northern, Central and Southern sectors (Fig. 4.1). On most reefs, four sites were sampled that represented one of four habitats that differed in exposure to incident wave energy: exposed reef slope, moderately exposed slope, sheltered slope, and lagoons. On several of the larger reefs, additional sites across several habitats were established as extra replicates. Each site consisted of four 12x6m plots, thus containing a total reef area of 288m^2. Adjacent plots were separated by at least 10 metres. These plots were in 4-6 m of water depth. Six reefs (Heron Island, Davies Reef, Moore Reef, Orpheus Island, Lizard Island and Masig) contained additional deep (13-15m) sites adjacent to the shallow plots in some habitats. Although the goal was to sample all habitats across all reefs, site conditions/access and reef architecture were not always amenable to the desired sample design, so some habitats were not sampled at every reef. Low coral cover in the Keppel Islands region necessitated that at some locations, only one to two of the four habitat types could be sampled adequately. The entire data set consisted of 352 total possible plots across 88 sites. However, poor image, and therefore reconstruction, quality meant that the final dataset used for this study consisted of 330 plots in total (detailed in Table S4.1). Data were collected between January and October 2021 depending on location. During this time, no significant bleaching events occurred. Coral health was surveyed in pilot trips prior to commencement of this study and condition of benthic communities were referenced against this baseline throughout the study period to determine whether disturbances had occurred and may affect results.

Habitat classification

Habitats were classified according to exposure to incoming wave energy. First, each reef slope site was placed into categories based on aspect relative to the prominent direction of incident wave energy: sheltered, moderately exposed and exposed. Two experienced coral reef ecologists independently assessed the benthic communities at each site as being typical of that location (i.e., exposed vs. sheltered reef slopes). The exposure categorisations were validated based on the modelled upper 95th percentile of incoming significant wave height using a fetch-based model (Callaghan et al. 2015), to ensure that the initial assessments were consistent with the expected wave energy gradients among sites at that reef. I chose to use categories consistent with ranges of wave energies rather than the modelled values because modelled wave data has important limitations regarding spatial resolution and accuracy at small scales. I classified the two depths as shallow (target depth 5m) and deep (target depth 13m). Within-plot depth ranges due to horizontal undulations and vertical slopes were mostly within 1m either side of the target depth; hence, the target depths approximately equate to average plot depths. The deep and shallow reef slope sites were orthogonal in design to compare structural complexity in directly perpendicular sites, and this depth gradient has been shown to reflect different communities (DeVantier et al. 2006; Jankowski et al. 2015).

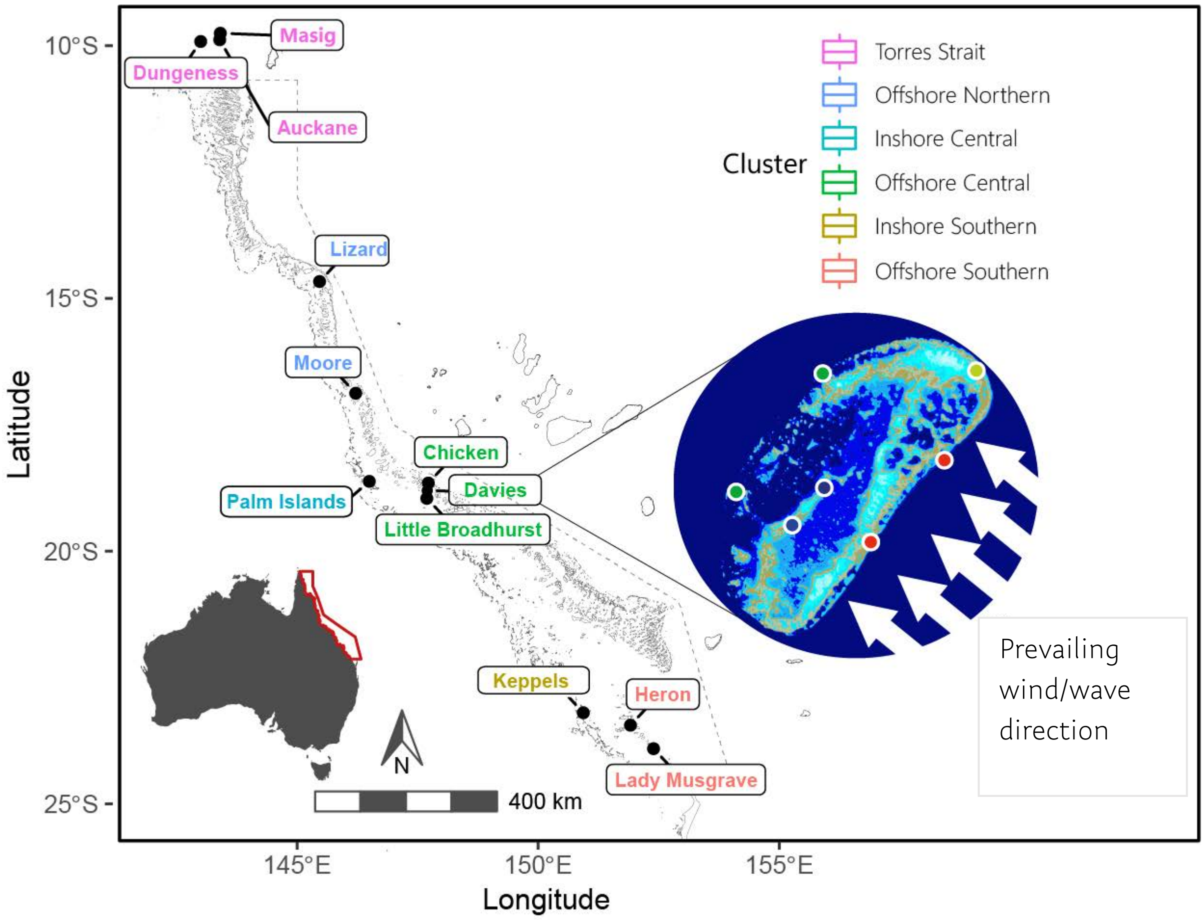

Figure 4.1| Map of the Queensland coast, eastern Australia, showing the location of the twelve study reefs. Note that the Keppel Islands cluster (yellow) was comprised of five separate reefs (Miall, Middle, Halfway, Great Keppel and North Keppel), each with a single site, due to low coral cover in exposed and moderately exposed reef slopes. (Inset) Example of study design at Davies Reef reflective of prevailing incoming wave energy exposure: Exposed slope (red dots), moderately exposed slope (yellow dot), sheltered slope (green dots) and lagoon (blue dots) sites.

Data collection

Each of the 330 permanent plots across the 12 reefs were imaged in 2021 using high-quality DSLR camera systems (Nikon D850) paired with underwater housings (Nauticam) to obtain the highest possible quality reconstructions. A pair of cameras were mounted to an aluminium frame, with the cameras separated by 57cm. Each camera was controlled independently and thus differed from a true stereo system, but this approach allowed for a larger image footprint than using a single camera, and reduced the time required to image a larger area underwater. The imaging swim pattern used followed that of most aerial photogrammetry surveys, consisting of several passes over the area of interest with the camera systems facing directly downwards, i.e., nadiral imagery (Fig. 4.2). Oblique imagery was also captured to achieve a final model mesh that captured the 3D characteristics of the area of interest as well as to significantly reduce model deformations (Nocerino et al. 2020). Divers swam five passes along both the X (long axes) and Y (short axes) axes of the permanent plots. Nadiral imagery was captured on X axes passes, and oblique imagery on Y axes passes. Since distortion tends to occur on the outer edges of models, a buffer area was captured around the permanent plots to ensure that the modelled area of interest was of high quality.

Two kinds of photogrammetry reference markers were used for model scaling and orientation: 'dumbbells' (X-Y scales) and 'triads' (X-Y-Z scales) (Fig. 4.S1). The second marker types were each fitted with spirit levels, to ensure correct orientation of the equipment in-water, to ensure that the reconstructions could later be oriented correctly. Both kinds of reference markers consisted of computer-detectable targets mounted on aluminium shapes of known dimensions. Plots contained five dumbbell markers placed across the depth range and one triad marker, level to 'real-world-up' using an X-Y bubble-level secured to its base. Reference markers were imaged during photogrammetry imaging passes of the area of interest. Depth measurements of all markers were also recorded using digital dive computers (accuracy ±0.2m), and data incorporated into the model processing workflow to scale and orient models in Agisoft Metashape Pro v1.7.2 (Agisoft LLC, St. Petersburg, Russia).

Image processing

Reconstructions of plots were built using Agisoft Metashape Professional v1.7.2 (Agisoft LLC, St. Petersburg, Russia). Processing instructions were delivered via a series of custom-coded python scripts taking advantage of the network processing feature in Metashape, which allows for the distribution of the computing workload across several 'nodes', increasing the scope of the software to deal with excessively large sets of high-quality images to achieve the highest possible model resolution. Details of processing settings and intermediary optimisation steps are presented (Table S1). I aimed to have a target number of 2000±200 images used in each reconstruction to avoid introducing any confounds, since the addition of more images leads to a higher resolution reconstruction with more faces and could affect surface measurements artificially (see **chapter 2**). Images were processed using medium quality settings, which downscales the images by a factor of four on each side. Most of the processing of images was conducted automatically, but experienced Metashape users reviewed several key model components during the reconstruction process, including reprojection error, number of photographs, marker projection error and scale bar error. Processing for each 72m^2 plot took approximately 4-6 hours depending on network load and reconstruction complexity, including the time taken to load the data and manual quality checks during reconstructions (processing times were also determined by computer hardware).

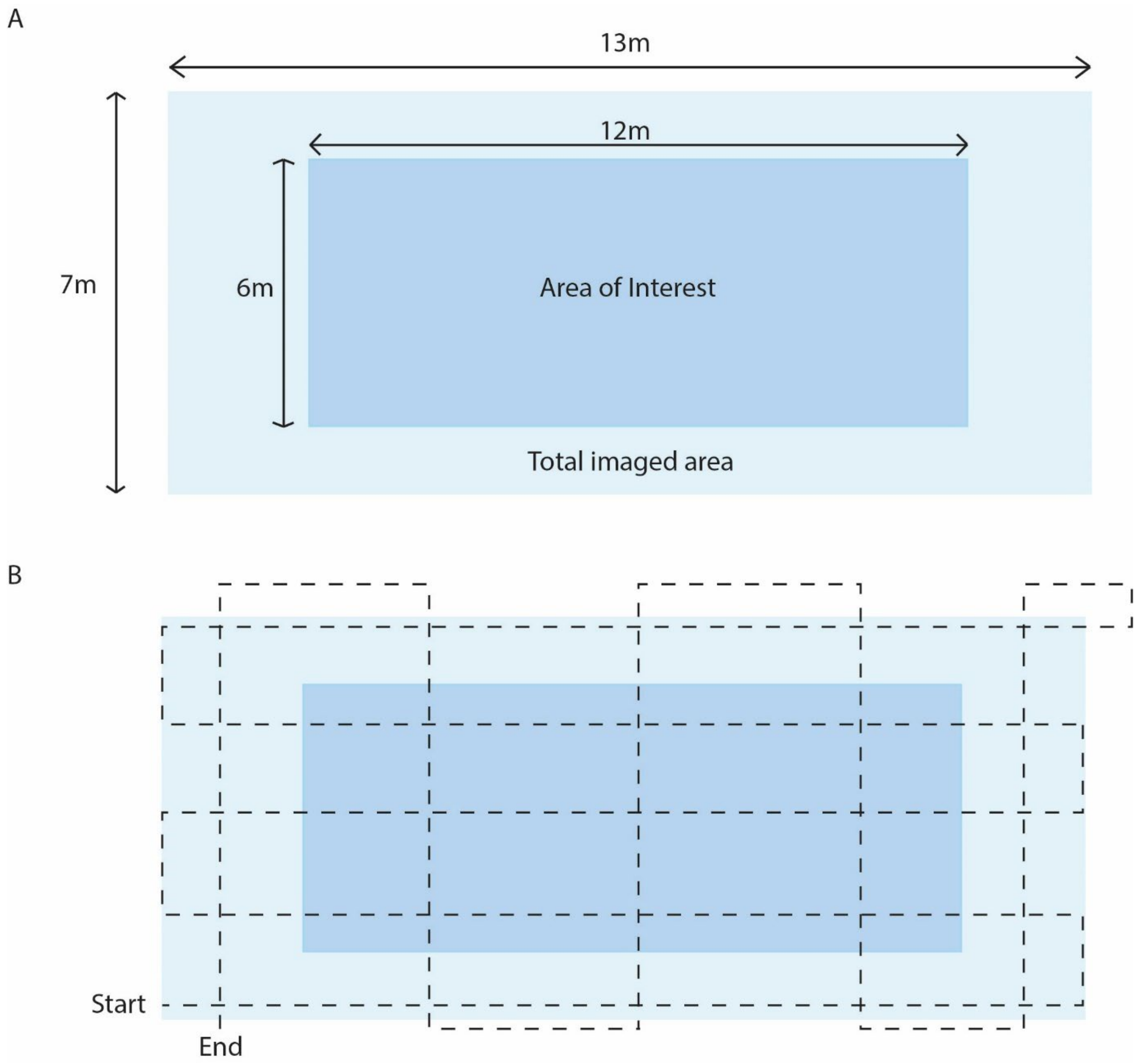

Figure 4.2| (A) Area of interest and total area of benthos imaged by divers during photo acquisition. (B) Swimming pattern of divers used during data capture, showing the five longways and five sideways passes of the total imaged area.

Extraction of structural complexity metrics from reconstructions

A custom-coded windows command-line tool was used to extract complexity metrics (i.e., rugosity and fractal dimension) from each of the 330 meshes. A tessellating series of 1x1m virtual quadrats was placed over each mesh and each metric was calculated in each of these before being aggregated up to the level of the entire mesh (i.e., averaged over all virtual quadrats). As a quality control procedure, quadrats with less than 50% of their 2D area occupied by contiguous mesh surface were excluded from analysis. A plane of best fit was also fitted to each plot to control for the effects of slope. Rugosity and fractal dimension were calculated with respect to this plane for each plot. Both of these metrics have been shown to be information-rich metrics that can be related to aspects of reef-associated fish communities and are useful descriptors of variation in the complexity and shape of objects in aquatic systems (Wilding et al. 2007; Tokeshi and Arakaki 2012; Torres-Pulliza et al. 2020). Rugosity is a relatively simple calculation of a surface's 3D surface area divided by its 2D planar area, whereas fractal dimension (or fractality) is a measure of how much complexity (in this case rugosity) is lost as meshes are successively smoothed to lower resolutions. Conceptually, fine-scale features such as those associated with complex corals are typically considered highly fractal surface features in this context (Fig. 4.3), since they are associated with an increase in rugosity but are quickly smoothed over if model resolution is reduced.

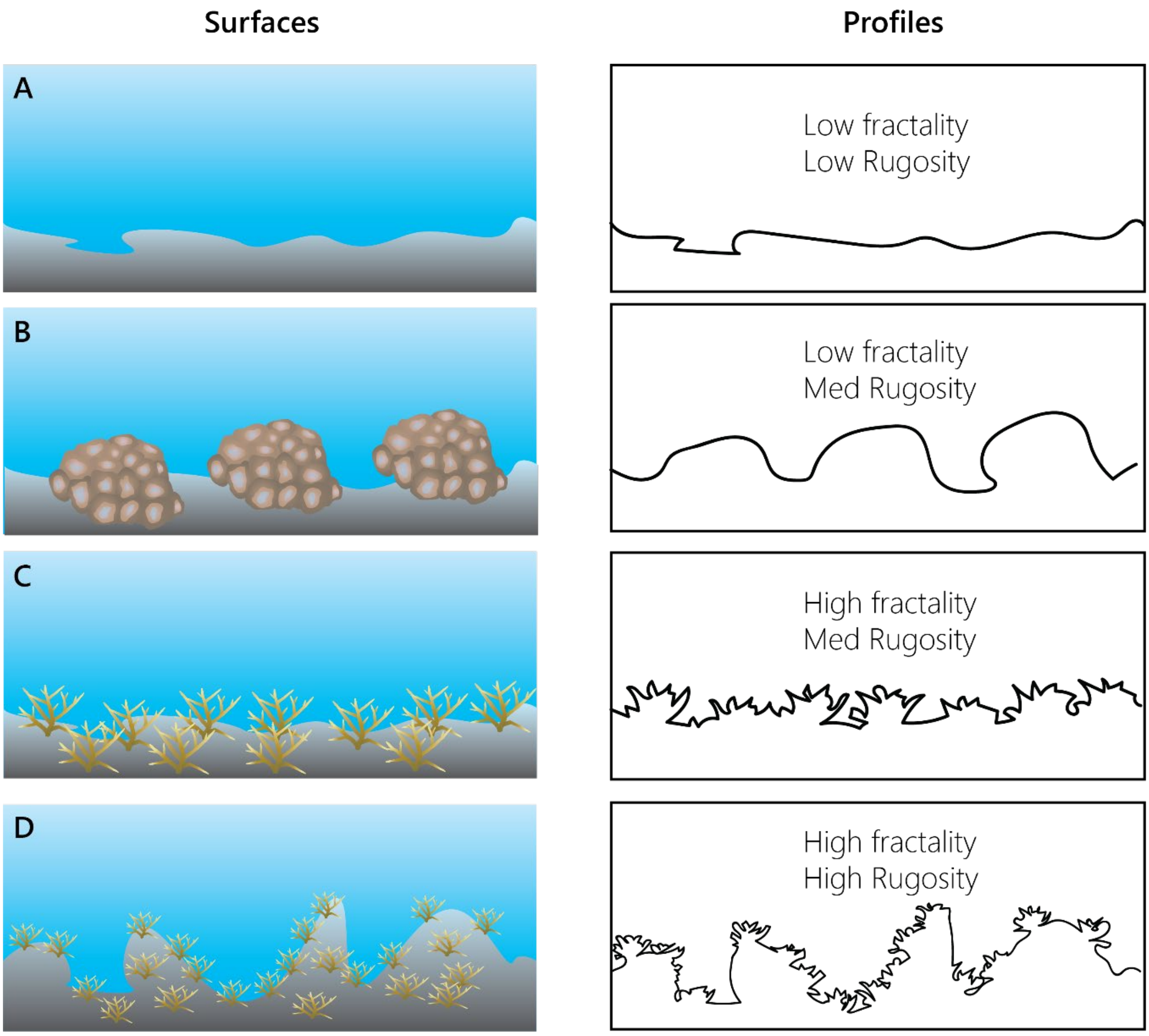

Figure 4.3| Increasing surface rugosity and surface fractality because of the inclusion of features of different size. The inclusion of large and relatively smooth features leads to higher rugosity but does not increase fractality much, since these features are well-preserved as the mesh is smoothed to a lower resolution. The

inclusion of both small, fine scale features as well as large features simultaneously increase rugosity (i.e., 3D surface area) whilst also increasing fractality.

To calculate fractal dimension, I used the variation method (Dubuc et al. 1987). The first step was a serial reduction in mesh resolution such that small faces were effectively joined together, smoothing out features of a progressively larger size, starting with the smallest. The native resolution of the mesh (~0.5 cm) was used as the first step, then 1 cm, 5 cm, 10 cm, 15 cm, 30 cm, 50 cm and 1 m. or nearly two orders of magnitude. Rugosity was calculated at each of these resolutions; since features were further smoothed at each step, rugosity always decreased as the model resolution became coarser. Surface fractality was defined by the slope of the line of the logged values of rugosity against the logged values of resolutions used, as per the equation:

$$S = \frac{\sum xy - \frac{\sum x - \sum y}{n}}{\sum x^2 - \frac{(\sum x)^2}{n}}$$

Where S is the slope of the line, n is the number of resolutions used, and x is the logged metric (in this case rugosity), and y is the logged set of resolutions. Fractal dimension D was calculated following Dubuc et al. (1987) as:

$$D = 2 - S$$

Therefore, my calculated value of fractal dimension for each case was a numerical descriptor of the loss in rugosity caused by serially depleting the meshes from their input resolution (5 mm^2 average face size) five times down to a low resolution of 1 m^2. Since the slope of the line is bound by a lower limit of 0, the value of D has a lower limit of 2, and higher values of D indicate a steeper slope, and a greater loss in complexity at successively depleted mesh resolutions. Comparatively therefore, plots with higher fractality are likely to be typified by an overabundance of small-scale features that are quickly smoothed out as mesh resolution is depleted. Where the complexity generating elements in a scene are of larger size, rugosity will be maintained as resolutions are depleted, resulting in a shallower slope and a lower value of fractal dimension. Whilst natural surfaces are not perfectly fractal and the complexity is not reduced by an identical amount with each resolution depletion, this method provides a simple means of determining the degree to which complexity in a reconstruction is generated by fine versus large-scale complexity. The inherent difficulties with calculating fractal dimension of natural surfaces accurately has been discussed (Loke and Chisholm 2022), and these are not discounted. I minimised the sources of error as much as possible by using high resolution models of large areas and choosing resolution ranges spanning two orders of magnitude for this reason.

Statistical analyses

All statistical analyses were conducted using the programming environment R ver. 4.1.0 (https://www.r-project.org). To provide insights into the dominant environmental drivers which might contribute to complexity, statistical analyses were structured around two response variables; rugosity and fractal dimension. A total of six generalised linear mixed effects models (GLMM) models were fitted to the data to assess differences in complexity with a variety of potential environmental drivers (habitat zone, depth, and geographic region) (Table S4.2). In line with the hypotheses that structural complexity would be influences by local and regional environmental drivers, these were used to investigate differences in plane-fitted three-dimensional rugosity and fractal dimension among different regions, shelf locations, habitats, and depths, each of which was a predictor variable in the fitted models. GLMMs account for the nested sampling design (plots nested within habitats at two depths across different reefs) (Bolker et al. 2009). Both fixed and random effects structures of each model were determined using comparisons of Akaike's information criterion (AIC) values of respective models to find which model was the most parsimonious (Yu and Yau 2012). The two response variables in the models (rugosity and fractal dimension) were modelled using gaussian data distributions. Each model was run with both rugosity and fractal dimension as the response variable to simultaneously test for differences in overall structural complexity as well as the extent to which the complexity within each plot was generated by fine-scale features.

Since not all sampling locations included adjacent deep and shallow sites, only data from shallow sites were used when testing for differences between regions and between habitats (12 reefs, 40 sites, 231 plots). When testing directly for differences between depths, depth was included as a fixed effect and a subset of the data including only the reefs with paired deep and shallow sites was used (6 reefs, 18 sites, 196 plots). Models were fit with the package *'glmmTMB'* (Brooks et al. 2017) using restricted maximum likelihood estimation (REML) and assessed using simulated DHARMa residuals (package: *'DHARMa'*(Hartig 2022)) to check for outliers as well as deviations from a normal distribution and homogeneity of variance (Nimon 2012). Tukey's post-hoc tests were used to investigate pairwise differences in the fixed effects for all models using all effects simultaneously, coming at a cost of statistical power but reducing the chance of a type-1 error (Ruxton and Beauchamp

2008). Planned-comparisons tests were used to inspect differences between offshore and inshore locations with shared latitudes (southern and central sectors).

4.3 Results

The rugosity of individual plots varied from 1.7 to 8.9, corresponding to an almost five-fold difference in the three-dimensional surface area present in the 72m^2 planar area of the plots. Variability in rugosity in the same habitats often exceeded the between-habitat variation in complexity within an individual reef. Notably, sheltered slopes (SS) were the most variable in terms of complexity (Fig. 4.4). Generally, habitat structural complexity (both rugosity and fractal dimension) was explained best by finer-scale (i.e., habitat zone) than broader-scale environmental variables (i.e., geographic region/shelf position). Rugosity was particularly strongly driven by both habitat zone and depth, whilst fractal dimension varied significantly with depth, but not strongly with habitat zone.

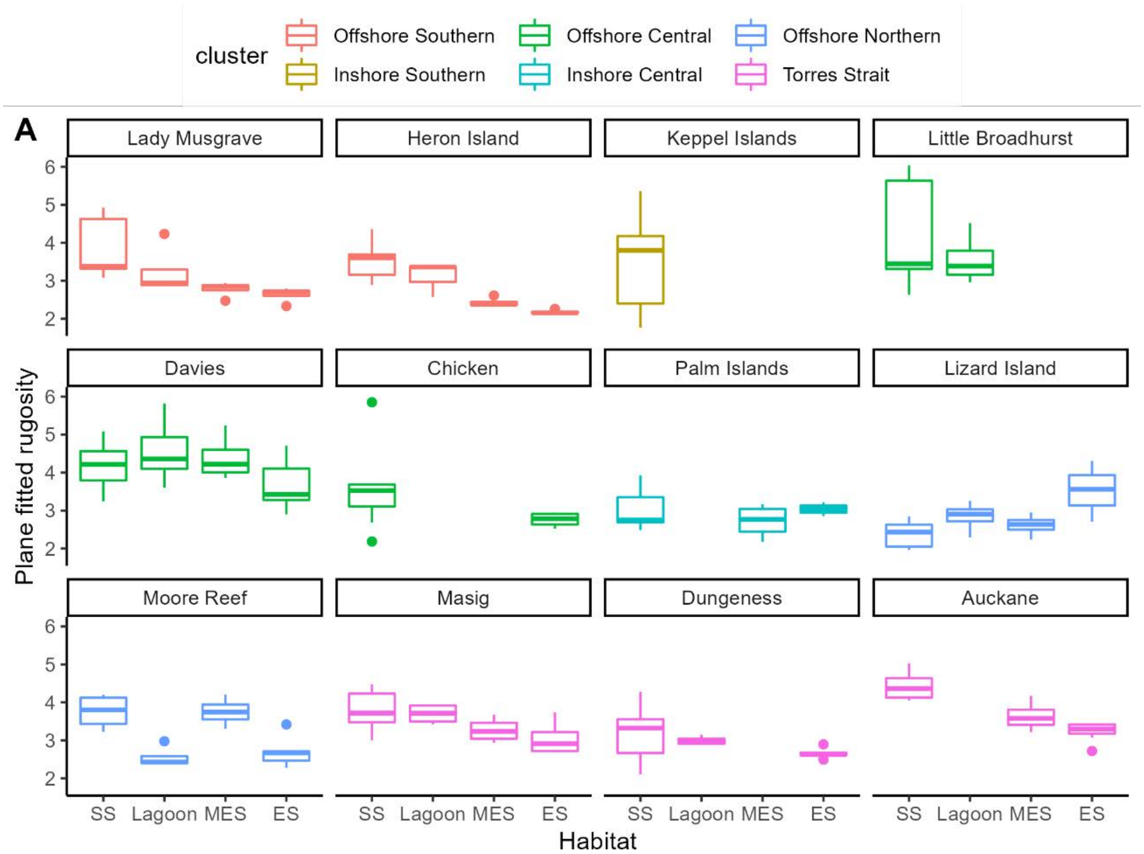

Figure 4.4|Rugosity measurements across all habitats and reefs (shallow sites) across the entire sample. Plots are arranged in order of descending latitude and are colour coded according to region. Habitat classes are

denoted by the following acronyms: SS = sheltered slope, MES = moderately exposed slope, ES = exposed slope, Lagoon habitats were generally within the same range of incoming wave energy as sheltered slopes.

There were no statistically significant differences in rugosity between any of the study regions (Fig. 4.5A; model details in Table S4.2). Interestingly, planned pairwise comparison testing revealed no significant differences between inshore reefs and their offshore counterparts in the central and southern sectors, where the study sites spanned a cross-shelf gradient. However, examining differences in fractal dimension across the six regions revealed that the surface fractality was significantly higher for the offshore central region than all other regions (Fig. 4.5B). This difference, combined with the slightly higher (though not significant) mean rugosity for the offshore central region, suggests that the complexity generating features are slightly more numerous and tend towards being a smaller size.

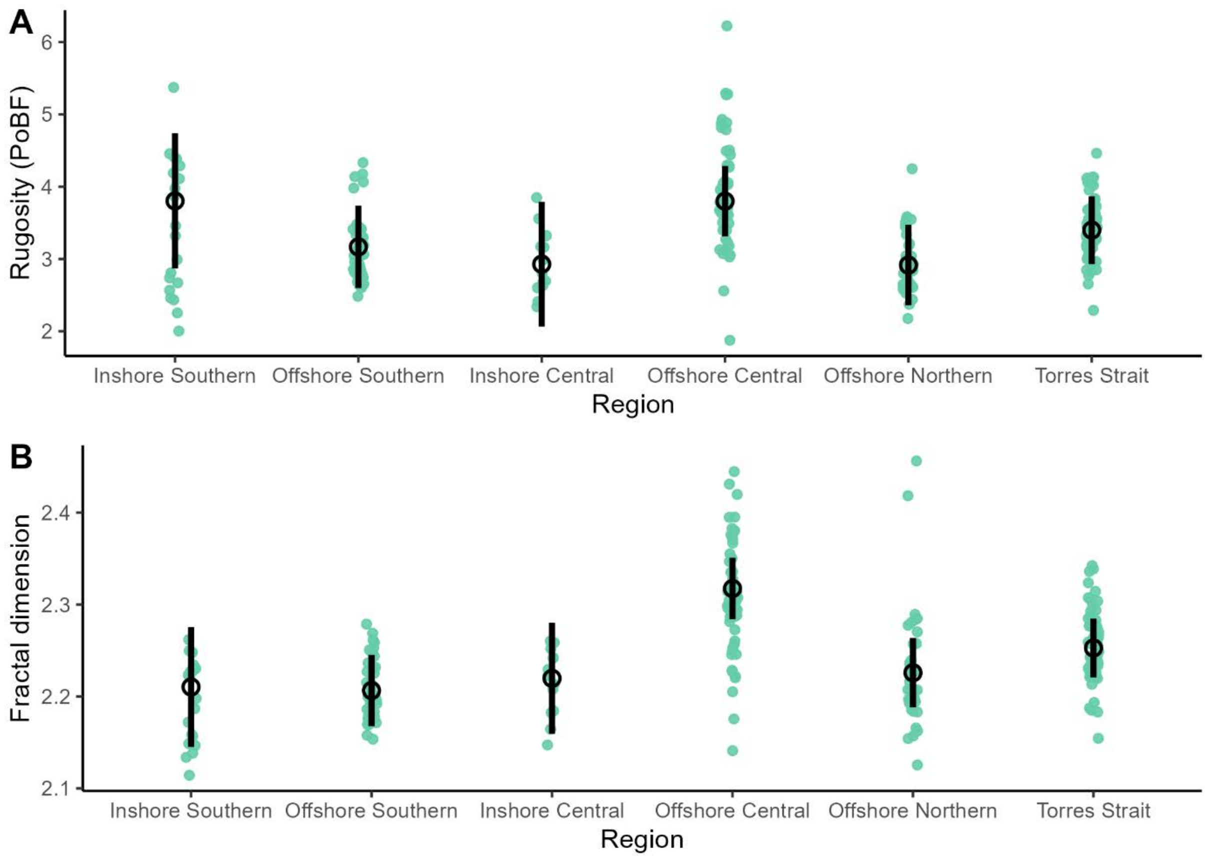

Figure 4.5| Model-fitted rugosity values (A) and fractal dimension (B) across all shallow sites within each of the reef sectors considered in this study.

Rugosity varied significantly between the four reef habitats across the entire sample design (Fig.4.6A). Shallow-water, sheltered reef slopes, generally typified by the lowest predicted wave energies, were the most complex habitats (Fig. 4.6, estimated marginal mean (EMM) rugosity = 3.61) and were significantly more complex than both moderately exposed slopes (EMM rugosity = 3.18) and exposed slopes (EMM rugosity = 2.88; p=0.01 and p<0.001 respectively). Lagoon sites provided an intermediate level of rugosity (EMM = 3.35) between sheltered and moderately exposed reefs and did not differ significantly from either in terms of complexity, however they were significantly more complex than the fully exposed slopes (p<0.001). In contrast, surface fractality did not differ among any of the habitats (Fig.5B), suggesting that exposure to wave energy in shallow-water habitats, whilst affecting overall complexity, has little influence on the overall distribution of feature sizes.

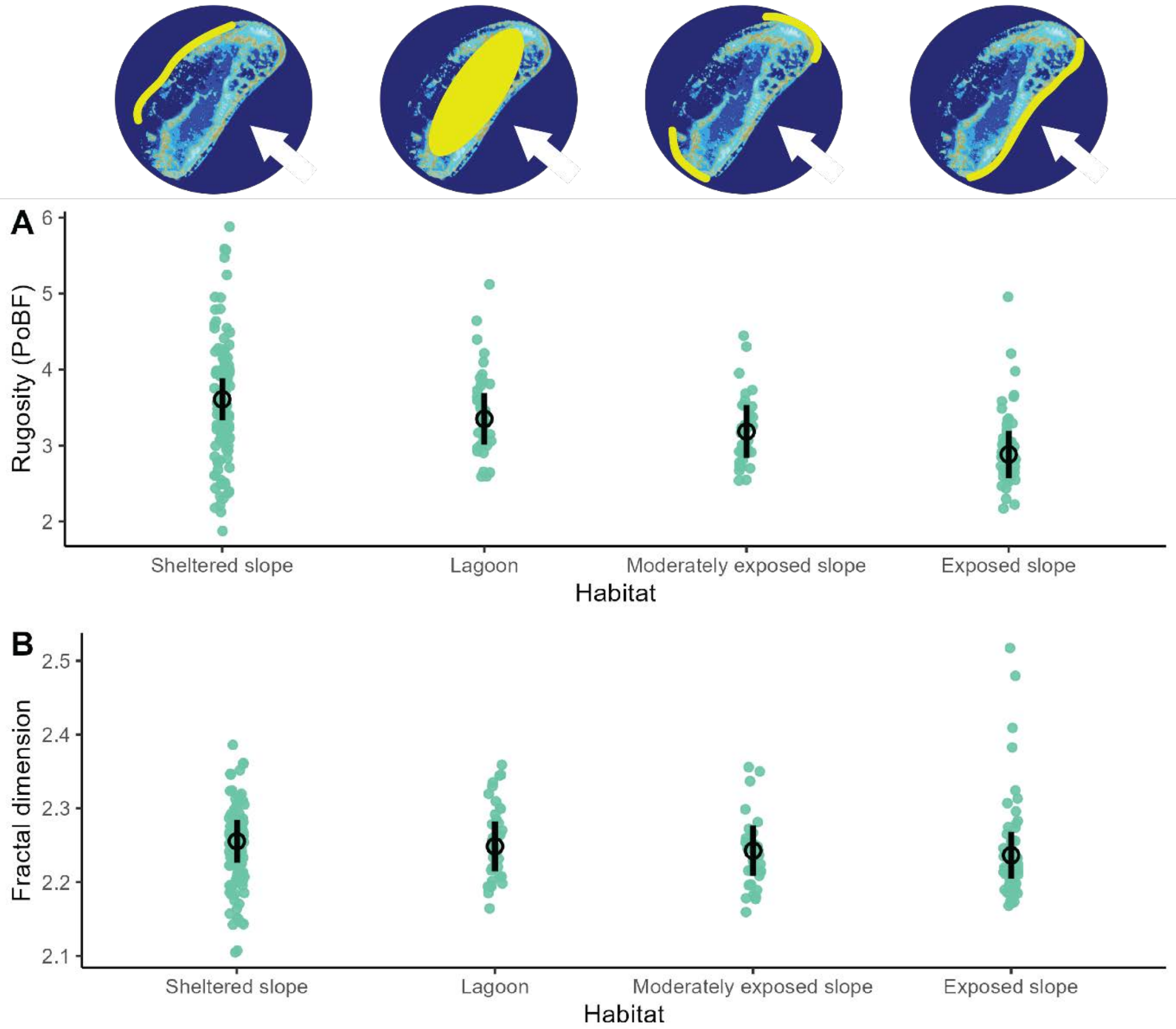

Figure 4.6| Rugosity across different habitats for all shallow sites within each habitat (n =231). Circles indicate the average estimated mean for each group, black bars indicate 95% confidence intervals. Coloured points represent overlaid raw data points representing complexity metrics in each plot.

There were differences in structural complexity between different depths within habitats, although this effect varied according to the specific habitat identity. The most complex habitats, shallow water sheltered reef slopes, were significantly more rugose than their adjacent deep-water counterparts (Fig. 4.7A). However, in the two higher wave-energy habitats (moderately exposed and exposed), there were no significant differences in rugosity between deep and shallow sites.

Fractal dimension differed in a similar manner to rugosity, with significant differences between paired deep and shallow sheltered slopes (Fig. 4.7B), but not moderately exposed or exposed slopes, although these relationships were not as strong as for rugosity (Fig. 4.7A, marginal R^2 = 0.23). The similar patterns in rugosity and fractal dimension suggest that the high levels of complexity that are typical of calm, shallow water environments are due in large part to an overabundance of fine-scale features in the 1-5cm size class, since the rate of loss of complexity as model resolution is depleted is high. Notably though, several reef plots deviated from this trend (Fig. 4.7B) with high rugosity and low fractality (indicative of a higher proportion of large-scale features/undulations), as well as plots with low rugosity but relatively high fractality (indicative of a relatively small amount of overall complexity yet made up primarily of fine-scale features).

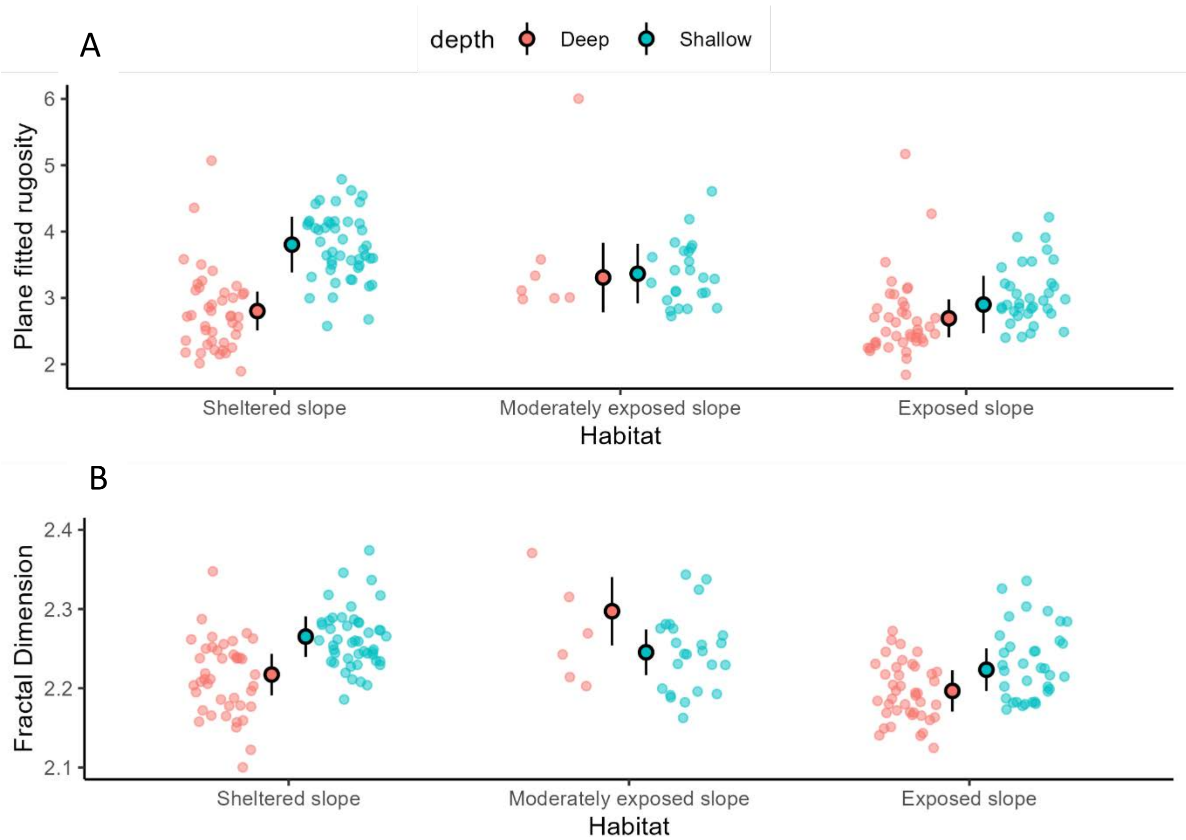

Figure 4.7|Comparisons of both rugosity (A) and fractal dimension (B) among sites and habitat zones with adjacent deep and shallow sites (6 reefs, 18 sites, 196 plots).

4.4 Discussion

The division of coral reefs into zones based on different habitats or depths with environmental and ecological reasonings is commonplace, with classification often related to the composition of the benthic and motile animal communities (Williams et al. 2013). More recently, structural differences between these habitats has begun to be assessed (Oakley-Cogan et al. 2020). The use of 3D photogrammetry provides an extremely practical method to accurately quantify important traits that can be used to compare key habitat features simultaneously across large spatial expanses. Here, it is demonstrated that habitat zonation based on relative exposure does influence structural complexity. My findings show that structural complexity exhibits a high level of variation across both regional and local scales. Generally, both components of structural complexity were best explained by fine-scale environmental drivers at the smaller, local scales, with differences in complexity reflective of varying depths and levels of exposure to wave energy. The same trends across intra-reef habitat zones and across depths were present among almost all sampling locations, with sheltered reef slopes being on average 25% more rugose than their exposed counterparts. These results indicate some level of structural complexity zonation occurs in response to gradients in environmental conditions, primarily incoming wave energy.

The most prominent gradients in complexity were among habitats within reefs. It is likely that the prominent driver of the patterns in complexity that existed between habitats was wave energy, which affects coral communities, the major reef builders and contributors to complexity, in multiple ways. First, distinct communities of complexity-generating organisms tend to be found in exposed versus sheltered habitats (Easton et al. 2018), with more highly branching and complex morphologies often growing best in sheltered locations, since dislodgment and mechanical damage is less likely to occur (Madin 2005). The relative calmness of these habitats may lead to a community containing more older, larger corals of different morphologies, contributing both coarse (e.g., massive *Porites*) and fine scale (branching *Acropora* and *Pocillopora*) complexity. Second, the highly dynamic environments of exposed reef slopes tend to lead to more spatially clustered coral cover in pockets of local shelter where conditions are more amenable to coral growth (Williams et al. 2013). Thirdly, the phenotypic plasticity exhibited by corals results in more compact phenotypes in places where incoming wave energy is typically high (Doszpot et al. 2019). Given these tendencies, it was expected that in shallow, sheltered environments, structural complexity would be highest, which was largely supported by the results. Regardless of the specific location of individual reefs, both rugosity (overall structural complexity) and fractal dimension (the relative inclusion of fine-scale complexity) was highest in more sheltered environments.

Patterns emerged among different depths across the sampling regions. In sheltered locations, shallow slopes (3-5m) were more rugose and fractal than their adjacent deep (13-15m) counterparts. Conversely, in exposed locations, both deep and shallow slopes were typically low rugosity, low fractality. This could be caused by a combination of several factors, relating to both species' composition and morphological diversity in reef builders that are known to change with depth in response to changing resource availability (Cooper et al. 2007) and hydrodynamics (Lowe and Falter 2015). Mechanistically, it is probable that these patterns (high complexity and high fractality) were driven by higher abundances of large corals that generate lots of fine scale structure.

Although intra- and inter-reef irradiance and wave energy gradients vary considerably, others have shown that in exposed shallow water environments, high oscillatory water flow (Madin 2005; Madin et al. 2014) and excessive irradiance (Brown 1997) can prevent high coral cover and/or lead to different morphologies of corals due to high sunlight and mechanical stress. Additionally, where irradiance is lower (for example at greater depth or where water clarity is poor), studies have shown that even members of the same genotype of coral taxa have flatter, light-capturing growth morphologies compared to their high-irradiance conspecifics which are more highly branching (Muko et al. 2000; Roberts et al. 2015). Whilst the shape of individual reef-building elements (i.e., coral colonies) were not measured here, the lower rugosity and fractality of coral morphotypes on deeper (lower irradiance) slopes compared to their adjacent shallow, sheltered counterpart offer a likely explanation for this pattern.

The ability to detect fine-scale gradients in structural complexity over space and time has several implications in understanding and predicting the future trajectory of coral reefs. The combination of rugosity and structural complexity can be used to infer the ability of reefs to host other organisms (Madin et al. 2023), avoid the harshest effect of disturbances and recover best when disturbances do happen. The identification of such traits that can be managed to promote resilience and preserve key functions can be accomplished using high-resolution habitat models such as those used in this study (Urbina-barreto et al. 2021). It is understood that structural complexity is positively correlated with reef resilience (Friedlander et al. 2003; Darling et al. 2017; Yuval et al. 2023). High levels of complexity promote bleaching avoidance through the provision of shading by reef structures (Hoogenboom et al. 2017) that may be beneficial for the long-term health of reefs. Fine-scale complexity on the other hand, may aid in recovery following perturbations since small crevices provide refugia from predation and harsh environmental conditions , increasing the survivability of small corals (Doropoulos et al. 2017; Gallagher and Doropoulos 2017) and enhancing recovery. Conversely, habitats that are generally typified by a low level of both overall and fine scale structural complexity, such as the exposed deep and shallow reef slopes observed in this study across multiple individual reefs, may be the most vulnerable and slow to recover following perturbations. For natural and active restoration, the identification of areas likely to have higher post-settlement survival rates using high-resolution appropriate complexity metrics to quantify beneficial traits may be helpful (Randall et al. 2021).

Interestingly, I was unable to detect any differences in rugosity on a regional basis, and there were no structural differences between inshore and offshore reefs in comparable habitats. The structural similarity of reefs across latitudes and the continental shelf here suggests that perhaps some level of homogenisation has occurred over time (Zawada et al. 2019b). It was expected that the different metrics of structural complexity would differ among geographic regions due to variation in environmental conditions (e.g., water quality, temperature) and disturbance history according to both latitude and shelf position (Doszpot et al. 2019; Mellin et al. 2019; Cumming and Bellwood 2023). However, no statistically significant differences between regions, apart from slightly higher rugosity and fractality in the offshore central region, were apparent. Coral reefs are highly dynamic, with the complex biotic interactions that shape their health and functioning being mediated constantly by background physical drivers (Sheppard 1982) and sporadically by disturbances of varying magnitude (De'ath et al. 2012; Cheal et al. 2017; Hughes et al. 2018). These perturbations have led to a widespread reduction in complexity, marked by shifts in the assemblage composition of reef communities (Dornelas et al. 2014), which has been documented in both the Caribbean and the Indo-Pacific (Alvarez-Filip et al. 2009; Rogers et al. 2014; Newman et al. 2015). Previous analyses have suggested that the morphology of corals is inherently linked to their bleaching susceptibility, and that highly complex morphologies are the most likely to be lost from communities during disturbances (Hughes et al. 2018; Zawada et al. 2019b). Although here, I did not include disturbance histories of reefs or regions in any of the models, it is possible that the combined effects of disturbances led to some of the structural similarities between different regions and sites in this study (Dornelas et al. 2014, Hughes et al. 2019b).

This study presents the first large-scale assessment of gradients in key high-resolution structural complexity metrics that have important implications for the functional capacity and resilience of coral reef ecosystems. Rugosity and fractal dimension have been identified as key indicators for resilience and recovery that should be promoted as part of management efforts (Torres-Pulliza et al. 2020), so understanding the spatial distribution of preferential features is important. The stability of the patterns uncovered in this study i.e., the consistent gradients in complexity among habitats within the same reef, regardless of the region in which each reef is located, is of ecological importance for several reasons. Whilst the use of physical variables such as wave exposure can be an effective proxy for some broad-scale processes, their resolution and accuracy are usually too coarse to predict important fine-scale trends in the habitats themselves. The stability of patterns in complexity regardless of geographic region and any related broad-scale differences in environmental drivers that may result is noteworthy. In the future, high-resolution complexity metrics such as those presented here should be paired with more ecological information such as coral demographics (species and size-frequency distributions). Pairing these metrics with the correct data would likely help to explain a large portion of the remaining variance in complexity gradients (Williams et al. 2013; Carlot et al. 2020), as well as helping to determine the proximal cause of variation in complexity i.e., the relative contribution of coral community organisation and successional state versus landform features (Graham et al. 2014).

4.5 Conclusions

High structural complexity is undoubtedly a positive feature within reefs, since it confers a greater propensity to support diverse and more resilient benthic and fish communities and aids recovery potential when disturbances occur. Here, we found that local-scale gradients in depth and exposure were the dominant drivers of coral reef structural complexity, and that there were no detectable differences in the reef structure across regions. The consistent patterns across specific habitats uncovered in this study suggest that they possess characteristics, by nature of a combination of their physical settings, and most likely their inhabitant benthic communities, which are the primary controllers of structural complexity. Peak levels of complexity, generally found in either sheltered, shallow-water reef slopes or patch reefs located in lagoons, which are both well-protected from incoming waves, are associated with high abundances of small-scale features typical of those generated by large branching coral colonies. In the future, the broad-scale variation in structural complexity documented here and the spatial arrangement of structure-generating elements should be reconciled with coral abundance, size frequency distribution and cover, as well as vital rates and species distributions within these areas.

Chapter 5 Three-dimensional rugosity and fractal dimension of habitats influence the abundance and diversity of small-bodied reef fish assemblages across broad spatial scales on the Great Barrier Reef

5.1 Introduction

Structural complexity is a component of habitats whose importance transcends any one ecosystem (Graham and Nash 2013; Gigliotti et al. 2021). The structural complexity of habitats is generally positively related to the abundance and diversity of associated animal communities, such that in two otherwise comparable environments with differing levels of habitat structural complexity, the environment with greater complexity would harbour a more abundant, and diverse animal community (Williams et al. 2002; Taniguchi et al. 2003; Griffiths et al. 2006; Pamela Delarue et al. 2015). These differences have been related to a range of factors, namely that complex habitats tend to provide greater refugia from predation (e.g., Hesterberg et al. 2017), create a greater number and diversity of microhabitats thereby reducing competition for available habitat (e.g., Mumby & Wabnitz 2002, Finstad et al. 2007), provide greater foraging opportunities due to an increased surface area which can support more of a given organism's food source (e.g., Oakley-Cogan et al. 2020), and facilitate a greater range of species by reducing environmental conditions to tolerable levels (Bruno et al. 2003; Johansen et al. 2007, 2008). Whilst these principals have been demonstrated across multiple ecosystems, recent advancement of technologies used to measure complexity have revealed the relationship between animals and their habitats is nuanced. Complex habitats do not lead to higher abundances of all trophic groups (Fukunaga et al. 2020b; Urbina-barreto et al. 2021), with the competitive advantage/s conferred to animals occupying specific trophic levels being context dependent (Nunes et al. 2015; Chan et al. 2018; Quadros et al. 2019).

Research into how complexity moderates interactions between animals has been particularly concentrated on the marine realm, however its importance in terrestrial scenarios has also been shown (Dorph et al. 2020; Gigliotti et al. 2020, 2021). For example, highly complex terrestrial systems may reduce predation risk for small-bodied animals through the provision of more refugia (Aben et al. 2017; Floros and Schleyer 2017), whilst impeding the movement and predation success of larger, roving predators (Iribarren and Kotler 2012; Gaynor et al. 2019). However, areas of high physical structure often lead to a trade-off between increased availability of refugia and decreased distance at which predators can be detected by prey and an escape response initiated (Nunes et al. 2015; Quadros et al. 2019). Thus, the relationship between animal biodiversity and/or abundance with their surrounding habitat often varies in direction and strength with specific habitat attributes and the traits of individuals (Ferrari et al. 2017b). The size of refugia relative to animal body size are of particular importance in terms of conferring any benefit; individuals do not benefit directly from refuges if they are too small to access themselves, or large enough that their predators can also gain access (Moran and Reaka 1988; Finstad et al. 2007; Noonan et al. 2012; González-Rivero et al. 2017; Rogers et al. 2018b).

In the context of coral reefs various factors have led to discrepancies across the literature in the importance of complexity as a driver of fish biodiversity and/or abundance (Komyakova et al. 2013). Coarse estimates, or proxies, of structural complexity often fail to adequately capture important aspects of complexity that shape the distribution of the target organisms (Pygas et al. 2020). Thus, when investigating the importance of habitat complexity, consideration should be given to ensure the spatial scale of the habitat attributes are relevant to the body size and/or behaviour of the species or assemblages of interest (Fukunaga et al. 2019). For example, small, site-attached fish species are highly likely to be influenced by fine-scale habitat attributes in their small home ranges (e.g., gaps between coral branches), but larger geomorphologic features (e.g., spur-and-groove formations) are more likely to be reflected in the abundances of larger, roving species (Robinson et al. 2011). Recent advances in the measurement of marine structural complexity with the rapid uptake of 3D photogrammetry have led to new quantitative indices that have uncovered new relationships between the structural attributes of habitats and their inhabitant animal communities (D'Urban Jackson et al. 2020, Chan et al. 2018).

The abundance of a particular species or group of animals is also mediated by factors beyond simple habitat availability, such as nutritional resources (Oakley-Cogan et al. 2020), and competition resulting from functional overlap of inhabitants in a particular locality (Hixon and Menge 1991; Mumby and Wabnitz 2002; Finstad et al. 2007). Regional-scale environmental variation has also been found to shape community distributions, particularly in respect to small, site-attached species (Emslie et al. 2010, 2012). External physical drivers that may make an otherwise suitable habitat uninhabitable by a particular group of animals also play a role (Johansen et al. 2007). For example, small fish with a relatively poor swimming ability, are less likely to be found in high-energy environments since the energetic costs associated with living in high currents outweigh any benefits they might receive (Bellwood and Wainwright 2001).

Given these complexities, assessing fish-habitat relationships using a trait-based approach (e.g., foraging behaviour) rather than a community-wide, or species specific approach, may provide useful insights into the relative importance of certain structural attributes of the habitat to fish communities (Madin et al. 2016). Characteristics such as body size are important in fish habitat selection (Finstad et al. 2007; Nash et al. 2013), and trait-based information on foraging behaviour tends to influence how they interact with their environment (Hitt et al. 2011; Helder et al. 2022). Incorporating these factors into analyses offers the opportunity to uncover important responses to changes in environmental variables that may occur through space and over time, applicable across species (Madin et al. 2016).

With the health of tropical coral reefs under threat (Hughes et al. 2018), it is critical to uncover mechanisms that allow for more accurate forecasting of the trajectory of fish communities. This requires an understanding of what factors determine fish community distributions and abundance using the best available technologies. The aim of this study was to investigate the relationship between habitat structural complexity and the abundance and diversity of small-bodied fish species. Small-bodied fishes are common on coral reefs, and important conduits of energy to higher trophic levels (Brandl et al. 2019). We surveyed small-bodied reef fish assemblages related to the 3-dimensional rugosity and fractal dimension of 276 habitat patches (each ~12 x 6m), across 12 reefs spanning the length of the Great Barrier Reef. The two complexity metrics were investigated alongside environmental data (geographical region, depth, and exposure) as drivers of fish abundance/diversity. Relationships were investigated for the entire small-bodied fish assemblage and for five feeding guilds (herein referred to as trophic groups: carnivore, planktivore, herbivore, omnivore and invertivore) independently.

5.2 Methods

Study Design

Several reefs spanning 1500km of latitude across the Great Barrier Reef and Torres Strait were selected, representing both inshore and offshore locations across Northern, Central and Southern regions (Fig. 5.1). On each reef, three habitat zones were sampled that differed in exposure to incident wave energy: exposed reef slope, moderately exposed slope, and sheltered slope (see **chapter 4**). Sites located in lagoons were surveyed in some reefs, but this habitat zone was not captured with sufficient replication across the geographic breadth of the sampling to be included in the final analysis for this study. A total of 276 plots contained overlapping fish and photogrammetry surveys, the details of which are described below. Sites with low visibility were also not included due to problems with surveying fish in such conditions (i.e., in the Keppel Islands).

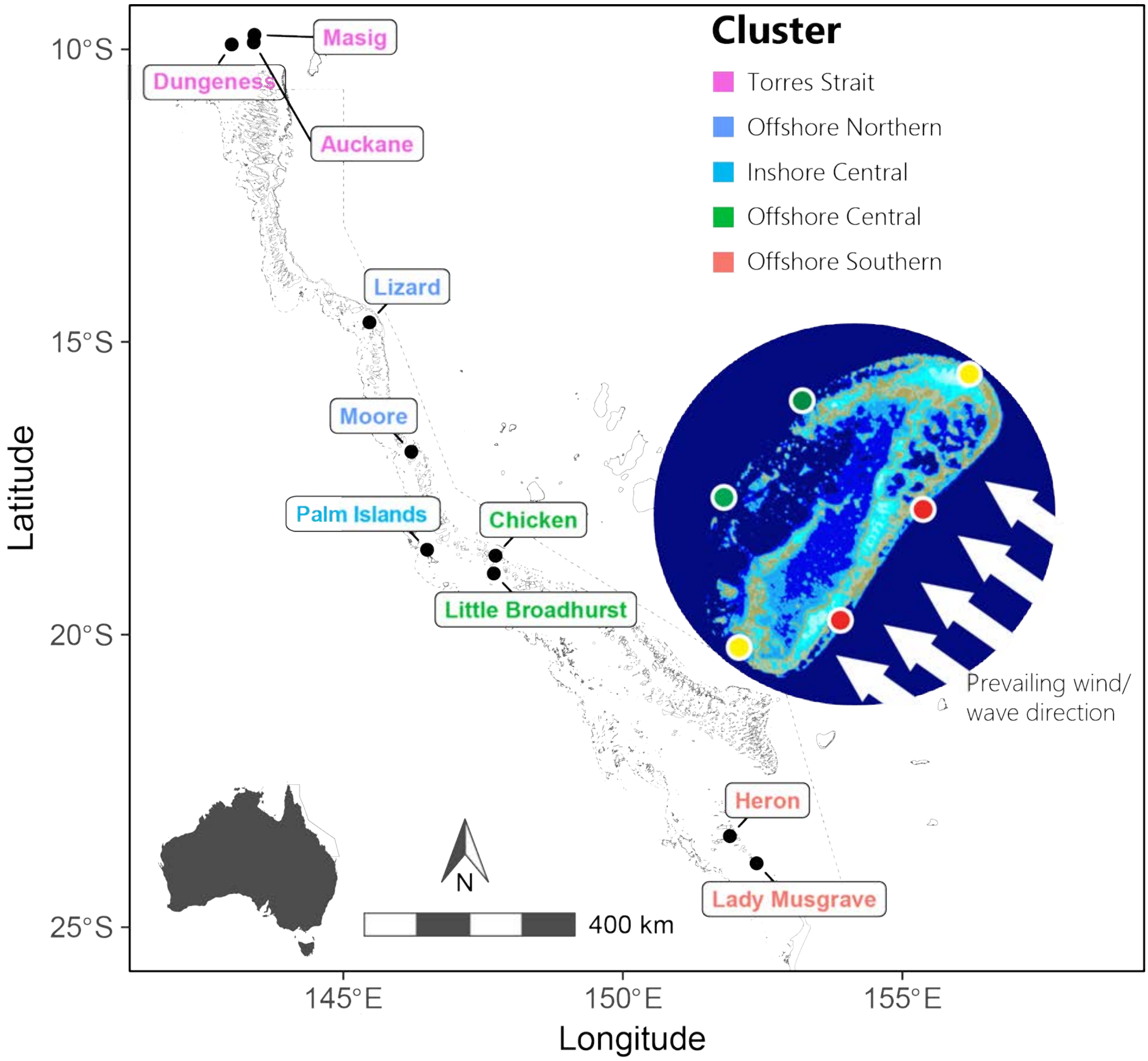

Figure 5.1| Map of the Queensland coast showing the location of the study reefs. (Inset) Example of study design reflective of prevailing incoming wave energy exposure: Exposed slope (red dots), moderately exposed slope (yellow dots) and sheltered slope (green dots).

Structural complexity assessments

We used high-resolution, dual-mounted DSLR cameras (Nikon D850 with 20mm fixed lenses, paired with 8-inch dome ports fitted to nauticam housings) combined with Agisoft Metashape Professional (ver. 1.7.6) to generate sub-centimetre resolution habitat maps (Agisoft LLC, St. Petersburg, Russia). By incorporating both nadiral and oblique imagery, we were able ensure that the resultant surface models were fully three-dimensional, which is important in accurate calculations of structural complexity measurements (Marre et al. 2019). Divers operating the DSLR camera system initially swam in a mow-the-lawn pattern to capture nadiral imagery over the 12x6m plots, before capturing additional images from oblique angles on several subsequent passes through each plot. Flying elevation was ~2m for the nadiral and ~1m for the oblique imagery and was adjusted slightly according to water visibility. Photogrammetry surveys were postponed when the desired flying elevation exceeded in-water visibility. To deal with the high volume of data to be processed whilst maintaining consistency across reconstructions and to attain fine-resolution reconstructions, we utilised a series of custom-coded python processing scripts in tandem with Metashape's support of network-based processing, splitting the computing load across several nodes simultaneously. In total, approximately 500,000 photographs were used to build reconstructions of 276 12x6m plots, with each model taking approximately 4-8 hours to process from end-to-end depending on the complexity of the surface to be reconstructed and the loading of the computing network. See **chapter 4** for basic processing settings. See also section *4.2: Extraction of structural complexity metrics from reconstructions* for a detailed workflow of the extraction of structural complexity metrics from reconstructions. Here, rugosity and fractal dimension were used as the complexity metrics. Although a larger suite of metrics was originally extracted from the reconstructions, exploratory analyses revealed that additional common metrics such as slope and height deviation (Torres-Pulliza et al. 2020) yielded negligible additional predictive power. Thus, in the interest of parsimony, these two metrics were satisfactory for all analyses.

Fish surveys

Within each of the 12x6m plots, fish assemblages were surveyed along a 10 x 1m belt transect by an experienced observer. All small (<15cm total length, TL) site-attached fishes within the 1m-wide belt were identified to species, and their total length estimated to the nearest centimetre. Cryptic species (e.g., those from the families Gobiidae and Blenniidae) were not included due to difficulties with detection and identification in the field. Surveys were constrained to include only small-bodied fish since these have the closest direct relationship with the benthos (Alvarez-Filip et al. 2011b) and have small home ranges (Ceccarelli et al. 2005), so should be influenced directly by their surrounding habitat. Fish were categorised in to one of five trophic groups based on feeding behaviour (herbivore, carnivore, omnivore, invertivore, planktivore; trophic groupings for each species are presented in table S5.1). These categorisations were informed by previously published data (Sano et al. 1984; Froese and Pauly 2010). Fish surveys were conducted prior to imaging the plots, to minimise any potential effects of diver presence on fish assemblages.

Statistical analyses

To investigate relationships between the abundance and diversity of fishes, and the environmental and structural complexity metrics, I used boosted regression tree (BRT) modelling. Unlike most modelling approaches, which simultaneously take a set of predictor variables and fit the data to a single parsimonious model, BRTs fit many models in a machine-learning approach using simple regression trees. They employ stochastic gradient boosting to deliver an additive regression model with minimal fitting error (Elith et al. 2008). By using cross-validation to evaluate models, BRTs resample the data many times during fitting, helping to reduce any spatial autocorrelation that may be present. In addition, missing data and mixing of categorical with continuous variables, as well as inherent robustness to departures from selected data distributions, make BRTs an appropriate choice for observational ecological data (Knudby et al. 2010). BRTs have been utilised effectively to model species-habitat relationships since the addition of many predictor variables does not hinder the model's ability to produce solutions (Leathwick et al. 2006; Pittman et al. 2009; Aston et al. 2019).

I modelled the abundance and diversity of the entire small-bodied fish assemblage in each of the 276 plots, using the following five potential predictor variables: Region, Habitat, Depth, Rugosity and Fractal dimension (Table 5. 1). Following this, data were parsed to split the fish community into six trophic groups; herbivores, carnivores, corallivores, planktivores, omnivores and invertivores. However, due to the low overall abundance of corallivorous fish in these samples, the BRT model was not able to model their abundance against the predictor variables, and these were not considered further. Separate BRT models were then fitted for the abundance of each of the five remaining groups, to determine whether fish-habitat relationships differed according to trophic groups. Due to the schooling nature and sometimes large variability in abundance of small-site attached fish species, abundance data were log-transformed. This also helped to achieve normally distributed data; hence, the log-abundance of fish in each case was modelled against a gaussian data distribution. Shannon-Weiner diversity was calculated with respect to each 72m^2 plot (Shannon and Weaver 1949).

To optimise and produce each BRT model, the packages 'gbm' (Ridgeway 2022) and 'dismo' (Hijmans 2022) were used. I used a custom loop routing to find the optimal combination of three model parameters using the function 'dismo::gbm.step': bag fraction (*bf*; the proportion of data to be used in each step), tree complexity (*tc*; the number of splits permitted in each individual regression tree) and learning rate (*lr*; the contribution of each tree allowed to the final model). The final model maximised cross-validation deviance (CVD) over possible parameters of 0.5, 0.7 and 0.8 *bf*, 1-5 *tc* and 0.01, 0.001 and 0.0001 *lr*, with a maximum of 30,000 trees permitted in each model. To explore the relative contribution of each predictor variable on the amount of deviance explained in each model (expressed as a percentage), and to plot 2D and 3D partial dependency plots to visualise these contributions, I used the package 'ggBRT' (Jouffray et al. 2019). Model outputs are displayed as partial dependency plots, which visualise the conditional relationship between one (2D) or two (3D) predictor variables on the response variable, after simultaneously accounting for the effect of all other predictors used in the model.

Table 5. 1 | List of predictor variables used in boosted regression tree models

Variable	Type of variable (number of classes)	Definition	List of classes/range of values
Region	Categorical (5)	Based on location and cross-shore location as shown in Fig.1.	Torres Strait Offshore Northern Inshore Central Offshore Central Offshore Southern
Habitat	Categorical (3)	Based on relative exposure to wave energy	exposed reef slope moderately exposed slope sheltered slope
Depth	Categorical (2)	Based on average target depth of each plot	Shallow – 5(+/-3)m Deep – 13(+/-2)m
Rugosity	Continuous	Three-dimensional area divided by the planar two-dimensional area (see section *Structural complexity assessments*)	Lower limit 1, general range 2-8
Fractal dimension	Continuous	Ratio of the change in detail to the change in scale (see section *Structural complexity assessments*)	Lower limit 2, general range 2-2.3

5.3 Results

In total, 25,192 small site-associated fish across 144 species were recorded, with the majority of these belonging to the families Pomacentridae and Labridae. By far the most abundant trophic groups were planktivores and omnivores (n=13122 and 8657 respectively), followed by generalist carnivores (n=1642) and herbivores (n=1007) and finally, invertivores (n=645) and corallivores (n=112).

Model performance of the BRTs of the abundance and diversity of small fish assemblages was relatively good, explaining 52% and 45% of the variance, respectively (Fig. 5.2). Geographic region was the strongest predictor of the abundance and diversity of the entire assemblage, followed by rugosity and fractal dimension. In both models, the relative influence of depth and habitat was low, explaining little variation in abundance and diversity of overall small-bodied fish communities.

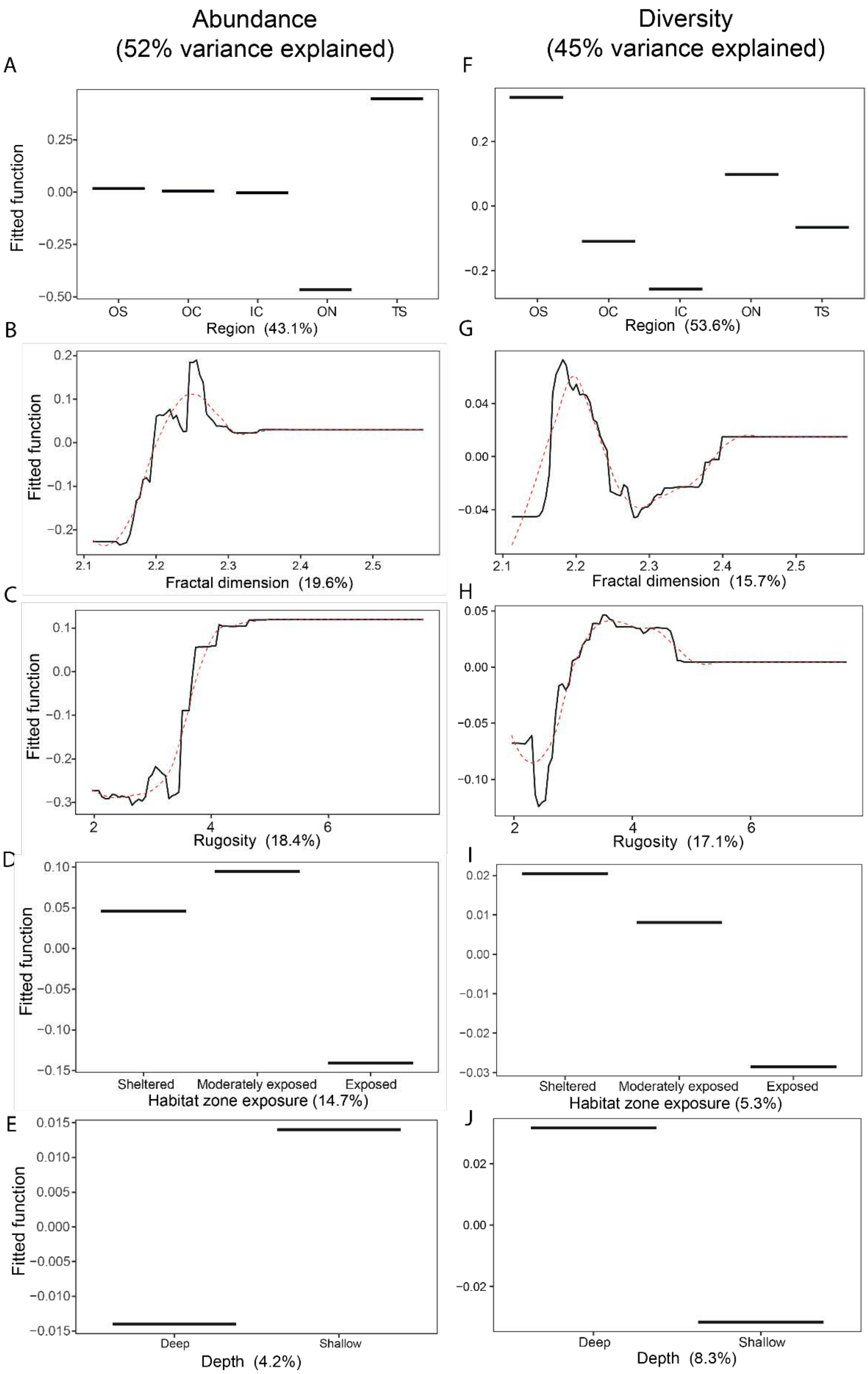

Figure 5.2 | Partial Dependency plots showing the influence of each of the five predictor variables on overall small-bodied fish abundance (left column) and Shannon-wiener diversity (right column). Percentages under each panel represent the relative influence of each variable, whilst percentages at the top of columns represent overall variance explained by the model. Note that panels are not necessarily in order of most to least influential variables and the different scales on panels. Region codes: I = Inshore, O = Offshore, N = Northern, C = Central, S = Southern, TS = Torres Strait. Habitat zone codes: SS = Sheltered slope, MES = Moderately exposed slope, ES = Exposed slope

Abundance of small fish

After accounting for the effect of geographic region, structural complexity metrics contributed significantly to explaining fish abundance and diversity. Both fractal dimension and rugosity were positively related to abundance, with a marked increase in abundance occurring between fractal dimensions of 2.15-2.25 and rugosity of 3.5-4, and after which there was limited effect of either metric on abundance. It also was apparent that the highest levels of fish abundance occurred when both the effects of fractality and rugosity were considered together (Fig. 5.3A). Their conditional effect on fish abundance was greater than each individual predictor, highlighting that the combined effects of overall complexity and the distribution of feature sizes considered together are important in structuring fish abundance.

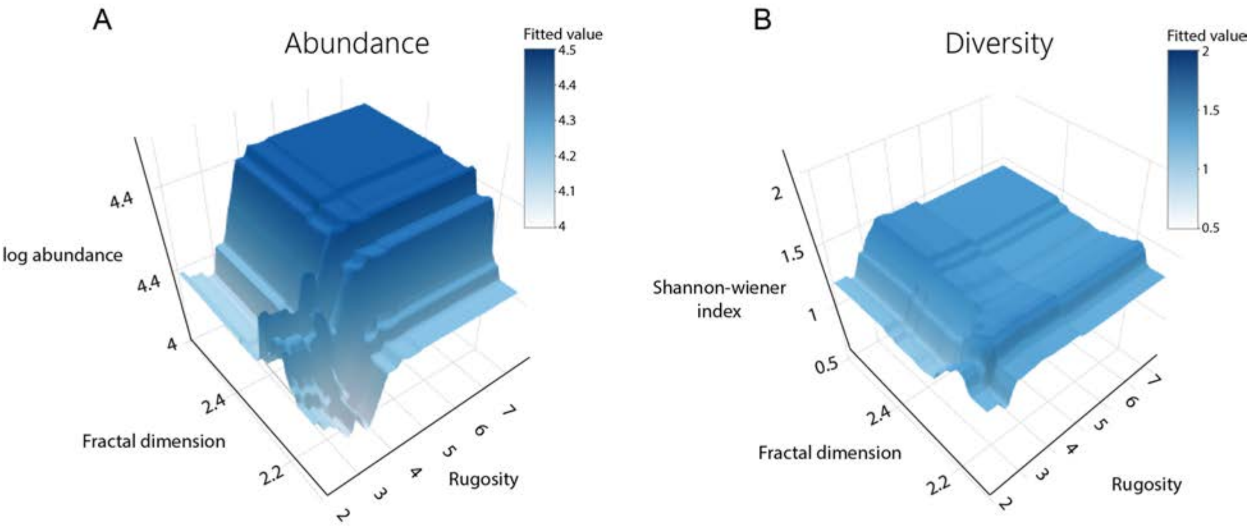

Figure 5.3 | Three-dimensional interaction plots from BRT models showing the combined effects of structural complexity metrics on fitted values of small-bodied fish abundance (A) and diversity (B) across all plots in all regions. Darker shades indicate higher fitted values (I.e., greater abundance or diversity).

Diversity of small fish

The relationship between small-bodied fish diversity and complexity metrics were less clear (Fig. 5.3B). Although the least diverse fish communities occurred in plots with both low complexity and low fractality, rugosity and fractal dimension independently appeared to have varying effects. As rugosity increased, there appeared to be a peak in its positive influence on fish diversity at a rugosity of ~3.6, beyond which there was no further effect (Fig. 5.2H). Fractal dimension on the other hand, appeared to positively influence fish diversity up to a value of 2.2, after which its influence was negative until it reached a value of 2.28, beyond which there was a positive, but less pronounced, effect on diversity (Fig. 5.2G). However, the interaction between rugosity and fractal dimension suggests that fish diversity was at its greatest when rugosity values were towards intermediate values (i.e., 4-5) and fractal dimension was towards its upper values (above 2.4) (Fig. 5.3B).

Trophic group responses

Model performance of BRTs varied across the five functional groups, explaining between 29.0% and 60.1% of the overall variance in abundance of each group (Fig. 5.4). The most influential predictors on fish abundance varied according to group, with geographic region being the most influential predictor for three of the five groups (herbivores, omnivores, planktivores; Fig. 5.4A, B and D). Fractal dimension was the most influential predictor for the abundance of the two remaining groups (i.e., carnivores and invertivores; Figure 5.4C, E). Habitat zone and depth were poor predictors of fish abundance except herbivores and carnivores, where habitat zone's relative influence was 17.1% and 16.5% respectively (Figure 5.5). Depth was the worst predictor in three of the five BRT models (planktivore, carnivore and invertivore) and the second worst in the remaining two (omnivore and herbivore).

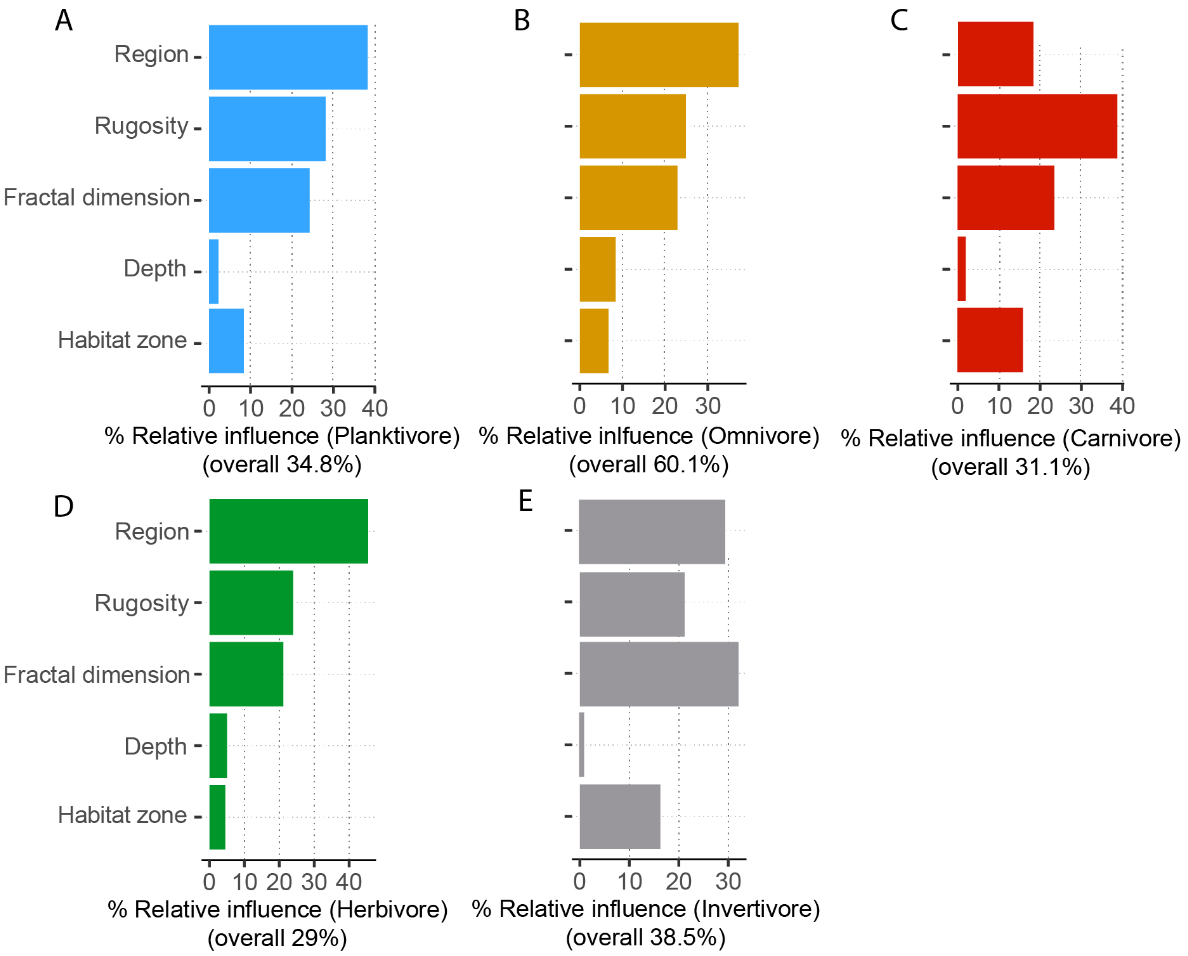

Figure 5.4 | Influence of predictor variables in each BRT model relative to the overall variance explained by the model for each trophic group.

Generally, among geographic region, habitat zone and depth, there were no clear patterns in strength or direction shared among the five trophic groups (Fig. 5.5). Unexpectedly, some trophic groups were absent in some regions (Fig. 5.5G and M), For example, invertivorous fish were not observed in the central region (both shelf positions), whilst no carnivores were observed in the Torres Strait. It was however notable that in the Torres Strait, very high abundances of planktivores, omnivores and herbivores were observed (Fig. 5.5A, D and J respectively). Habitat zone showed little influence except for carnivores and invertivores (Fig. 5.5H and N) where moderate levels of wave exposure drove the highest abundance.

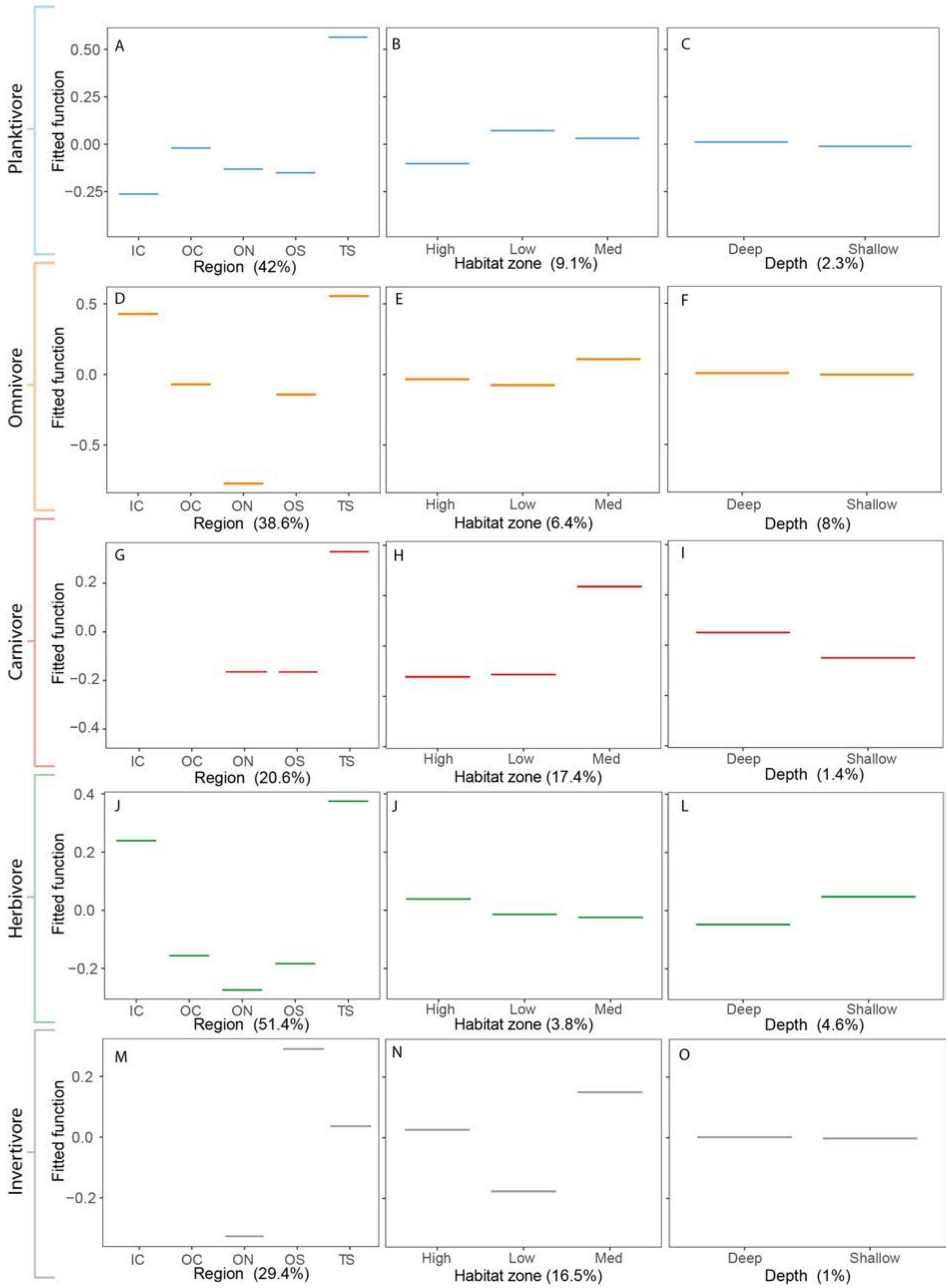

Figure 5.5 | Partial dependency plots showing effects of categorical variables on the abundance of each of the five trophic groups, across all sampling locations. Percentages are the relative influence of each variable for that model and are not reflective of absolute values of variance explained. Region codes: I = Inshore, O = Offshore, N = Northern, C = Central, S = Southern, TS = Torres Strait.

Complexity metrics were good predictors of abundance across all five trophic groups (Fig. 5.4; Table 5.2). The combined effects of the two complexity metrics accounted for between 40.2 – 72.8% of the relative influence of predictors across the five trophic group models. In absolute terms, the proportion of variation in fish abundance explained by the combined complexity metrics varied between 11.6 and 33.0%. The strongest overall model was the BRT for planktivores, which explained 60.1% of the variation in abundance; complexity metrics alone accounted for 33.0% of the total variance.

Table 5.2 | Relative and absolute performance of structural complexity metrics in BRT's predicting the abundance of each trophic group

Trophic group	Overall variance explained	Relative influence / Absolute variance explained (Rugosity) (%)	Relative influence/ absolute variance explained (Fractal dimension) (%)	Combined relative influence from complexity metrics (%)	Total variance explained from complexity metrics (%)
Planktivore	34	29.4 / 10.0	19.2 / 6.5	53.2	16.5
Omnivore	60.1	27.1 / 16.5	27.1 / 16.5	54.2	33
Carnivore	31.1	37.9 / 11.4	22.7 / 10.6	60.6	18.8
Herbivore	29	21.2 / 6.1	19 / 5.6	40.2	11.6
Invertivore	38.5	21 / 8.1	31.2 / 12	52.2	20.1

For both rugosity (Fig. 5.6A) and fractal dimension (Fig 5.6B), the influence on abundance of the five trophic groups appeared to cease above values of 3.9-4.2 and 2.29-2.33 respectively. Neither rugosity nor fractal dimension was a uniformly better predictor across trophic groups (Fig. 5.4). The effect of complexity metrics also varied in both direction and strength according to group identity (Fig. 5.6), and these were the strongest predictors for carnivores and invertivores (Fig 5.4C and E). The abundance of omnivores, planktivores, carnivores and herbivores all were positively influenced by increasing values of rugosity to varying degrees, up to values of 3.8-4.2 depending on the specific trophic group (Fig. 5.6A), above which there was no further increase in abundance. Invertivores were the only group to show minimal response to rugosity.

The relationship between fractal dimension and fish abundance was mare variable among trophic groups (Fig. 5.6B). Both carnivorous and omnivorous fish abundance correlated negatively with increasing fractal dimension, though the relationship differed slightly. For carnivores, a steep decline in abundance occurred between values of 2.2-2.25, whereas for omnivores, a similar decline occurred over a range of 2.2-2.3 in fractal dimensions. Herbivores and Invertivores did not have a strongly directional correlation with fractality. Planktivorous fish were the only group to respond positively to fractal dimension.

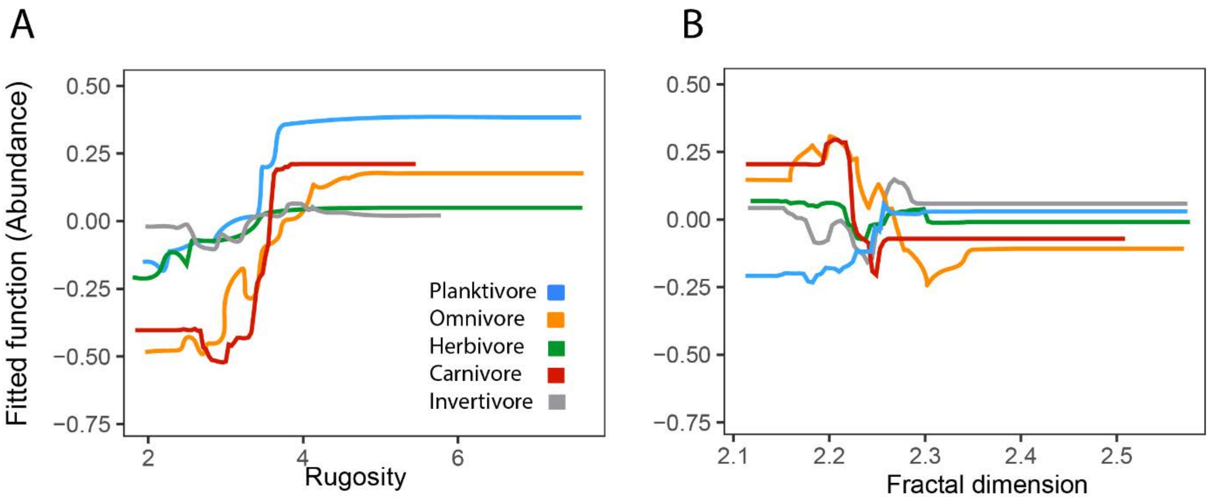

Figure 5.6 | Partial dependency plots showing the effects of (A) rugosity and (B) fractal dimension on the abundance of individual fish trophic groups across the sample, taken from each BRT model. Note that the percentage of variance explained by these complexity metrics varied between models (See Fig. 5.3)

5.4 Discussion

My results show that small-bodied reef fish abundance and diversity are both influenced positively by structural complexity, supporting the general consensus across the literature that greater habitat complexity results in higher biodiversity (Alvarez-Filip et al. 2011b; Emslie et al. 2014; Rogers et al. 2018b; van Lier et al. 2018; Helder et al. 2022). The abundance and diversity of small-bodied reef fish assemblages were positively influenced by rugosity and fractal dimension, while depth and relative wave exposure habitat zones were poor predictors. Generally, higher values of both rugosity and fractal dimension led to increased diversity and abundance of small-bodied fishes, however, both measures peaked at intermediate values of complexity metrics, suggesting that excessive complexity is not necessarily beneficial for overall fish abundance or diversity, a finding supported by others at both the patch (Paxton et al. 2017) and colony scale (Noonan et al. 2012; Brooker et al. 2013). Small-scale studies have suggested that intermediate levels of complexity (i.e., branch density in individual corals) are the most beneficial for small-bodied fish to hide since they obstruct predator access (Noonan et al. 2012), and that large inter-branch spacing is detrimental for fish fitness (Pereira and Munday 2016). Here, the peak abundances and species diversities were reached at intermediate values of complexity, beyond which there were no further increases in either measure of the fish community. This suggests that even at the patch-scale, whilst low levels of complexity result in fewer fish, ever increasing complexity does not always equate to the most abundant and diverse fish assemblages.

There is a growing literature identifying the variable relationships that different groups of fishes have with their surrounding environment based on structural complexity (Jankowski et al. 2015; Agudo-Adriani et al. 2016; Ferrari et al. 2017b; Castaño et al. 2021; Helder et al. 2022). Different trophic groups of small-bodied fishes interact differently with their environment due to their different foraging behaviours, yet all these fish share a need for the protection offered by complex reef structure (Willis and Anderson 2003; Alvarez-Filip et al. 2011b). It was found that the response to the two-complexity metrics was not ubiquitous across all trophic groups. Instead, the strength and direction of the relationship with either complexity metric varied dependent on group identity. The varying response of individual trophic groups to rugosity and fractal dimension may represent trade-offs between the quality of preferred dietary targets and ability to detect and/or evade predators (Nunes et al. 2015; Chan et al. 2018; Quadros et al. 2019). Planktivores, which were made up almost entirely of species belonging to Pomacentridae (damselfish), were positively associated with both rugosity and fractal dimension. The most abundant five species in this trophic group accounted for over 80% of its total abundance (*Neopomacentrys azysron, Chromis nitida, Neopomacentrus bankieri, Pomacentrus lepidogenys* and *Chromis atripectoralis*). Many small-bodied planktivorous fish display schooling or shoaling behaviour, and have a tendency to associate with highly complex branching coral structure (Richardson et al. 2017b), where refuge can quickly be taken among the branches of corals to avoid predation. The likely mechanism for the positive relationship between planktivores and both metrics of complexity is the availability of small refuge spaces, that complement both their feeding tendencies and need to avoid predation (Helder et al. 2022). Others have found that schooling fish tend to associate with highly complex environments; Helder et al. (2023) found that schooling/shoaling herbivores are positively correlated with small-scale complexity.

Omnivores were positively correlated with rugosity, but negatively correlated with fractal dimension, suggesting a selective preference for habitats that have many complexity features, but where that complexity is made up of relatively large feature size. An example of a low fractality, high rugosity environment would be one that has high vertical relief generated by spur and groove formations and/or large bommies rather than lots of small branching corals on a relatively flat surface. The species complex making up omnivores in this study consisted mainly of *Pomacentrus moluccensis, Pomacentrus brachialis* and *Pomacentrus amboinensis*. In contrast to the schooling planktivores, these species typically occur in small groups, and feed on a mixture of algae and some zooplankton. *Amblyglyphidodon curacao,* a solitary omnivore with a larger body size that feeds mainly on plankton as well as some benthic algae (Curtis-quick et al. 2012), was also highly abundant in general. It is possible that the different foraging tendencies and smaller group sizes lead to a preference for habitats that are not excessively complex; habitats with less coral cover may be beneficial because of a higher potential grazing surface area (Oakley-Cogan et al. 2020), as well as greater visual acuity afforded by the less fractal environment. Such combinations of habitat traits may satisfy the need for solitary/shoaling omnivores to feed successfully whilst being able to view predators and assess risk (Chan et al. 2018). Others have shown the importance of visual acuity in predator detection (Rilov et al. 2007; González-Rivero et al. 2017), and habitat fractality may be important for small fish closely associated with the benthos for this reason. Experimental manipulation of the benthos has shown that feeding rates in *P. amboinensis* is reduced in highly complex environments, most likely because lower visual acuity impairs the ability to detect predators and leads to more conservative behaviour (McCormick and Löonnstedt 2013).

Interestingly, carnivores, dominated by *Cheilodipterus quinquelineatus* (f. Apogonidae), (Gardiner and Jones 2010) had very similar relationships with both rugosity and fractal dimension to omnivores. As a nocturnal species (Nay et al. 2015), *C. quinquelineatus* uses the reef during the day as a resting site (Gardiner and Jones 2010) and is likely to select for habitats primarily on a shelter-quality basis. The similar relationship that these fish appeared to have with complexity is likely reflective of their body-size and gregarious behaviour. Low fractality sites tend to be less fragmented and thus have shelter at a scale that fish with slightly larger body sizes (10-15cm) can use, and the high rugosity of the sites that *C. quinquelineatus* associated with suggest that these sites had a high density of such features, amenable to schooling aggregations.

Herbivores (mostly made up of *Pomacentrus adelus, P. wardi, Stegastes apicalis*, and *S. lacrymatus,* previously *Plectroglyphidodon lacrymatus*) appeared to be weakly positively associated with rugosity and did not have much association with fractal dimension (though it did appear to be slightly negative). Others have recently found that the distribution of herbivorous fish is closely related to the availability of grazing surface area rather than the complexity of the habitat (Oakley-Cogan et al. 2020). However, given their inherent vulnerability to predation (Noonan et al. 2012; Nunes et al. 2015; Quadros et al. 2019), the positive correlation between rugosity and abundance of small-bodied herbivores does suggest some dependence on complexity for shelter. Further, the herbivorous damsel species making up most of this trophic group were highly territorial (or farming) species (Sano et al. 1984; Hoey and Bellwood 2010; Emslie et al. 2012), and as such 'weed' algae in their home patches. It is likely, given the specific habitat requirements of farming herbivores, that habitat attributes decoupled from complexity and not measured in this study (e.g., live versus dead coral cover, algal cover etc.,) exert stronger control over their distribution. Farming herbivores are a complex group; different species have different behaviours in terms of their territory sizes and farming intensities and have been shown to respond differently to disturbances that affect complexity in the past (Emslie et al. 2014). Whilst they are reliant on complexity for shelter due to their small body size (explaining the positive relationship between rugosity and abundance observed here), herbivorous fish distribution may be best explained when coral demographics and health are incorporated into analyses or may be best divided into further subgroups of differing farming home ranges and intensities.

Geographic region was a strong driver of variation in diversity and abundance of small fish at the assemblage level and for some of the individual trophic groups. Previously, latitude and shelf position have been identified as important determinants of the distribution of other groups of fish (Russ 1984; Newman et al. 1997; Gust et al. 2001; Emslie et al. 2010). The broad representation of latitudes (north, central and south) and shelf position (inshore versus outer shelf) here led to different abundances/diversities of the whole assemblage, and different abundances of individual trophic groups. However, these differences could not be related solely to the directional effects of either latitude or shelf position. Rather than the observed fish assemblage being related to either of these geographic components, specific regions varied markedly. Specific attributes of certain sites are likely to drive the abundances of some groups. For example, herbivores were particularly abundant at both the inshore central and the Torres Strait regions. With just one inshore location from the Great Barrier Reef included in this analysis it is difficult to identify the underlying drivers with any certainty, but it is possible that conditions in these areas were more amenable to algal productivity compared to offshore reefs due gradients in water quality (Déath and Fabricius 2010). Planktivorous fish were at their lowest abundance at the inshore central section but were found in their highest abundances in the Torres Strait. The relatively high abundance of this trophic group in offshore locations may have been driven by gradients in both the availability of highly suitable habitat and abundant food sources at these more remote locations typical of offshore reefs (Emslie et al. 2019). Further investigation into these proximal drivers shaping the distribution of planktivorous fish and the specifics of complexity generating elements (i.e., coral demographics) would complement the analyses presented here.

Across almost all BRT models, depth emerged as the least influential driver of fish abundance. Whilst the relationship between fish communities and depth is complex and by no means ubiquitous, the lack of an effect in this analysis is noteworthy since depth is usually an influential driver in fish species distribution models (Melo-Merino et al. 2020; Pickens et al. 2021). Previously it has been shown that tropical fish communities show stratification along depth gradients, with abundance sometimes peaking in the top few metres of water (Hay 1981; Hall and Kingsford 2021). The results here do not necessarily contradict previous results, rather they suggest that the combined effects of complexity metrics were a stronger predictor for the abundance of the small site-attached fishes considered in this study, and once these effects were accounted for, depth explained very little additional variance in abundance of either assemblages or trophic groups. In the sites mapped in this study, particularly in sheltered locations, deeper sites tended to be less complex (see chapter 4). Whilst it is difficult to disentangle depth from structural complexity as a driver, the stronger selection for complexity metrics over depth among the BRT models suggests that it is a stronger driver over the depth ranges considered here (I.e., 3-8 m and 12-15m). Others have found that herbivores and carnivores are found in higher abundances on shallow reef slopes (Hay 1981), whilst omnivores and planktivores are more abundant further down the slope, mostly due to differences in food availability relative to each group (Jankowski et al. 2015), with depth supplanting structural complexity as a driver (Medeiros et al. 2010). It is possible that the depth ranges used in this study (the target depths of deep and shallow sites were 8m apart) were not sufficient to illicit strong responses in the fish community in comparison with the effects of the other variables considered (i.e., structural complexity metrics and geographic region).

Coral reefs have undergone drastic change over the past several decades, with overall declines in coral cover as well as shifts in the species composition of the remaining coral communities (Wilson et al. 2006; Knowlton and Jackson 2008; Kok et al. 2016; Hughes et al. 2018). Therefore, the total habitat availability, as well as the size distribution of shelter spaces within those habitats, has also undoubtedly changed. By breaking down the fish community into constituent trophic groups and focussing on small-bodied fish that by nature are generally site attached (Medeiros et al. 2010), I show that, even within this cohort, different groups of fish have different responses to structural complexity along the Great Barrier Reef and Torres Strait. Elucidating this may allow for more accurate predictions of the implications of future reef changes to fish communities. Different trophic groups appeared to respond to rugosity and fractal dimension differently in both the strength and direction of the effect, depending on their feeding mode and by extension, the relationships they have with their surrounding habitat. This study suggests that, whilst regionality plays an important role in structuring fish communities, complexity metrics also play a strong role in structuring the wider fish assemblage and individual feeding guilds. This underlines the importance of measuring complexity metrics at appropriate spatial scales (i.e., patch rather than the colony scale) and spatial resolutions (i.e., sub-centimetre). The unprecedentedly broad spatial extent of this study, which spans over ~1500km of latitude, and the focus on the foraging traits of different trophic groups rather than species identity, suggests that these patterns may be broadly applicable to tropical reef ecosystems. In the future, the incorporation of more benthic community metrics, such as coral coverage, size frequency distributions and taxonomic composition (all of which are available in the orthomosaics captured at each plot in this study) may aid in explaining the remainder of variance in abundance of these fish, which typically have strong associations with specific habitat types. Overall, this study highlights the importance of complexity in determining the composition and abundance of small fish communities and the need to consider the distribution of sizes of complexity generating elements, dependent on the group of fish being considered.

Chapter 6 General Discussion

Over the past few years (beginning in ca. 2015), three-dimensional habitat mapping has transformed from a novel research approach with good potential (Burns et al. 2015; Micheletti et al. 2015), into a widely adopted practise among research groups, since it is easily accessible (Raoult et al. 2016; Lange and Perry 2020) and requires less effort in the field than methods that return comparatively less rich data (Bayley et al. 2019). Yet, as with any emerging technologies, they should be explored fully prior to placing full trust in the results. Whilst this may seem unnecessary at first glance, especially given the apparent realism of 3D models on-screen, it is recognised that photogrammetry should be viewed with a critical lens and that there are gaps to be filled and criteria met before too much emphasis is placed on the ecological conclusions that result (Rossi et al. 2021). This thesis advances both the methodology and applications of underwater photogrammetry in this context by addressing some of the critical issues that might hinder the efficacy of how we obtain and extract data using three-dimensional habitat reconstructions. By critically assessing the outputs of photogrammetry via experimental manipulation in **chapter 2**, and developing a protocol to automate model processing in **chapter 3,** this thesis developed a scientifically robust, efficient and replicable methodology crucial to demonstrate meaningful ecological comparisons. By using the high-quality and repeatable routines established, **chapters 4 and 5** demonstrate the ecological principals that can be captured using photogrammetry to accomplish two of the main goals of habitat mapping studies; spatial comparisons in complexity to understand how and why various habitats differ among regions, and, to relate structural habitat attributes to inhabitant communities of other organisms (in this case fish). In the following discussion, I will focus on the key findings of, and linkages between, these four chapters and how together they advance the utility of habitat reconstructions built using photogrammetry and their application and interpretation in an ecological context.

6.1 Significance and ecological interpretations of this thesis

6.1.1 Methodological advancements in photogrammetry

This thesis makes novel contributions to both the implementation and interpretation of photogrammetry-based reconstructions of coral reefs. Together, **chapters 2 and 3** demonstrate both the facilitation and the importance of repeatability within the data gathering and reconstruction routines when using photogrammetry. Repeatability is critical, especially in the context of observational ecology (Powers and Hampton 2019), where variation in a multitude of natural processes cause differences in the community, and inform actionable science and management policies. **Chapter 2** addresses some novel aspects of comparability that may arise when reconstructions of habitats are built using different routines in both data collection and data processing protocols. Different researchers inevitably will use different means and processes to achieve similar goals and because of this, it is important to quantify and mitigate the resultant deviations this may cause. Hitherto, most studies addressing repeatability have focused primarily on a constrained set of performance metrics, notably reprojection error (Figueira et al. 2015; Raoult et al. 2017; Marre et al. 2019), which compares observed versus expected locations of points in 3D space to determine deviation from reality across the reconstruction. Instead, I chose to focus on the outputs of photogrammetry and how they may differ according to the choices researchers make based on constraints and needs of different studies. The analyses reveal that image density and resolution have a strong effect on 3D model resolution, but only image resolution strongly affected the rugosity (i.e., measured 3D surface area) of resultant models. Given the propensity for archival, 3D data to be shared and incorporated into complex analyses from across different studies and regions, it is highly important that studies report the image resolution and density used both in data collection and processing to assure comparability across datasets.

Chapter 3 furthers the concept of repeatability by introducing a freely available toolset with which to build models and extract a set of ecologically relevant structural complexity metrics from the models in a standardised manner. Using the principals of repeatability established in the previous chapter, a dataset comprising models of individual colonies was used in thematic analyses to explore scaling relationships of three-dimensional metrics among colonies of different size, taxonomic identity, and growth morphology. Using identical processing and metrics extraction routines across the sample, analyses revealed that the combination of simple metrics (colony diameter and morphotaxa) explained up to 95% of the variance in three-dimensional shelter provisioning of coral colonies. This supports the idea that simple metrics can be used as accurate proxies for 3D metrics when paired with appropriate information (House et al. 2018). Given the established importance of coral colonies as habitat for fish (Holbrook et al. 2002; Noonan et al. 2012; Agudo-Adriani et al. 2016; Pereira and Munday 2016), these two chapters together demonstrate how inconsistencies in methodologies can compromise model comparability, as well as the effectiveness of models, built using the correct procedures, to accurately glean ecologically useful information.

The demonstration of parameters affecting repeatability (**chapter 2**) and the use of the highly repeatable routines (**chapters 2-5**) presented in this thesis have the potential to improve on the accuracy of 3D growth rates versus routines where manual quality control is required during processing (Lange and Perry 2020; Lange et al. 2022). Further, the automatic derivation of a suite of metrics assessing different components of colony-level structural complexity (**chapter 3**) increases the available information with which to make accurate and relevant ecological comparisons within and among species (Million et al. 2021; Lange et al. 2022). Finally, the efficiency and speed at which processing can occur using automation tools that require little to no coding knowledge to implement means that both throughput and accessibility issues are largely negated (Million et al. 2021). By combining the use of automated tools with reporting of equipment and software specifications used to obtain metrics at any given spatial extent (colony or patch scale), the shareability of data will be enhanced, and ecological questions concerning the function of reefs can be answered more reliably.

Further, the three-dimensional metrics presented in **chapter 3** suggest that different morphotaxa deliver spatial refuge in different ways, with different groups tending towards relatively small or large shelter spaces. The suite of metrics extracted combined with the relevant thematic analyses demonstrate that using repeatable, automated routines that make identical decisions each time during the photogrammetric reconstruction and metrics extraction processes, ecologically meaningful comparisons between different benthic groups can be made. Others have demonstrated the importance of single coral colonies as habitat for fish (Noonan et al. 2012; Agudo-Adriani et al. 2016), which can be advanced by using the method presented in **chapter 3**. The analyses also show that there is an exceedingly strong correlation between colony diameter and the level of spatial refuge provided by a colony, according to its morphotaxa. These demonstrable principals, shown with a relatively small dataset, prove the concept, and the published tools provide others with a way of making the best use of their own photographic data, such that comparisons and the amalgamation of datasets to better answer ecological questions is possible. In addition, the growth rates of colonies, which hitherto have widely been measured using annual or radial extension rates, can be measured in greater detail using photogrammetry. Finally, the repeatable relationship between two- and three-dimensional metrics at the colony scale suggests that, with more data (the training dataset here consisted of 69 colonies), it may be possible to accurately estimate several higher order metrics of complexity from simple measurements in the absence of 3D reconstructions.

6.1.2 Ecological implications of the thesis

This thesis furthers our understanding of the importance of complexity in an ecological context using an unprecedented dataset covering 330 patches at 12 reefs (a total mapped area of over 23,000m^2) covering a cross-shelf gradient over 1,500km of latitudinal change at extremely high resolution (<5mm pixel size) (**chapters 4 and 5**). Broadly speaking, although the importance of structural complexity is well recognised (Graham and Nash 2013; Emslie et al. 2014; Graham 2014), it is of interest to determine exactly how and why the physical structure of reefs varies at multiple spatial extents (i.e., between individual reef patches, habitats and regions). Since it is becoming increasingly apparent that different structural attributes of environments relate directly to components of the animal community dependent on what relationship they have with their environment (Ferrari et al. 2017b; González-Rivero et al. 2017; Helder et al. 2022), characterisation of habitat complexity over broad spatial scales is especially useful.

Chapter 4 used the principals of repeatability established in **chapters 2 and 3** to generate a robust dataset comprising over 700,000 photographs worth of models covering a total reef area of some 23,760m^2. Given the potential for confounds that arise via differences in image density and resolution, as well as the increase in repeatability gained via the use of automated tools to generate and extract information, the robustness of this dataset generated over such a large spatial extent is unprecedented. The results described in **chapter 4**'s thematic analyses revealed varying patterns in two highly informative metrics of structural complexity, rugosity and fractal dimension, which appeared to mainly be driven by wave exposure. That these patterns were found to be consistent over 12 reef systems spanning over 1500km in latitude is an important step towards characterising structural complexity at broad, ecologically meaningful scales. Studies concerning spatial patterns in complexity or community organisation tend to be assessed primarily at relatively small spatial scales of patches on single reefs (Oakley-Cogan et al. 2020; Baum et al. 2022; Helder et al. 2022). This thesis suggests it is possible to generalise relationships across broad spatial scales. This is useful, particularly (as is most often the case) where highly detailed 3D habitat reconstructions, such as those produced in this thesis, are not available. Given the differences in the hydrodynamic conditions experienced at regional scales along the GBR caused by oceanic current circulation and the cross-shelf gradients in water quality and exposure to oceanic swell (Cumming and Bellwood 2023), it was an interesting and notable finding that significant differences in complexity were only found at local scales. According to the results of **chapter 4**, the primary driver for differences in complexity operate at local scales within reefs, rather than cross-shelf or latitudinal. Across the six regions, the only predictable patterns in structural complexity gradients were found on an intra-reef basis, with complexity decreasing along increasing gradients of wave exposure and depth.

That none of the six regions showed outstandingly high or low complexity across any habitat was somewhat unexpected given regional differences in environmental conditions and history of disturbance events such as bleaching, cyclones and crown-of-thorns starfish outbreaks. It is difficult to draw meaningful comparisons with other studies since **chapter 4** relates to a spatial analysis of habitat structure on a scale that has not before been presented in the literature. One comparable study, the Australian Institute of Marine Science's Long Term Monitoring Program (LTMP), monitored structural complexity over decadal timescales along the length of the Great Barrier Reef (Emslie et al. 2014) using video transects to visually estimate structural complexity on a scale of 1 (low complexity) to 5 (high complexity) , but in only one habitat (moderately exposed slopes) at each site. That study indicated that habitat complexity on certain reefs appeared to decline substantially from 2005 to 2010, mainly on those sites located in the offshore southern region. Methodological differences and temporal changes in the >10 years between that study and this thesis, and differential site selection could all account for the slightly different findings presented in **chapter 4**. High resolution habitat maps captured over relatively small spatial extents such as those captured here are unlikely to relate well to qualitative measures over larger scales, so future work on the relationship between complexity at small versus large extents at multiple resolutions would help to build a greater understanding of variation in reef structure.

The importance of coral reef structural complexity stems largely from the many processes that it facilitates, whether this is in relation to fish (Ferrari et al. 2017b; Fukunaga et al. 2020b; Helder et al. 2022) and/or other animal communities (Fuchs 2013), or some physical mediation that affects other processes (e.g., coastal protection) (Monismith et al. 2015; Harris et al. 2018). In terms of fish distributions, both regional and local-scale variables are influential to varying extents (Nash et al. 2014). Overall, geographic ranges of reef-dwelling species tend to be influenced by broad-scale environmental variables such as temperature ranges and connectivity between different reefs (Cumming and Bellwood 2023). At local, within-reef extents though, smaller scale habitat attributes are likely to be much more influential (Helder et al. 2022) as they vary greatly over considerably smaller distances (as evidenced in **chapter 4** which showed intra-reef variability to be greater than inter-reef variability). Further, it has been suggested that the spatial extent of structural complexity (i.e., the area over which complexity metrics are calculated and related to the biotic community) influences different fish groups according to home range extents, with roving pelagics responding strongly to broader-scale complexity, for example (Robinson et al. 2011).

Chapter 5 employs the principals of **chapters 2 and 3**, and furthers the spatial patterns shown in **chapter 4** to explore local and regional gradients in the distribution of small, predominantly site-attached fish species. A large body of research beginning in the 1970s suggested the importance of structural complexity for maintaining fish diversity (Risk 1972; Luckhurst and Luckhurst 1978) and abundance/biomass (Gratwicke and Speight 2005), but these were mainly based on a single, coarse metric of complexity. The coarse nature and low dimensionality of chain and tape rugosity limits its capability to discern complex biotic interactions that organisms with different strategies have with their environment (Komyakova et al. 2013). Technologies that permit 3D reconstructions of habitats though, have led to the quantification of different aspects of complexity (see **chapters 2, 3, 4**), which may relate to different components of the animal community (Harborne et al. 2011, 2012; Ferrari et al. 2017b) depending on their body size (Agudo-Adriani et al. 2016) and/or behavioural traits (Helder et al. 2022). The performance of structural complexity metrics in explaining variation in fish communities varies among studies, and it has been suggested that this is mainly due to mismatches between the spatial extent or scales of measurement and those of the target organisms (Pygas et al. 2020).

For most fish guilds, the paucity of data and species distribution maps is well-recognised, as is the need to consider the life history and ecology of different species complexes (Pickens et al. 2021). In this thesis, a trait-based approach (i.e., feeding guilds) was used to group together several species in a manner that reflected their different relationships with habitat features. By tailoring the extent of fish surveys ($10m^2$ transects) to areas encompassing the home range of small species (the surrounding ~70-$80m^2$), the habitat surveys were closely matched to their inhabitants. Using two metrics of structural complexity (rugosity and fractal dimension) that independently assess different aspects of complexity (see **chapter 4**), I showed that different trophic groups have different relationships with complexity. Although higher values of both measures of complexity were associated with higher overall abundances and diversity of small fish, relationships differed in both direction and strength with both components of complexity according to trophic group. The intricacies of these relationships revealed by high resolution habitat reconstructions at scales appropriate to the target organisms provide a much-needed mechanistic understanding of how reef ecosystems deliver their functions (Williams and Graham 2019).

Taken together, the findings of this thesis in terms of spatial distributions of complexity and the association of fish with certain components thereof have some implications and utility in determining the future trajectory of coral reefs and their inhabitants. Identifying reefscape traits that can be managed to preserve the functions delivered to and by fish groups is a key management objective (Maynard et al. 2015; Duarte et al. 2020), and this thesis supports other studies that have linked certain trait-based groups of fish to their surrounding habitat. It has been recognised for some time that reefscapes with higher levels of complexity foster resilience to perturbations (Friedlander et al. 2003; Darling et al. 2017; Yuval et al. 2023), and the type of data presented in this thesis promotes the accurate quantification of such traits. **Chapter 5**'s results indicate that there are certain, relatively narrow, ranges of complexity (rugosities of 2.5-4) over which sharp changes in abundance occur for some trophic groups of fish (carnivores, planktivores and invertivores). It appears that habitat patches with rugosity values of 4 and above are best able to support abundant small fish communities across multiple trophic groups. Although rugosity values above 4 were not associated with further increases in abundance of any of the considered trophic groups, these extremely high levels of complexity may still be beneficial. Such high levels of complexity may be indicative of areas that will provide a safeguard against the loss of complexity that often follows acute perturbations, since the structure of the habitat may be more likely to be retained above this level following disturbances. Areas with high levels of complexity currently (such as reef slopes sheltered from incoming wave energy) are likely to be somewhat protected from mechanical disturbances, and the high complexity may offer shading during temperature extremes, enabling them to resist disturbances and recover better when they do occur. Combined with the results of **chapter 4**, which identified key gradients in complexity at the intra-reef scale, present across the entire Great Barrier Reef and Torres Strait region, it is possible to predict locations where complexity is likely to be high even in the absence of high-resolution habitat reconstructions.

The results of **chapter 5** also indicate that changes in reefscapes are likely to differentially affect trophic groups since they are influenced in different ways by certain elements (i.e., metrics) of complexity. For example, planktivorous fish were positively correlated with both rugosity and fractal dimension, suggesting a preference for abundant fine-scale complexity, owing to their small body size and tendency to aggregate in schools. The non-random loss of corals depending on their ability to withstand disturbances (Marshall and Baird 2000; Graham et al. 2014), and the tendency for the small-scale complexity generated by high abundances of branching corals to be at the greatest risk (Dornelas et al. 2014; Hughes et al. 2018), implies that fish groups that associate the closest with fine-scale structure (such as small schooling planktivores) are the most at risk in the immediate aftermath of disturbances. Conversely, in **chapter 5** it was also found that small-bodied carnivores and omnivores were negatively associated with fractal dimension, instead being found in higher abundances in habitats comprising relatively large feature sizes. Such differential relationships highlight that, as reefscapes change under intense disturbance regimes, the effects on different components of even the small-bodied fish assemblage may be specific to different groups according to their habitat relationships. A shift (whether temporary or permanent) towards more structurally simple environments may be less detrimental to groups that do not rely on fine-scale complexity since their preferred habitat may still be sufficiently available to support healthy communities. The findings of this thesis highlight the importance of considering different aspects of the structure of habitats and the differential relationships various groups may have with their surroundings in explaining their distribution and predicting future trajectories under regimes of change. However, as previously noted (Brandl et al. 2016), it is important when conducting future research that trait-based approaches in their inherent broadness do not mask the loss of potentially important functions delivered by key species even if other members of the same group persist in the face of future disturbances.

From a management perspective, the trends and relationships presented in the second half of my thesis can inform decisions on management by helping to target key habitat areas for consideration in facilitating resilience and/or restoration efforts. Across the literature, complex habitats have been shown to promote bleaching avoidance or resilience through the provision of shelter from extreme conditions (i.e., shade from light and heat) (Hoegh-Guldberg 1999; Hoogenboom et al. 2017; Vo et al. 2019). Further, the provisioning of fine-scale complexity may provide enhanced resilience for corals since larvae can both attach and avoid predation in refuges provided by small structures. The ability of rugosity combined with fractal dimension to easily determine both the overall amount of structure and whether it is provided by comparatively small or large sized features make these two metrics valuable in assessing the relationships between reef organisms and their habitat.

6.2 Future research directions

This thesis presents a step forward in enhancing the repeatability of photogrammetry studies and uses an unprecedentedly large and high-resolution dataset to demonstrate the effectiveness of high-quality reconstructions in making spatially expansive comparisons among reef habitats. Whilst the power of thoughtfully collected, rigorously and replicably processed 3D datasets is apparent, there are many exciting avenues that will transform the method into a tool that can be used to collaborate globally to achieve management outcomes, accomplished by sheer data volume. Particularly in respect to **chapter 2**, which was aimed at quantifying the error associated with different equipment choices that arise due to time and budgetary constraints, there is still room to better quantify why models vary from one another in terms of their measured surfaces. I simulated the effect of choosing a high versus a low-quality camera setup by manipulating Metashape's quality settings, which down samples images according to the setting chosen. Whilst this provides a good broad overview of the effect of, for example, choosing a DSLR camera against a GoPro, it would be of great use to ecologists to test this directly. Whilst there are expectations in terms of what the effect of changing a particular parameter will be, **chapter 2** exemplifies that these expectations are by no means always met. Clearly, image resolution and density have compensatory effects on the resolution of the models, but this did not equate to the expected differences in rugosity. As such, the true nature of variation among different samples is not yet fully quantified, and it is not possible to compare models with absolute certainty when the methodologies used to build them are not subject to standardisation (i.e., a combination of the same camera, image collection protocols, automated processing protocols) for every model that is to be compared. If this deviation among methodologies can be fully understood and quantified, it can be accounted for, unlocking the powerful and hitherto unrealised potential to compare across studies and bolster our understanding of how reef systems function. In the future, the utility of metrics may be developed to better capture heterogeneity within each patch by developing further metrics that are able to capture variation of metrics that occur within different sections of the same habitat reconstruction.

Regarding the ecological applications of photogrammetry-derived 3D habitat maps, this thesis identifies some of the knowledge gaps that can be addressed in the future. **Chapters 4 and 5** present spatially expansive analyses of structural complexity variation and how different components of complexity relate to the inhabitant small fish community. A simple set of two metrics (rugosity and fractal dimension) highlighted some stark contrasts across habitats and depths in the structural characteristics of reefs located along the length of the Great Barrier Reef and Torres Strait islands. In the future, the further upscaling of research to include more habitat types (e.g., reef crests and flats along wider depth gradients) and reef conditions will lead to a more accurate understanding of the spatial variation in structural complexity.

Further, the enhanced understanding of how animals are supported by different components of complexity can be used to inform spatially explicit management strategies that are targeted more accurately at preserving key functions. To further this goal, future work should seek to complement **chapter 5** by determining the aspects and scale of complexity that benefit different trophic groups of larger-bodied fish species. The commercial importance of large, roving fish is one of the most important ecosystem services provided by reefs (Nagelkerken et al. 2005; Emslie et al. 2014), so better understanding factors related to the structure of the reef that influence their distribution should be a key management objective.

The unprecedented scale and detail of the dataset presented in this thesis serves as an important baseline of reef structural complexity across the Great Barrier Reef and the Torres Strait Islands. The repeatable differences in structural complexity at the intra-reef scale highlighted across shelf positions and latitudes and can be monitored in the context of change following disturbances. Further, repeated surveys of fish communities that may occur because of shifting structural characteristics can be used to determine how well fish communities are retained if losses in complexity do occur following further bleaching events, further informing future active management efforts. The flexibility of three-dimensional reconstructions in terms of the data that can be extracted is likely to result in more key complexity metrics that are important ecological indicators relating to specific components of the fish community, further bolstering the utility of the data presented. Paired with the relevant data on benthic communities (i.e., benthic cover, species composition and size-frequency distributions), it will be possible to determine more holistically the reasons for variation in structural complexity, and the resultant effects on concurrent faunal communities.

6.3 Final thoughts

The future of coral reefs is uncertain; global-scale perturbations are marked by declines in reef health that manifest as reconfigured or lost habitats, which places their functioning at risk. Society has recently awakened to the fact that humans are planetary stewards, and as such, management objectives evolve rapidly as the scientific community and policymakers arm themselves with better information. As of now, management of reef ecosystems focuses largely on how best to maintain reef functionality to support resilient benthic and animal communities. The exploration of new technologies such as photogrammetry has led to a rise in popularity of trait-based approaches, i.e., identifying quantifiable traits of ecosystems that infer functional attributes, which can be measured through time. One of the key features of habitats is their structural complexity, and the benefits it confers to different groups of inhabitant animals. The primary utility in using accurate metrics derived from 3D reconstructions is an improvement in our ability to uncover mechanistic relationships between animals and their environment, enabling more accurate predictions of the trajectory of animal communities under certain scenarios of change. Using new and emerging technologies is an exciting route to collaboration among the scientific community at a global scale, which is an approach that is necessary to effectively understand, maintain and restore fragile habitats. Understanding in detail how different aspects of structural complexity vary across spatial scales and influence different components of animal communities will promote more effective management.

7. Bibliography

Aben J, Pellikka P, Travis JMJ (2017) A call for viewshed ecology: Advancing our understanding of the ecology of information through viewshed analysis. Methods Ecol Evol 9:624–633

Adam TC, Brooks AJ, Holbrook SJ, Schmitt RJ, Washburn L, Bernardi G (2014) How will coral reef fish communities respond to climate-driven disturbances? Insight from landscape-scale perturbations. Oecologia 176:285–296

Agudo-Adriani EA, Cappelletto J, Cavada-Blanco F, Croquer A (2016) Colony geometry and structural complexity of the endangered species Acropora cervicornis partly explains the structure of their associated fish assemblage . PeerJ 4:e1861

Agudo-Adriani EA, Cappelletto J, Cavada-Blanco F, Cróquer A (2019) Structural Complexity and Benthic Cover Explain Reef-Scale Variability of Fish Assemblages in Los Roques National Park, Venezuela. Front Mar Sci 6:1–12

Almany GR (2004) Differential effects of habitat complexity, predators and competitors on abundance of juvenile and adult coral reef fishes. Oecologia 141:105–113

Althaus F, Hill N, Ferrari R, Edwards L, Przeslawski R, Schönberg CHL, Stuart-Smith R, Barrett N, Edgar G, Colquhoun J, Tran M, Jordan A, Rees T, Gowlett-Holmes K (2015) A standardised vocabulary for identifying benthic biota and substrata from underwater imagery: The CATAMI classification scheme. PLoS One 10:1–18

Alvarez-Filip L, Côté IM, Gill JA, Watkinson AR, Dulvy NK (2011a) Region-wide temporal and spatial variation in Caribbean reef architecture: Is coral cover the whole story? Glob Chang Biol 17:2470–2477

Alvarez-Filip L, Dulvy NK, Gill JA, Côté IM, Watkinson AR (2009) Flattening of Caribbean coral reefs: Region-wide declines in architectural complexity. Proc R Soc B Biol Sci 276:3019–3025

Alvarez-Filip L, Gill JA, Dulvy NK (2011b) Complex reef architecture supports more small-bodied fishes and longer food chains on Caribbean reefs. Ecosphere 2:art118

Álvarez-Noriega M, Baird AH, Dornelas M, Madin JS, Cumbo VR, Connolly SR (2016) Fecundity and the demographic strategies of coral morphologies. Ecology 97:3485–3493

Anderson KD, Heron SF, Pratchett MS (2015) Species-specific declines in the linear extension of branching corals at a subtropical reef, Lord Howe Island. Coral Reefs 34:479–490

Aston EA, Williams GJ, Green JAM, Davies AJ, Wedding LM, Gove JM, Jouffray JB, Jones TT, Clark J (2019) Scale-dependent spatial patterns in benthic communities around a tropical island seascape. Ecography (Cop) 42:578–590

Banner KM, Irvine KM, Rodhouse TJ (2020) The use of Bayesian priors in Ecology : The good , the bad and the not great. Methods Ecol Evol 11:882–889

Baum JK, Claar DC, Tietjen KL, Magel JMT, Maucieri DG, Cobb KM, Mcdevitt-Irwin JM (2022) Transformation of coral communities subjected to an unprecedented heatwave is modulated by local disturbance. Sci Adv 9:eabq5615

Bayley DTI, Mogg AOM (2020) A protocol for the large-scale analysis of reefs using Structure from Motion photogrammetry. Methods Ecol Evol 11:1410–1420

Bayley DTI, Mogg AOM, Koldewey H, Purvis A (2019) Capturing complexity: field-testing the use of ‘structure from motion’ derived virtual models to replicate standard measures of reef physical structure. PeerJ 7:e6540

Bellwood DR, Wainwright P (2001) Locomotion in labrid fishes: Implications for habitat use and cross-shelf biogeography on the Great Barrier Reef. Coral Reefs 20:139–150

Bolker BM, Brooks ME, Clark CJ, Geange SW, Poulsen JR, Stevens MHH, White JSS (2009) Generalized linear mixed models: a practical guide for ecology and evolution. Trends Ecol Evol 24:127–135

Brandl SJ, Emslie MJ, Ceccarelli DM (2016) Habitat degradation increases functional originality in highly diverse coral reef fish assemblages. Ecosphere 7:

Brandl SJ, Tornabene L, Goatley CHR, Casey J., Morais R, Cote I., Baldwin C., Parravicini V, Schiettekatte NM., Bellwood DR (2019) Demographic dynamics of the smallest marine vertebrates fuel coral-reef ecosystem functioning Simon. Science (80-) 364:1189–1192

Brooker RM, Munday PL, Mcleod IM, Jones GP (2013) Habitat preferences of a corallivorous reef fish: Predation risk versus food quality. Coral Reefs 32:613–622

Brooks ME, Kristensen K, van Benthem KJ, Magnusson A, Berg CW, Nielsen A, Skaug HJ, Mächler M, Bolker BM (2017) glmmTMB balances speed and flexibility among packages for zero-inflated generalized linear mixed modeling. R J 9:378–400

Brown BE (1997) Coral bleaching: Causes and consequences. Coral Reefs 16:129–138

Bruno JF, Stachowicz JJ, Bertness MD (2003) Inclusion of facilitation into ecological theory. Trends Ecol Evol 18:119–125

Bryson M, Ferrari R, Figueira W, Pizarro O, Madin J, Williams S, Byrne M (2017) Characterization of measurement errors using structure-from-motion and photogrammetry to measure marine habitat structural complexity. Ecol Evol 7:5669–5681

Bürkner PC (2017) brms: An R package for Bayesian multilevel models using Stan. J Stat Softw 80:

Burn D, Heron S, Pratchett D, Hoey A, Pratchett M, Thompson C (2018) Limited Cross-Shelf Variation in the Growth of Three Branching Corals on Australia’s Great Barrier Reef. Diversity 10:122

Burns JHR, Delparte D (2017) Comparison of commercial structure-from-motion photogrammety software used for underwater three-dimensional modeling of coral reef environments. Int Arch Photogramm Remote Sens Spat Inf Sci - ISPRS Arch 42:127–131

Burns JHR, Delparte D, Gates RD, Takabayashi M (2015) Utilizing underwater three-dimensional modeling to enhance ecological and biological studies of coral reefs. Int Arch Photogramm Remote Sens Spat Inf Sci - ISPRS Arch 40:61–66

Burns JHR, Delparte D, Kapono L, Belt M, Gates RD, Takabayashi M (2016) Assessing the impact of acute disturbances on the structure and composition of a coral community using innovative 3D reconstruction techniques. Methods Oceanogr 15–16:49–59

Bythell J, Pan P, Lee J (2001a) Three-dimensional morphometric measurements of reef corals using underwater photogrammetry techniques. Coral Reefs 20:193–199

Bythell J, Pan P, Lee J (2001b) Three-dimensional morphometric measurements of reef corals using underwater photogrammetry techniques. Coral Reefs 20:193–199

Calders K, Phinn S, Ferrari R, Leon J, Armston J, Asner GP, Disney M (2020) 3D Imaging Insights into Forests and Coral Reefs. Trends Ecol Evol 35:6–9

Callaghan DP, Leon JX, Saunders MI (2015) Wave modelling as a proxy for seagrass ecological modelling: Comparing fetch and process-based predictions for a bay and reef lagoon. Estuar Coast Shelf Sci 153:108–120

Carlot J, Lenihan HS, Kayal M, Pérez-Rosales G, Hedouin L, Parravicini V, Vousdoukas M, Rovere A, Adjeroud M, Perez-Rosales G (2022) Coral reef structural complexity loss exposes coastlines to waves. Under Rev Sci Reports 1–8

Carlot J, Rovère A, Casella E, Harris D, Grellet-Muñoz C, Chancerelle Y, Dormy E, Hedouin L, Parravicini V (2020) Community composition predicts photogrammetry-based structural complexity on coral reefs. Coral Reefs 39:967–975

Casella E, Collin A, Harris D, Ferse S, Bejarano S, Parravicini V, Hench JL, Rovere A (2017) Mapping coral reefs using consumer-grade drones and structure from motion photogrammetry techniques. Coral Reefs 36:269–275

Castaño D, Morales-de-Anda D, Prato J, Cupul-Magaña AL, Echeverry JP, Santos-Martínez A (2021) Reef Structural Complexity Influences Fish Community Metrics on a Remote Oceanic Island: Serranilla Island, Seaflower Biosphere Reserve, Colombia. Oceans 2:611–623

Ceccarelli DM, Jones GP, McCook LJ (2005) Foragers versus farmers: Contrasting effects of two behavioural groups of herbivores on coral reefs. Oecologia 145:445–453

Chan Y, Lo S, Quan A, Blumstein DT (2018) Ontogenetic shifts in perceptions of safety along structural complexity gradients in a territorial damselfish. Curr Zool 65:183–188

Chase JM, Blowes SA, Knight TM, Gerstner K, May F (2020) Ecosystem decay exacerbates biodiversity loss with habitat loss. Nature 584:238–243

Cheal A, Emslie M, Miller I, Sweatman H (2012) The distribution of herbivorous fishes on the Great Barrier Reef. Mar Biol 159:1143–1154

Cheal AJ, MacNeil MA, Emslie MJ, Sweatman H (2017) The threat to coral reefs from more intense cyclones under climate change. Glob Chang Biol 23:1511–1524

Chong-Seng KM, Mannering TD, Pratchett MS, Bellwood DR, Graham NAJ (2012) The influence of coral reef benthic condition on associated fish assemblages. PLoS One 7:1–10

Cignoni P, Callieri M, Corsini M, Dellepiane M, Ganovelli F, Ranzuglia G (2008) MeshLab: An open-source mesh processing tool. 6th Eurographics Ital Chapter Conf 2008 - Proc 129–136

Connell JH, Series N, Mar N, Connell JH (2010) A Celebration and Exploration of Joseph H. Connell's Conceptual and Empirical Influence, Inspiration, and Legacy in Ecological Research and Education. Bull Ecol Soc Am 91:464–466

Cooper TF, Uthicke S, Humphrey C, Fabricius KE (2007) Gradients in water column nutrients, sediment parameters, irradiance and coral reef development in the Whitsunday Region, central Great Barrier Reef. Estuar Coast Shelf Sci 74:458–470

Cruz-Trinidad A, Aliño PM, Geronimo RC, Cabral RB (2014) Linking Food Security with Coral Reefs and Fisheries in the Coral Triangle. Coast Manag 42:160–182

Cumming GS, Bellwood DR (2023) Broad-scale analysis of fish community data suggests critical need to support regional connectivity of coral reefs. Ecol Appl e2849

Cunliffe AM, Brazier RE, Anderson K (2016) Ultra-fine grain landscape-scale quantification of dryland vegetation structure with drone-acquired structure-from-motion photogrammetry. Remote Sens Environ 183:129–143

Curtis-quick JA, Ahmadia GN, Smith DJ (2012) Feeding plasticity of reef fish. Proc 12th Int Coral Reef Symp Cairns, Aust 9–13

D'Urban Jackson T, Williams GJ, Walker-Springett G, Davies AJ (2020) Three-dimensional digital mapping of ecosystems: A new era in spatial ecology. Proc R Soc B Biol Sci 287:1–10

Dalben A, Floeter SR (2012) Cryptobenthic reef fishes: Depth distribution and correlations with habitat complexity and sea urchins. J Fish Biol 80:852–865

Darling ES, Pratchett MS, Januchowski-Hartley FA, Wilson SK, Graham NAJ, Nash KL (2017) Relationships between structural complexity, coral traits, and reef fish assemblages. Coral Reefs 36:561–575

De'ath G, Fabricius KE, Sweatman H, Puotinen M (2012) The 27-year decline of coral cover on the Great Barrier Reef and its causes. Proc Natl Acad Sci 109:17995–17999

Déath G, Fabricius K (2010) Water quality as a regional driver of coral biodiversity and macroalgae on the great barrier reef. Ecol Appl 20:840–850

DeVantier LM, De'ath G, Turak E, Done TJ, Fabricius KE (2006) Species richness and community structure of reef-building corals on the nearshore Great Barrier Reef. Coral Reefs 25:329–340

Dietzel A, Bode M, Connolly SR, Hughes TP (2021) The population sizes and global extinction risk of reef-building coral species at biogeographic scales. Nat Ecol Evol 5:663–669

Dornelas M, Gotelli NJ, McGill B, Shimadzu H, Moyes F, Sievers C, Magurran AE (2014) Assemblage time series reveal biodiversity change but not systematic loss. Science (80-) 344:296–299

Dornelas M, Madin JS, Baird AH, Connolly SR (2017) Allometric growth in reef-building corals. Proc R Soc B Biol Sci 284:

Doropoulos C, Evensen NR, Gómez-Lemos LA, Babcock RC (2017) Density-dependent coral recruitment displays divergent responses during distinct early life-history stages. R Soc Open Sci 4:

Dorph A, Swan M, Rochelmeyer E, Di Stefano J (2020) Complex habitat drives mammal communities in a flammable landscape. For Ecol Manage 462:

Doszpot N, McWilliam M, Pratchett M, Hoey A, Figueira W (2019) Plasticity in Three-Dimensional Geometry of Branching Corals Along a Cross-Shelf Gradient. Diversity 11:44

Duarte CM, Agusti S, Barbier E, Britten GL, Castilla JC, Gattuso JP, Fulweiler RW, Hughes TP, Knowlton N, Lovelock CE, Lotze HK, Predragovic M, Poloczanska E, Roberts C, Worm B (2020) Rebuilding marine life. Nature 580:39–51

Dubuc B, Roques-Carmes C, Tricot C, Zucker S (1987) The variation method: a technique to estimate the fractal dimension of surfaces. Vis Commun Image Process II 845:241–248

Duce S, Vila-Concejo A, McCarroll RJ, Yiu B, Perris LA, Webster JM (2022) Field measurements show rough fore reefs with spurs and grooves can dissipate more wave energy than the reef crest. Geomorphology 413:108365

Easton EE, Gaymer CF, Friedlander AM, Herlan JJ (2018) Effects of herbivores, wave exposure and depth on benthic coral communities of the Easter Island ecoregion. Mar Freshw Res

Eggertsen M, Chacin DH, van Lier J, Eggertsen L, Fulton CJ, Wilson S, Halling C, Berkström C (2020) Seascape configuration and fine-scale habitat complexity shape parrotfish distribution and function across a coral reef lagoon. Diversity 12:1–19

Elith J, Leathwick JR, Hastie T (2008) A working guide to boosted regression trees. J Anim Ecol 77:802–813

Emslie MJ, Cheal AJ, Johns KA (2014) Retention of habitat complexity minimizes disassembly of reef fish communities following disturbance: A large-scale natural experiment. PLoS One 9:e105384

Emslie MJ, Cheal AJ, Sweatman H, Delean S (2008) Recovery from disturbance of coral and reef fish communities on the Great Barrier Reef, Australia. Mar Ecol Prog Ser 371:177–190

Emslie MJ, Logan M, Ceccarelli DM, Cheal AJ, Hoey AS, Miller I, Sweatman HPA (2012) Regional-scale variation in the distribution and abundance of farming damselfishes on Australia's Great Barrier Reef. Mar Biol 159:1293–1304

Emslie MJ, Logan M, Cheal AJ (2019) The distribution of planktivorous damselfishes (pomacentridae) on the great barrier reef and the relative influences of habitat and predation. Diversity 11:

Emslie MJ, Pratchett MS, Cheal AJ, Osborne K (2010) Great Barrier Reef butterflyfish community structure: The role of shelf position and benthic community type. Coral Reefs 29:705–715

Feary DA, Almany GR, Jones GP, McCormick MI (2007) Coral degradation and the structure of tropical reef fish communities. Mar Ecol Prog Ser 333:243–248

Ferrari R, Bryson M, Bridge T, Hustache J, Williams SB, Byrne M, Figueira W (2016a) Quantifying the response of structural complexity and community composition to environmental change in marine communities. Glob Chang Biol 22:1965–1975

Ferrari R, Figueira WF, Pratchett MS, Boube T, Adam A, Kobelkowsky-Vidrio T, Doo SS, Atwood TB, Byrne M (2017a) 3D photogrammetry quantifies growth and external erosion of individual coral colonies and skeletons. Sci Rep 7:1–9

Ferrari R, Lachs L, Pygas DR, Humanes A, Sommer B, Figueira WF, Edwards AJ, Bythell JC, Guest JR (2021) Photogrammetry as a tool to improve ecosystem restoration. Trends Ecol Evol 36:1093–1101

Ferrari R, Malcolm HA, Byrne M, Friedman A, Williams SB, Schultz A, Jordan AR, Figueira WF (2017b) Habitat structural complexity metrics improve predictions of fish abundance and distribution. Ecography (Cop) 41:1077–1091

Ferrari R, Marzinelli EM, Ayroza CR, Jordan A, Figueira WF, Byrne M, Malcolm HA, Williams SB, Steinberg PD (2018) Large-scale assessment of benthic communities across multiple marine protected areas using an autonomous underwater vehicle. PLoS One 13:1–20

Ferrari R, McKinnon D, He H, Smith RN, Corke P, González-Rivero M, Mumby PJ, Upcroft B (2016b) Quantifying multiscale habitat structural complexity: A cost-effective framework for underwater 3D modelling. Remote Sens 8:rs8020113

Ferrario F, Beck MW, Storlazzi CD, Micheli F, Shepard CC, Airoldi L (2014) The effectiveness of coral reefs for coastal hazard risk reduction and adaptation. Nat Commun 5:1–9

Figueira W, Ferrari R, Weatherby E, Porter A, Hawes S, Byrne M (2015) Accuracy and precision of habitat structural complexity metrics derived from underwater photogrammetry. Remote Sens 7:16883–16900

Finstad AG, Einum S, Forseth T, Ugedal O (2007) Shelter availability affects behaviour, size-dependent and mean growth of juvenile Atlantic salmon. Freshw Biol 52:1710–1718

Floros C, Schleyer MH (2017) The functional importance of Acropora austera as nursery areas for juvenile reef fish on South African coral reefs. Coral Reefs 36:139–149

Forsmoo J, Anderson K, Macleod CJA, Wilkinson ME, DeBell L, Brazier RE (2019) Structure from motion photogrammetry in ecology: Does the choice of software matter? Ecol Evol 9:12964–12979

Franklin JF, Pelt R Van (2004) Spatial apects of structural complexity in old-growth forests. J For 102:22–28

Friedlander AM, Brown EK, Jokiel PL, Smith WR, Rodgers KS (2003) Effects of habitat, wave exposure, and marine protected area status on coral reef fish assemblages in the Hawaiian archipelago. Coral Reefs 22:291–305

Froese R, Pauly D (2010) FishBase. FishBase

Fryer JG (1983) Stereoscopic coral maps from underwater photogrammetry. Cartogr J 20:23–25

Fuchs T (2013) Effects of habitat complexity on invertebrate biodiversity. Immed Sci Ecol 2:1–10

Fukunaga A, Burns J, Craig B, Kosaki R (2019) Integrating three-dimensional benthis habitat characterization techniques into ecological monitoring of coral reefs. J Mar Sci Eng 7:27

Fukunaga A, Burns JHR (2020) Metrics of coral reef structural complexity extracted from 3D mesh models and digital elevation models. Remote Sens 12:

Fukunaga A, Burns JHR, Pascoe KH, Kosaki RK (2020a) Associations between benthic cover and habitat complexity metrics obtained from 3D reconstruction of coral reefs at different resolutions. Remote Sens 12:

Fukunaga A, Kosaki RK, Pascoe KH, Burns JHR (2020b) Fish assemblage structure in the northwestern hawaiian islands is associated with the architectural complexity of coral-reef habitats. Diversity 12:1–19

Fukunaga A, Pascoe KH, Pugh AR, Kosaki RK, Burns JHR (2022) Underwater Photogrammetry Captures the Initial Recovery of a Coral Reef at Lalo Atoll. Diversity 14:1–8

Gallagher C, Doropoulos C (2017) Spatial refugia mediate juvenile coral survival during coral–predator interactions. Coral Reefs 36:51–61

Gardiner NM, Jones GP (2010) Synergistic effects of habitat preference and gregarious behaviour on habitat use in coral reef cardinalfish. Coral Reefs 29:845–856

Gaynor KM, Brown JS, Middleton AD, Power ME, Brashares JS (2019) Landscapes of Fear: Spatial Patterns of Risk Perception and Response. Trends Ecol Evol 34:355–368

George EE, Mullinix JA, Meng F, Bailey BA, Edwards C, Felts B, Haas AF, Hartmann AC, Mueller B, Roach TNF, Salamon P, Silveira C, Vermeij MJA, Rohwer F, Luque A (2021) Space-filling and benthic competition on coral reefs. PeerJ 9:

Gigliotti LC, Slotow R, Hunter LTB, Fattebert J, Sholto-Douglas C, Jachowski DS (2020) Habitat complexity and lifetime predation risk influence mesopredator survival in a multi-predator system. Sci Rep 10:

Gigliotti LC, Slotow R, Sholto-Douglas C, de Vos C, Jachowski DS (2021) Short-term predation risk and habitat complexity influence cheetah antipredator behaviours. Anim Behav 178:175–184

González-Rivero M, Bongaerts P, Beijbom O, Pizarro O, Friedman A, Rodriguez-Ramirez A, Upcroft B, Laffoley D, Kline D, Bailhache C, Vevers R, Hoegh-Guldberg O (2014) The Catlin Seaview Survey - kilometre-scale seascape assessment, and monitoring of coral reef ecosystems. Aquat Conserv Mar Freshw Ecosyst 24:184–198

González-Rivero M, Harborne AR, Herrera-Reveles A, Bozec YM, Rogers A, Friedman A, Ganase A, Hoegh-Guldberg O (2017) Linking fishes to multiple metrics of coral reef structural complexity using three-dimensional technology. Sci Rep 7:1–15

Goreau T (1959) The Ecology of Jamaican Coral Reefs I. Species Composition and Zonation. Ecology 40:67–90

Graham MH (2004) Effects of local deforestation on the diversity and structure of southern California giant kelp forest food webs. Ecosystems 7:341–357

Graham NAJ (2014) Habitat complexity: Coral structural loss leads to fisheries declines. Curr Biol 24:R359–R361

Graham NAJ, Chong-Seng KM, Huchery C, Januchowski-Hartley FA, Nash KL (2014) Coral reef community composition in the context of disturbance history on the Great Barrier Reef, Australia. PLoS One 9:

Graham NAJ, Nash KL (2013) The importance of structural complexity in coral reef ecosystems. Coral Reefs 32:315–326

Graham NAJ, Wilson SK, Jennings S, Polunin NVC, Bijoux JP, Robinson J (2006) Dynamic fragility of oceanic coral reef ecosystems. Proc Natl Acad Sci U S A 103:8425–8429

Graham NAJ, Wilson SK, Pratchett MS, Polunin NVC, Spalding MD (2009) Coral mortality versus structural collapse as drivers of corallivorous butterflyfish decline. Biodivers Conserv 18:3325–3336

Gratwicke B, Speight M. (2005) The relationship between fish species richness, abundance and habitat complexity in a range of shallow tropical marine habitats. J Fish Biol 66:650–667

Green S, Bevan A, Shapland M (2014) A comparative assessment of structure from motion methods for archaeological research. J Archaeol Sci 46:173–181

Griffiths SP, Davis AR, West RJ (2006) Role of habitat complexity in structuring temperate rockpool ichthyofaunas. Mar Ecol Prog Ser 313:227–239

Groves SH, Holstein DM, Enochs IC, Kolodzeij G, Manzello DP, Brandt ME, Smith TB (2018) Growth rates of Porites astreoides and Orbicella franksi in mesophotic habitats surrounding St. Thomas, US Virgin Islands. Coral Reefs 37:345–354

Guo T, Capra A, Troyer M, Gruen A, Brooks AJ, Hench JL, Schmitt RJ, Holbrook SJ, Dubbini M (2016) Accuracy assessment of underwater photogrammetric three dimensional modelling for coral reefs. Int Arch Photogramm Remote Sens Spat Inf Sci - ISPRS Arch 41:821–828

Gust N, Choat JH, McCormick MI (2001) Spatial variability in reef fish distribution, abundance, size and biomass: A multi-scale analysis. Mar Ecol Prog Ser 214:237–251

Hall A, Kingsford MJ (2021) Habitat type and complexity drive fish assemblages in a tropical seascape. J Fish Biol 99:1364–1379

Harborne AR, Mumby PJ, Ferrari R (2012) The effectiveness of different meso-scale rugosity metrics for predicting intra-habitat variation in coral-reef fish assemblages. Environ Biol Fishes 94:431–442

Harborne AR, Mumby PJ, Kennedy E V., Ferrari R (2011) Biotic and multi-scale abiotic controls of habitat quality: Their effect on coral-reef fishes. Mar Ecol Prog Ser 437:201–214

Harris DL, Pomeroy A, Power H, Casella E, Rovere A, Webster JM, Parravicini V, Canavesio R, Collin A

(2018) Coral reef structural complexity provides important coastal protection from waves under rising sea levels. Sci Adv 4:eaao4350

Hartig F (2022) DHARMa: Residual Diagnostics for Hierarchical (Multi-Level / Mixed) Regression Models. R package version 0.4.6. R Packag version 046

Hay M (1981) Spatial patterns of grazing intensity on a caribbean barrier reef: herbivory and algal distribution. Aquat Bot 11:97–109

Helder NK, Burns JHR, Green SJ (2022) Intra-habitat structural complexity drives the distribution of fish trait groups on coral reefs. Ecol Indic 142:109266

Hesterberg SG, Duckett CC, Salewski EA, Bell SS (2017) Three-dimensional interstitial space mediates predator foraging success in different spatial arrangements. Ecology 98:1153–1162

Hijmans R. (2022) No Title. Doc R Packag "dismo" ver 13-9

Hitt S, Pittman SJ, Nemeth RS (2011) Diel movements of fishes linked to benthic seascape structure in a caribbean coral reef ecosystem. Mar Ecol Prog Ser 427:275–291

Hixon M., Beets J. (1993) Predation, prey refuges, and the structure of coral-reef fish assemblages. Ecol Monogr 63:77–101

Hixon MA, Menge BA (1991) Species diversity: Prey refuges modify the interactive effects of predation and competition. Theor Popul Biol 39:178–200

Hoegh-Guldberg O (1999) Climate change, coral bleaching and the future of the world's coral reefs. Mar Freshw Res 50:839–866

Hoegh-Guldberg O, Mumby PJ, Hooten AJ, Steneck RS, Greenfield P, Gomez E, Harvell CD, Sale PF, Edwards AJ, Caldeira K, Knowlton N, Eakin CM, Iglesias-Prieto R, Muthiga N, Bradbury RH, Dubi A, Hatziolos ME (2007) Coral reefs under rapid climate change and ocean acidification. Science 318:1737–42

Hoey AS, Bellwood DR (2010) Damselfish territories as a refuge for macroalgae on coral reefs. Coral Reefs 29:107–118

Hoey AS, Brandl SJ, Bellwood DR (2013) Diet and cross-shelf distribution of rabbitfishes (f. Siganidae) on the northern Great Barrier Reef: Implications for ecosystem function. Coral Reefs 32:973–984

Holbrook SJ, Brooks AJ, Schmitt RJ (2002) Variation in structural attributes of patch-forming corals and in patterns of abundance of associated fishes. Mar Freshw Res 53:1045–1053

Hoogenboom MO, Frank GE, Chase TJ, Jurriaans S, Álvarez-Noriega M, Peterson K, Critchell K, Berry KLE, Nicolet KJ, Ramsby B, Paley AS (2017) Environmental drivers of variation in bleaching severity of Acropora species during an extreme thermal anomaly. Front Mar Sci 4:1–16

House JE, Brambilla V, Bidaut LM, Christie AP, Pizarro O, Madin JS, Dornelas M (2018) Moving to 3D: relationships between coral planar area, surface area and volume. PeerJ 6:e4280

Hughes T., Barnes M., Bellwood DR, Cinner J., Cumming G., Jackson JB., Kleypas J, van de Leemput I., Lough J., Morrison T., Palumbi S., van Nes E., Scheffer M (2017a) Coral reefs in the anthropocene. Nature 546:82–90

Hughes TP, Kerry JT, Álvarez-Noriega M, Álvarez-Romero JG, Anderson KD, Baird AH, Babcock RC, Beger M, Bellwood DR, Berkelmans R, Bridge TC, Butler IR, Byrne M, Cantin NE, Comeau S, Connolly SR, Cumming GS, Dalton SJ, Diaz-Pulido G, Eakin CM, Figueira WF, Gilmour JP, Harrison HB, Heron SF, Hoey AS, Hobbs JPA, Hoogenboom MO, Kennedy E V., Kuo CY, Lough JM, Lowe RJ, Liu G, McCulloch MT, Malcolm HA, McWilliam MJ, Pandolfi JM, Pears RJ, Pratchett MS, Schoepf V, Simpson T, Skirving WJ, Sommer B, Torda G, Wachenfeld DR, Willis BL, Wilson SK (2017b) Global warming and recurrent mass bleaching of corals. Nature 543:373–377

Hughes TP, Kerry JT, Baird AH, Connolly SR, Chase TJ, Dietzel A, Hill T, Hoey AS, Hoogenboom MO, Jacobson M, Kerswell A, Madin JS, Mieog A, Paley AS, Pratchett MS, Torda G, Woods RM (2019a) Global warming impairs stock–recruitment dynamics of corals. Nature 568:387–390

Hughes TP, Kerry JT, Baird AH, Connolly SR, Dietzel A, Eakin CM, Heron SF, Hoey AS, Hoogenboom MO, Liu G, McWilliam MJ, Pears RJ, Pratchett MS, Skirving WJ, Stella JS, Torda G (2018) Global warming transforms coral reef assemblages. Nature 556:492–496

Hughes TP, Kerry JT, Connolly SR, Baird AH, Eakin CM, Heron SF, Hoey AS, Hoogenboom MO, Jacobson M, Liu G, Pratchett MS, Skirving W, Torda G (2019b) Ecological memory modifies the cumulative impact of recurrent climate extremes. Nat Clim Chang 9:40–43

Iglhaut J, Cabo C, Puliti S, Piermattei L, O'Connor J, Rosette J (2019) Structure from Motion Photogrammetry in Forestry: a Review. Curr For Reports 5:155–168

Iribarren C, Kotler BP (2012) Foraging patterns of habitat use reveal landscape of fear of Nubian ibex Capra nubiana. Wildlife Biol 18:194–201

Jankowski MW, Gardiner NR, Jones GP (2015) Depth and reef profile: Effects on the distribution and abundance of coral reef fishes. Environ Biol Fishes 98:1373–1386

Januchowski-Hartley FA, Graham NAJ, Wilson SK, Jennings S, Perry CT (2017) Drivers and predictions of coral reef carbonate budget trajectories. Proc R Soc B Biol Sci 284:

Johansen JL, Bellwood DR, Fulton CJ (2008) Coral reef fishes exploit flow refuges in high-flow habitats. Mar Ecol Prog Ser 360:219–226

Johansen JL, Fulton CJ, Bellwood DR (2007) Avoiding the flow: Refuges expand the swimming potential of coral reef fishes. Coral Reefs 26:577–583

Jouffray J, Wedding LM, Norstro A V, Donovan MK, Williams GJ, Crowder LB, Erickson AL, Friedlander AM, Graham NAJ, Gove JM, Kappel C V, Kittinger JN, Lecky J, Oleson KLL (2019) Parsing human and biophysical drivers of coral reef regimes. Proc R Soc B Biol Sci 286:20182544

Jupiter S, Roff G, Marion G, Henderson M, Schrameyer V, McCulloch M, Hoegh-Guldberg O (2008) Linkages between coral assemblages and coral proxies of terrestrial exposure along a cross-shelf gradient on the southern Great Barrier Reef. Coral Reefs 27:887–903

Karkarey R, Alcoverro T, Kumar S, Arthur R (2017) Coping with catastrophe: foraging plasticity enables a benthic predator to survive in rapidly degrading coral reefs. Anim Behav 131:13–22

Kerr JT, Ostrovsky M (2003) From space to species: Ecological applications for remote sensing. Trends Ecol Evol 18:299–305

Kerry JT, Bellwood DR (2015) Do tabular corals constitute keystone structures for fishes on coral reefs? Coral Reefs 34:41–50

Knowlton N, Jackson JBC (2008) Shifting baselines, local impacts, and global change on coral reefs. PLoS Biol 6:0215–0220

Knudby A, LeDrew E (2007) Measuring Structural Complexity on Coral Reefs. Proc Am Acadamy Underw Sci 26th Symp 181–188

Knudby A, LeDrew E, Brenning A (2010) Predictive mapping of reef fish species richness, diversity and biomass in Zanzibar using IKONOS imagery and machine-learning techniques. Remote Sens Environ 114:1230–1241

Kok JE, Graham NAJ, Hoogenboom MO (2016) Climate-driven coral reorganisation influences aggressive behaviour in juvenile coral-reef fishes. Coral Reefs 35:473–483

Komyakova V, Munday PL, Jones GP (2013) Relative importance of coral cover, habitat complexity and diversity in determining the structure of reef fish communities. PLoS One 8:1–12

Kotilainen AT, Kaskela AM (2017) Comparison of airborne LiDAR and shipboard acoustic data in complex shallow water environments: Filling in the white ribbon zone. Mar Geol 385:250–259

Kunkel CM, Hallberg RW, Oppenheimer M (2006) Coral reefs reduce tsunami impact in model simulations. Geophys Res Lett 33:4–7

Lange ID, Molina-Hernández A, Medellín-Maldonado F, Perry CT, Álvarez-Filip L (2022) Structure-from-motion photogrammetry demonstrates variability in coral growth within colonies and across habitats. PLoS One 17:1–15

Lange ID, Perry CT (2020) A quick, easy and non-invasive method to quantify coral growth rates using photogrammetry and 3D model comparisons. Methods Ecol Evol 11:714–726

Lavy A, Eyal G, Neal B, Keren R, Loya Y, Ilan M (2015) A quick, easy and non-intrusive method for underwater volume and surface area evaluation of benthic organisms by 3D computer modelling. Methods Ecol Evol 6:521–531

Leathwick JR, Elith J, Francis MP, Hastie T, Taylor P (2006) Variation in demersal fish species richness in the oceans surrounding New Zealand: an analysis using boosted regression trees J. Mar Ecol Prog Ser 321:267–281

van Lier JR, Wilson SK, Depczynski M, Wenger LN, Fulton CJ (2018) Habitat connectivity and complexity underpin fish community structure across a seascape of tropical macroalgae meadows. Landsc Ecol 33:1287–1300

Loke LHL, Chisholm RA (2022) Measuring habitat complexity and spatial heterogeneity in ecology. Ecol Lett 25:2269–2288

Lowe RJ, Falter JL (2015) Oceanic forcing of coral reefs. Ann Rev Mar Sci 7:43–66

Luckhurst BE, Luckhurst K (1978) Analysis of the influence of substrate variables on coral reef fish communities. Mar Biol 49:317–323

MacArthur R (1958) Population ecology of some Warblers of Northeastern coniferous forests. Ecology 39:599–619

MacArthur RH, MacArthur JW (1961) On Bird Species Diversity. Ecology 42:594–598

Madin J., Asbury M, Schiettekatte NM., Dornelas M, Pizarro O, Reichert J (2023) A word on habitat complexity. Ecol Lett 26:1021–1024

Madin JS (2005) Mechanical limitations of reef corals during hydrodynamic disturbances. Coral Reefs 24:630–635

Madin JS, Baird AH, Dornelas M, Connolly SR (2014) Mechanical vulnerability explains size-dependent mortality of reef corals. Ecol Lett 17:1008–1015

Madin JS, Connolly SR (2006) Ecological consequences of major hydrodynamic disturbances on coral reefs. Nature 444:477–480

Madin JS, Hoogenboom MO, Connolly SR, Darling ES, Falster DS, Huang D, Keith SA, Mizerek T, Pandolfi JM, Putnam HM, Baird AH (2016) A trait-based approach to advance coral reef science. Trends Ecol Evol 31:419–428

Magel JMT, Burns JHR, Gates RD, Baum JK (2019) Effects of bleaching-associated mass coral mortality on reef structural complexity across a gradient of local disturbance. Sci Rep 9:2512

Marre G, Holon F, Luque S, Boissery P, Deter J (2019) Monitoring Marine Habitats With Photogrammetry: A Cost-Effective, Accurate, Precise and High-Resolution Reconstruction Method. Front Mar Sci 6:1–15

Marshall PA, Baird AH (2000) Bleaching of corals on the Great Barrier Reef: Differential susceptibilities among taxa. Coral Reefs 19:155–163

Maynard JA, McKagan S, Raymundo L, Johnson S, Ahmadia GN, Johnston L, Houk P, Williams GJ, Kendall M, Heron SF, van Hooidonk R, Mcleod E, Tracey D, Planes S (2015) Assessing relative resilience potential of coral reefs to inform management. Biol Conserv 192:109–119

McCormick MI (1994) Comparison of field methods for measuring surface topography and their associations with a tropical reef fish assemblage. Mar Ecol Prog Ser 112:87–96

McCormick MI, Löonnstedt OM (2013) Degrading habitats and the effect of topographic complexity on risk assessment. Ecol Evol 3:4221–4229

McKinnon D, He H, Upcroft B, Smith RN (2011) Towards automated and in-situ, near-real time 3-D reconstruction of coral reef environments. Ocean - MTS/IEEE Kona, Progr B

Medeiros PR, Grempel RG, Souza AT, Ilarri MI, Rosa RS (2010) Non-random reef use by fishes at two dominant zones in a tropical, algal-dominated coastal reef. Environ Biol Fishes 87:237–246

Mellin C, Thompson A, Jonker MJ, Emslie MJ (2019) Cross-shelf variation in coral community response to disturbance on the Great Barrier Reef. Diversity 11:

Melo-Merino S, Reyes-Bonilla H, Lira-Noriega A (2020) Ecological niche models and species distribution models in marine environments: A literature review and spatial analysis of evidence. Ecol Modell 415:108837

Ménard A, Turgeon K, Roche DG, Binning SA, Kramer DL (2012) Shelters and their use by fishes on fringing coral reefs. PLoS One 7:e38450

Menna F, Nocerino E, Drap P, Remondino F, Murtiyoso A, Grussenmeyer P, Borlin N (2018) Improving underwater accuracy by empirical weighting of image observations. Int Arch Photogramm Remote Sens Spat Inf Sci XLII–2:699–705

Menna F, Nocerino E, Fassi F, Remondino F (2016a) Geometric and Optic Characterization of a Hemispherical Dome Port for Underwater Photogrammetry. Sensors 1–21

Menna F, Nocerino E, Remondino F (2016b) Photogrammetric Modelling of Submerged Structures : Influence of Underwater Environment and Lens Ports on Three- Dimensional (3D) Measurements. 279–303

Micheletti N, Chandler JH, Lane SN (2015) Investigating the geomorphological potential of freely available and accessible structure-from-motion photogrammetry using a smartphone. Earth Surf Process Landforms 40:473–486

Million WC, O'Donnell S, Bartels E, Kenkel CD (2021) Colony-Level 3D Photogrammetry Reveals That Total Linear Extension and Initial Growth Do Not Scale With Complex Morphological Growth in the Branching Coral, Acropora cervicornis. Front Mar Sci 8:1–12

Monismith SG, Rogers JS, Koweek D, Dunbar RB (2015) Frictional wave dissipation on a remarkably rough reef. Geophys Res Lett 42:4063–4071

Morais J, Morais R, Tebbett SB, Bellwood DR (2022) On the fate of dead coral colonies. Funct Ecol 3148–3160

Moran D, Reaka M (1988) Bioerosion and availability of shelter for benthic reef organisms. Mar Ecol Prog Ser 44:249–263

Morillo-Velarde PS, Briones-Fourzán P, Álvarez-Filip L, Aguíñiga-García S, Sánchez-González A, Lozano-Álvarez E (2018) Habitat degradation alters trophic pathways but not food chain length on shallow Caribbean coral reefs. Sci Rep 8:1–12

Mortelliti A, Fagiani S, Battisti C, Capizzi D, Boitani L (2010) Independent effects of habitat loss, habitat fragmentation and structural connectivity on forest-dependent birds. Divers Distrib 16:941–951

Mosbrucker AR, Major JJ, Spicer KR, Pitlick J (2017) Camera system considerations for geomorphic applications of SfM photogrammetry. Earth Surf Process Landforms 42:969–986

De Moustier C, Matsumoto H (1993) Seafloor acoustic remote sensing with multibeam echo-sounders and bathymetric sidescan sonar systems. Mar Geophys Res 15:27–42

Muko S, Kawasaki K, Sakai K, Takasu F, Shigesada N (2000) Morphological plasticity in the coral Porites sillimaniani and its adaptive significance. Bull Mar Sci 66:225–239

Mumby PJ (2017) Embracing a world of subtlety and nuance on coral reefs. Coral Reefs 36:1003–1011

Mumby PJ, Wabnitz CCC (2002) Spatial patterns of aggression, territory size, and harem size in five sympatric Caribbean parrotfish species. Environ Biol Fishes 63:265–279

Munday PL (2004) Habitat loss, resource specialization, and extinction on coral reefs. Glob Chang Biol 10:1642–1647

Nagelkerken I, Vermonden K, Moraes OCC, Debrot AO, Nagelkerken WP (2005) Changes in coral reef communities and an associated reef fish species, Cephalopholis cruentata (Lacépède), after 30 years on Curaçao (Netherlands Antilles). Hydrobiologia 549:145–154

Mac Nally R, Parkinson A, Horrocks G, Conole L, Tzaros C (2001) Relationships between terrestrial vertebrate diversity, abundance and availability of coarse woody debris on south-eastern Australian floodplains. Biol Conserv 99:191–205

Nash KL, Allen CR, Angeler DG, Barichievy C, Eason T, Garmestani AS, Graham NAJ, Granholm D, Knutson M, Nelson RJ, Nyström M, Stow CA, Sundstrom SM (2014) Discontinuities, cross-scale patterns, and the organization of ecosystems. Ecology 95:654–67

Nash KL, Graham NAJ, Wilson SK, Bellwood DR (2013) Cross-scale habitat structure drives fish body size distributions on coral reefs. Ecosystems 16:478–490

Naumann MS, Niggl W, Laforsch C, Glaser C, Wild C (2009) Coral surface area quantification-evaluation of established techniques by comparison with computer tomography. Coral Reefs 28:109–117

Nay TJ, Johansen JL, Habary A, Steffensen JF, Rummer JL (2015) Behavioural thermoregulation in a temperature-sensitive coral reef fish, the five-lined cardinalfish (Cheilodipterus quinquelineatus). Coral Reefs 34:1261–1265

Newman SJ, Williams DMB, Russ GR (1997) Patterns of zonation of assemblages of the Lutjanidae, Lethrinidae and Serranidae (Epinephelinae) within and among mid-shelf and outer-shelf reefs in the central Great Barrier Reef. Mar Freshw Res 48:119–128

Newman SP, Meesters EH, Dryden CS, Williams SM, Sanchez C, Mumby PJ, Polunin NVC (2015) Reef flattening effects on total richness and species responses in the Caribbean. J Anim Ecol 84:1678–1689

Nimon KF (2012) Statistical assumptions of substantive analyses across the general linear model: A mini-review. Front Psychol 3:1–5

Nocerino E, Menna F, Gruen A, Troyer M, Capra A, Castagnetti C, Rossi P, Brooks AJ, Schmitt RJ, Holbrook SJ (2020) Coral reef monitoring by scuba divers using underwater photogrammetry and geodetic surveying. Remote Sens 12:

Noonan SHC, Jones GP, Pratchett MS (2012) Coral size, health and structural complexity: Effects on the ecology of a coral reef damselfish. Mar Ecol Prog Ser 456:127–137

Nunes JACC, Sampaio CLS, Barros F (2015) The influence of structural complexity and reef habitat types on flight initiation distance and escape behaviors in labrid fishes. Mar Biol 162:493–499

Oakley-Cogan A, Tebbett SB, Bellwood DR (2020) Habitat zonation on coral reefs: Structural complexity, nutritional resources and herbivorous fish distributions. PLoS One 15:1–23

Osuka K, Kochzius M, Vanreusel A, Obura D, Samoilys M (2018) Linkage between fish functional groups and coral reef benthic habitat composition in the Western Indian Ocean. J Mar Biol Assoc United Kingdom 98:387–400

Ow YX, Todd PA (2010) Light-induced morphological plasticity in the scleractinian coral Goniastrea pectinata and its functional significance. Coral Reefs 29:797–808

Palma M, Casado MR, Pantaleo U, Cerrano C (2017) High resolution orthomosaics of African coral reefs: A tool for wide-scale benthic monitoring. Remote Sens 9:1–26

Pamela Delarue EM, Kerr SE, Lee Rymer T (2015) Habitat complexity, environmental change and personality: A tropical perspective. Behav Processes 120:101–110

Paxton AB, Pickering EA, Adler AM, Taylor JC, Peterson CH (2017) Flat and complex temperate reefs provide similar support for fish: Evidence for a unimodal species-habitat relationship. PLoS One 12:1–22

Pereira P, Munday P (2016) Coral colony size and structure as determinants of habitat use and fitness of coral-dwelling fishes. Mar Ecol Prog Ser 553:163–172

Perry CT, Murphy GN, Kench PS, Edinger EN, Smithers SG, Steneck RS, Mumby PJ (2014) Changing dynamics of Caribbean reef carbonate budgets: Emergence of reef bioeroders as critical controls on present and future reef growth potential. Proc R Soc B Biol Sci 281:

Pickens BA, Carroll R, Schirripa MJ, Forrestal F, Friedland KD, Taylor JC (2021) A systematic review of spatial habitat associations and modeling of marine fish distribution: A guide to predictors, methods, and knowledge gaps. PLoS One 16:1–21

Pittman SJ, Costa B, Jeffrey CFG, Caldow C (2010) Importance of Seascape Complexity for Resilient Fish Habitat and Sustainable Fisheries. Proc 63rd Gulf Caribb Fish Inst 420–426

Pittman SJ, Costa BM, Battista TA (2009) Using LiDAR bathymetry and boosted regression trees to predict the diversity and abundance of fish and corals. J Coast Res 10053:27–38

Polunin NVC, Roberts CM (1993) Greater biomass and value of target coral-reef fishes in two small Caribbean marine reserves. Mar Ecol Prog Ser 100:167–176

Powers SM, Hampton SE (2019) Open science, reproducibility, and transparency in ecology. Ecol Appl 29:1–8

Pratchett MS (2005) Dietary overlap among coral-feeding butterflyfishes (Chaetodontidae) at Lizard Island, northern Great Barrier Reef. Mar Biol 148:373–382

Pratchett MS, Hoey AS, Wilson SK (2014) Reef degradation and the loss of critical ecosystem goods and services provided by coral reef fishes. Curr Opin Environ Sustain 7:37–43

Purkis SJ, Graham NAJ, Riegl BM (2008) Predictability of reef fish diversity and abundance using remote sensing data in Diego Garcia (Chagos Archipelago). Coral Reefs 27:167–178

Pygas DR, Ferrari R, Figueira WF (2020) Review and meta-analysis of the importance of remotely sensed habitat structural complexity in marine ecology. Estuar Coast Shelf Sci 235:106468

Quadros ALS, Barros F, Blumstein DT, Meira VH, Nunes JACC (2019) Structural complexity but not territory sizes influences flight initiation distance in a damselfish. Mar Biol 166:

Randall CJ, Giuliano C, Heyward AJ, Negri AP (2021) Enhancing Coral Survival on Deployment Devices With Microrefugia. Front Mar Sci 8:

Raoult V, David PA, Dupont SF, Mathewson CP, O'Neill SJ, Powell NN, Williamson JE (2016) GoPros™ as an underwater photogrammetry tool for citizen science. PeerJ 4:e1960

Raoult V, Reid-Anderson S, Ferri A, Williamson J (2017) How reliable is structure from motion (SfM) over time and between observers? A case study using coral reef bommies. Remote Sens 9:740

Rees MJ, Knott NA, Neilson J, Linklater M, Osterloh I, Jordan A, Davis AR (2018) Accounting for habitat structural complexity improves the assessment of performance in no-take marine reserves. Biol Conserv 224:100–110

Reichert J, Backes AR, Schubert P, Wilke T (2017) The power of 3D fractal dimensions for comparative shape and structural complexity analyses of irregularly shaped organisms. Methods Ecol Evol 8:1650–1658

Reichert J, Schellenberg J, Schubert P, Wilke T (2016) 3D scanning as a highly precise, reproducible, and minimally invasive method for surface area and volume measurements of scleractinian corals. Limnol Oceanogr Methods 14:518–526

Richardson LE, Graham NAJ, Hoey AS (2017a) Cross-scale habitat structure driven by coral species composition on tropical reefs. Sci Rep 7:7557

Richardson LE, Graham NAJ, Pratchett MS, Eurich JG, Hoey AS (2018) Mass coral bleaching causes biotic homogenization of reef fish assemblages. Glob Chang Biol 24:3117–3129

Richardson LE, Graham NAJ, Pratchett MS, Hoey AS (2017b) Structural complexity mediates functional structure of reef fish assemblages among coral habitats. Environ Biol Fishes 100:193–207

Ridgeway G (2022) Generalized boosted regression models. Doc R Packag "gbm", ver 2181

Rilov G, Figueira WF, Lyman SJ, Crowder LB (2007) Complex habitats may not always benefit prey: Linking visual field with reef fish behavior and distribution. Mar Ecol Prog Ser 329:225–238

Risk M. (1972) Fish diversity on a coral reef in the Virgin Islands. Atoll Res Bull 153:1–5

Roberts TE, Moloney JM, Sweatman HPA, Bridge TCL (2015) Benthic community composition on submerged reefs in the central Great Barrier Reef. Coral Reefs 34:569–580

Robinson LM, Elith J, Hobday AJ, Pearson RG, Kendall BE, Possingham HP, Richardson AJ (2011) Pushing the limits in marine species distribution modelling: Lessons from the land present challenges and opportunities. Glob Ecol Biogeogr 20:789–802

Rogers A, Blanchard JL, Mumby PJ (2014) Vulnerability of coral reef fisheries to a loss of structural complexity. Curr Biol 24:1000–1005

Rogers A, Blanchard JL, Mumby PJ (2018a) Fisheries productivity under progressive coral reef degradation. J Appl Ecol 55:1041–1049

Rogers A, Blanchard JL, Newman SP, Dryden CS, Mumby PJ (2018b) High refuge availability on coral reefs increases the vulnerability of reef-associated predators to overexploitation. Ecology 99:450–463

Rossi P, Ponti M, Righi S, Castagnetti C, Simonini R, Mancini F, Agrafiotis P, Bassani L, Bruno F, Cerrano C, Cignoni P, Corsini M, Drap P, Dubbini M, Garrabou J, Gori A, Gracias N, Ledoux JB, Linares C, Mantas TP, Menna F, Nocerino E, Palma M, Pavoni G, Ridolfi A, Rossi S, Skarlatos D, Treibitz T, Turicchia E, Yuval M, Capra A (2021) Needs and Gaps in Optical Underwater Technologies and Methods for the Investigation of Marine Animal Forest 3D-Structural Complexity. Front Mar Sci 8:1–9

Russ G (1984) Distribution and abundance of herbivorous grazing fishes in the central Great Barrier Reef. I. Levels of variability across the entire continental shelf. Mar Ecol Prog Ser 20:23–34

Ruxton GD, Beauchamp G (2008) Time for some a priori thinking about post hoc testing. Behav Ecol 19:690–693

Sano M, Shimizu M, Nose Y (1984) Changes in structure of coral reef fish communities by destruction of hermatypic corals: observational and experimental views. Pacific Sci 38:51–79

Sass GG, Gille CM, Hinke JT, Kitchell JF (2006) Whole-lake influences of littoral structural complexity and prey body morphology on fish predator-prey interactions. Ecol Freshw Fish 15:301–308

Shaish L, Levy G, Katzir G, Rinkevich B (2010) Employing a highly fragmented, weedy coral species in reef restoration. Ecol Eng 36:1424–1432

Shannon CE&, Weaver W (1949) The mathematical theory of communication. Univ Illinois Urbana, Chicago, London 3–24

She M, Nakath D, Song Y, Köser K (2022) Refractive geometry for underwater domes. ISPRS J Photogramm Remote Sens 183:525–540

Sheppard C (1982) Coral Populations on Reef Slopes and Their Major Controls. Mar Ecol Prog Ser 7:83–115

Shortis M (2015) Calibration Techniques for Accurate Measurements by Underwater Camera Systems. Sensors 15:30810–30826

Skarlatos D, Agrafiotis P, Menna F, Nocerino E, Remondino F (2018) Ground control networks for underwater photogrammetry in archaeological excavations. IMEKO Int Conf Metrol Archaeol Cult Herit 2016–2018

Spalding MD, Brown BE (2015) Warm water coral reefs and climate change. Science (80-) 350:769–771

Storlazzi CD, Brown EK, Field ME, Rodgers K, Jokiel PL (2005) A model for wave control on coral breakage and species distribution in the Hawaiian Islands. Coral Reefs 24:43–55

Storlazzi CD, Dartnell P, Hatcher G., Gibbs A. (2016) End of the chain? Rugosity and fine-scale bathymetry from existing underwater digital imagery using structure-from-motion (SfM) technology. Coral Reefs 35:889–894

Streit RP, Cumming GS, Bellwood DR (2019) Patchy delivery of functions undermines functional redundancy in a high diversity system. Funct Ecol 33:1144–1155

Suchley A, Alvarez-Filip L (2018) Local human activities limit marine protection efficacy on Caribbean coral reefs. Conserv Lett 11:1–9

Taniguchi H, Nakano S, Tokeshi M (2003) Influences of habitat complexity on the diversity and abundance of epiphytic invertebrates on plants. Freshw Biol 48:718–728

Tews J, Brose U, Grimm V, Tielbörger K, Wichmann MC, Schwager M, Jeltsch F (2004) Animal species diversity driven by habitat heterogeneity/diversity: The importance of keystone structures. J Biogeogr 31:79–92

Tinkham WT, Swayze NC (2021) Influence of agisoft metashape parameters on uas structure from motion individual tree detection from canopy height models. Forests 12:1–14

Todd PA (2008) Morphological plasticity in scleractinian corals. Biol Rev 83:315–337

Tokeshi M, Arakaki S (2012) Habitat complexity in aquatic systems: Fractals and beyond. Hydrobiologia 685:27–47

Torres-Pulliza D, Dornelas MA, Pizarro O, Bewley M, Blowes SA, Boutros N, Brambilla V, Chase TJ, Frank G, Friedman A, Hoogenboom MO, Williams S, Zawada KJA, Madin JS (2020) A geometric basis for surface habitat complexity and biodiversity. Nat Ecol Evol 4:1495–1501

Trebilco R, Dulvy NK, Stewart H, Salomon AK (2015) The role of habitat complexity in shaping the size structure of a temperate reef fish community. Mar Ecol Prog Ser 532:197–211

Urbina-barreto I, Elise, Simon, Guilhaumon F, Bruggemann JH, Pinel R, Kulbicki M, Vigliola L, Mou-Tham G, Mahamadaly V, Facon M, Bureau S, Peignon C, Dutrieux E, Garnier R, Penin L, Adjeroud M (2021) Underwater photogrammetry reveals new links between coral reefscape traits and fishes that ensure key functions. Ecosphere 13:e3934

Urbina-barreto I, Pinel R, Fr L, Mahamadaly V, Elise S, Kulbicki M, Quod J, Dutrieux E (2020) Quantifying the shelter capacity of coral reefs using photogrammetric 3D modeling : From colonies to reefscapes.

Veal CJ, Holmes G, Nunez M, Hoegh-Guldberg O, Osborn J (2010) A comparative study of methods for surface area and three dimensional shape measurement of coral skeletons. Limnol Oceanogr Methods 8:241–253

Ventura D, Bonifazi A, Gravina MF, Belluscio A, Ardizzone G (2018) Mapping and Classification of Ecologically Sensitive Marine Habitats Using Unmanned Aerial Vehicle (UAV) Imagery and Object-Based Image Analysis (OBIA). Remote Sens 10:1331

Vine P (1974) Effects of algal grazing and aggressive behaviour of the fishes Pomacentrus lividus and Acanthurus sohal on coral-reef ecology. Mar Biol 24:131–136

Vivian DN, Yee SH, Courtney LA, Fisher WS (2019) Estimating 3-dimensional surface areas of small scleractinian corals. Caribb J Sci 49:192

Vo ST, Hua TT, Phan KH (2019) A study of coral reef resilience and implications of adaptive management and rehabilitation in Khanh Hoa Province, Vietnam. Acta Oceanol Sin 38:112–117

Warfe DM, Barmuta LA (2006) Habitat structural complexity mediates food web dynamics in a freshwater macrophyte community. Oecologia 150:141–154

Wasserman RJ, Alexander ME, Weyl OLF, Barrios-O'Neill D, Froneman PW, Dalu T (2016) Emergent effects of structural complexity and temperature on predator-prey interactions. Ecosphere 7:

Wearn O, Reuman D, Ewers R (2012) Extinction Debt and Windows of Conservation Opportunity in the Brazilian Amazon. Science (80-) 338:228–232

Wedding LM, Jorgensen S, Lepczyk CA, Friedlander AM (2019) Remote sensing of three-dimensional coral reef structure enhances predictive modeling of fish assemblages. Remote Sens Ecol Conserv 5:150–159

Wickham H (2016) ggplot2: Elegant graphics for data analysis. Springer-Verlag New York ISBN 978-3:https://ggplot2.tidyverse.org

Wild C, Hoegh-Guldberg O, Naumann MS, Colombo-Pallotta MF, Ateweberhan M, Fitt WK, Iglesias-Prieto R, Palmer C, Bythell JC, Ortiz JC, Loya Y, Van Woesik R (2011) Climate change impedes scleractinian corals as primary reef ecosystem engineers. Mar Freshw Res 62:205–215

Wilding TA, Rose CA, Downie MJ (2007) A novel approach to measuring subtidal habitat complexity. J Exp Mar Bio Ecol 353:279–286

Williams GJ, Graham NAJ (2019) Rethinking coral reef functional futures. Funct Ecol 33:942–947

Williams GJ, Smith JE, Conklin EJ, Gove JM, Sala E, Sandin SA (2013) Benthic communities at two remote pacific coral reefs: Effects of reef habitat, depth, and wave energy gradients on spatial patterns. PeerJ 2013:1–26

Williams SE, Marsh H, Winter J (2002) Spatial scale, species diversity, and habitat structure: Small mammals in Australian tropical rain forest. Ecology 83:1317–1329

Willis SC, Winemiller KO, Lopez-Fernandez H (2005) Habitat structural complexity and morphological diversity of fish assemblages in a Neotropical floodplain river. Oecologia 142:284–295

Willis TJ, Anderson MJ (2003) Structure of cryptic reef fish assemblages: Relationships with habitat characteristics and predator density. Mar Ecol Prog Ser 257:209–221

Wilson S., Burgess S., Cheal A., M E, Fisher R, Miller I, Polunin NV., Sweatman HP. (2008) Habitat utilization by coral reef fish: implications for specialists vs. generalists in a changing environment. J Anim Ecol 77:220–229

Wilson SK, Graham NAJ, Polunin NVC (2007) Appraisal of visual assessments of habitat complexity and benthic composition on coral reefs. Mar Biol 151:1069–1076

Wilson SK, Graham NAJ, Pratchett MS, Jones GP, Polunin NVC (2006) Multiple disturbances and the global degradation of coral reefs: Are reef fishes at risk or resilient? Glob Chang Biol 12:2220–2234

Yanovski R, Abelson A (2019) Structural complexity enhancement as a potential coral-reef restoration tool. Ecol Eng 132:87–93

Yao Y, Vehtari A, Simpson D, Gelman A (2018) Using stacking to average Bayesian predictive distributions (with discussion). Bayesian Anal 13:917–1007

Young GC, Dey S, Rogers AD, Exton D (2017) Cost and time-effective method for multi-scale measures of rugosity, fractal dimension, and vector dispersion from coral reef 3D models. PLoS One 13:1–18

Yu D, Yau KKW (2012) Conditional Akaike information criterion for generalized linear mixed models. Comput Stat Data Anal 56:629–644

Yuval M, Alonso I, Eyal G, Tchernov D, Loya Y, Murillo AC, Treibitz T (2021) Repeatable Semantic Reef-Mapping through Photogrammetry and Label-Augmentation. Remote Sens 13:659

Yuval M, Pearl N, Tchernov D (2022) 3D Imaging Reveals Resilience : Storm Impact on Coral Reef Structural Complexity. bioRxiv 1–21

Yuval M, Pearl N, Tchernov D, Martinez S, Loya Y, Bar-massada A, Treibitz T (2023) Assessment of storm impact on coral reef structural complexity. Sci Total Environ 891:164493

Zawada KJA, Dornelas M, Madin JS (2019a) Quantifying coral morphology. Coral Reefs

Zawada KJA, Madin JS, Baird AH, Bridge TCL, Dornelas M (2019b) Morphological traits can track coral reef responses to the Anthropocene. Funct Ecol 962–975

Zhang K, Yang F, Zhang H, Su D, Li Q (2017) Morphological characterization of coral reefs by combining lidar and MBES data: A case study from Yuanzhi Island, South China Sea. J Geophys Res Ocean 122:4779–4790

8. Supplementary Materials

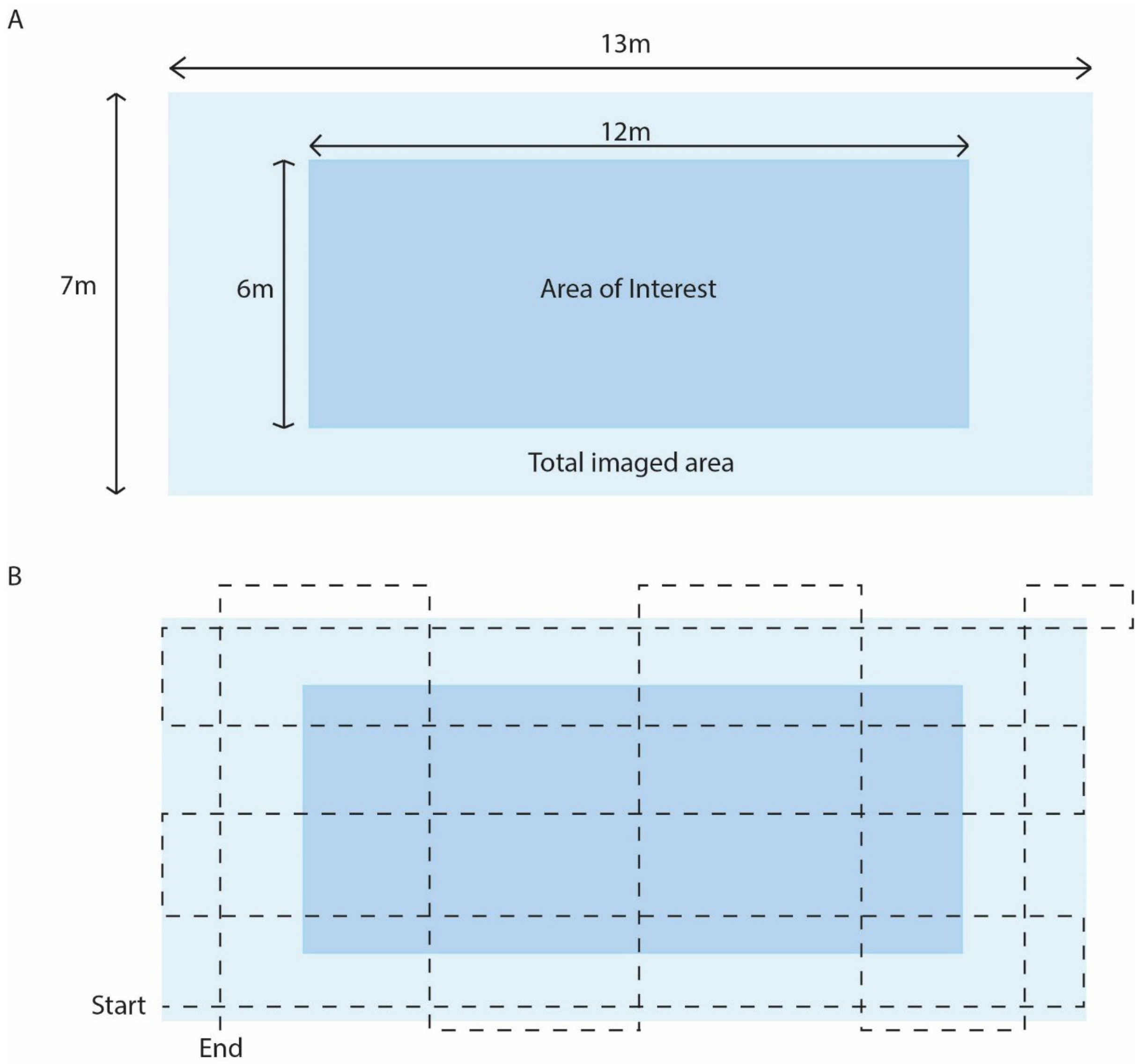

Figure S2.1 | (A) Area of interest and total area of benthos imaged by divers during photo acquisition. (B) Swimming pattern of divers used during data capture, showing the five longways and five sideways passes of the total imaged area.

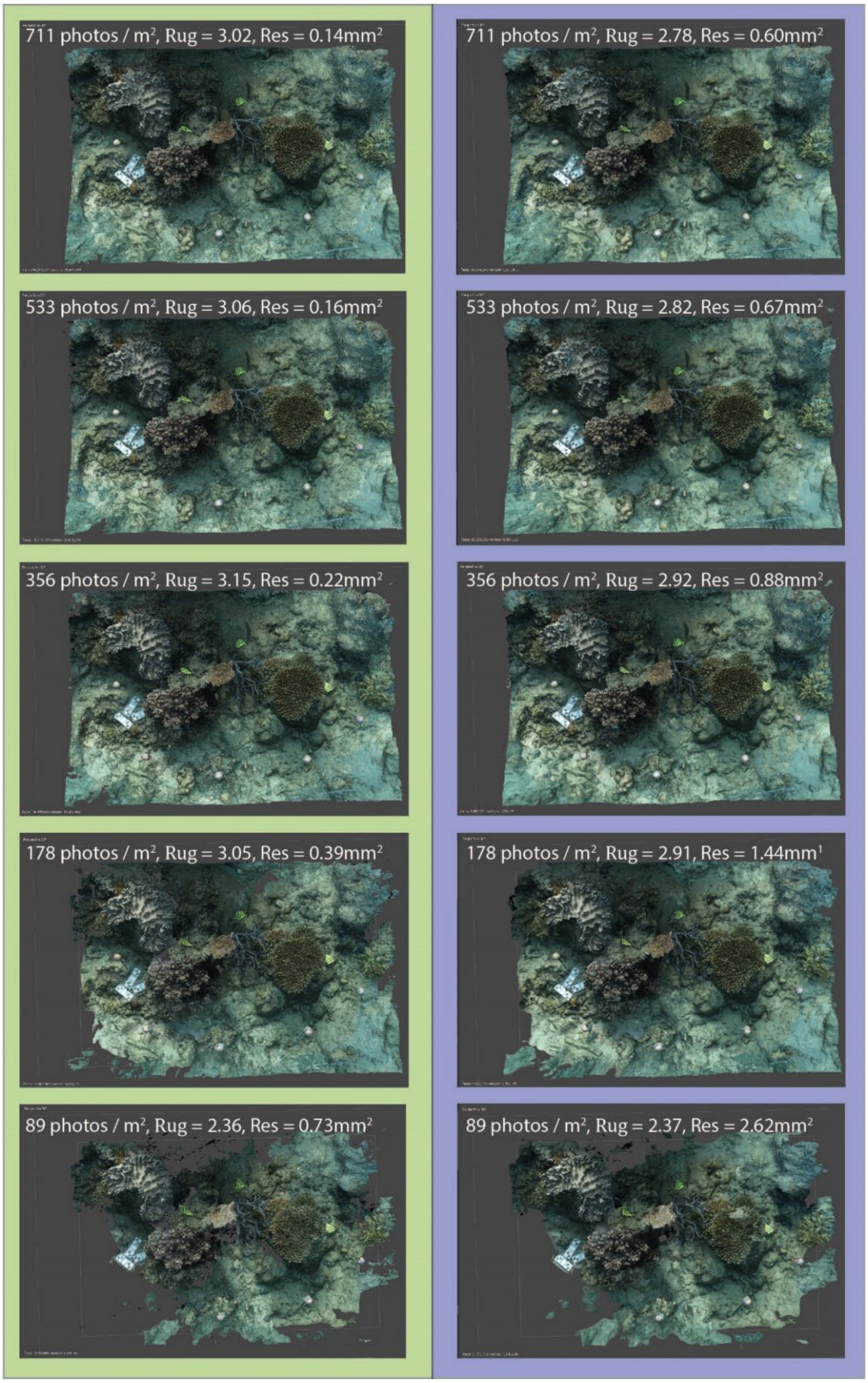

Figure S2.2 | Small spatial extent model example showing the change in resolution and progressive degradation in model completeness as photographs were removed from the dataset. Green indicates higher image resolution (medium dense cloud quality), blue indicates lower image resolution (low dense cloud quality).

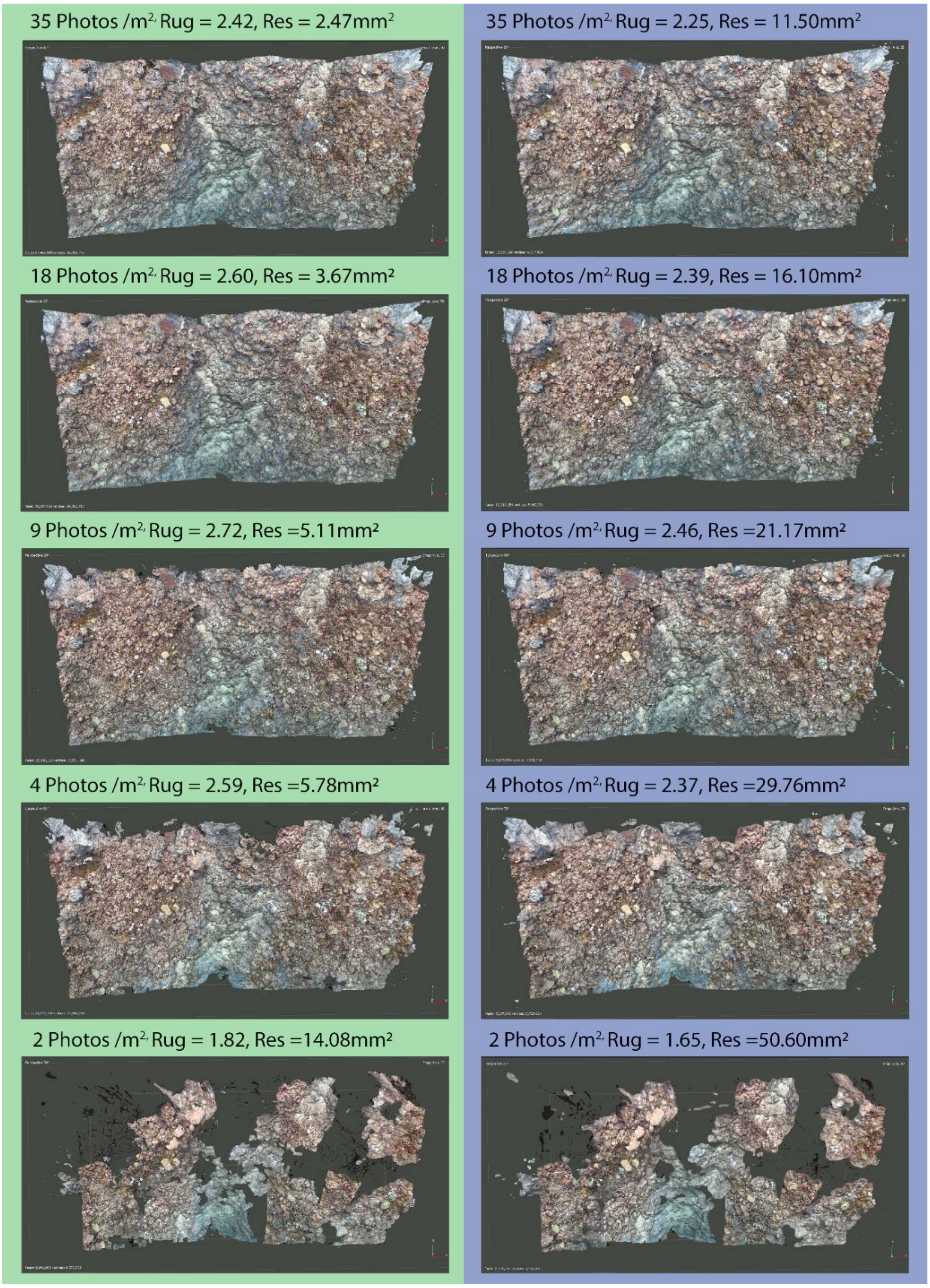

Figure S2.3 | Large spatial extent model example showing the change in resolution and progressive degradation in model completeness as photographs were removed from the dataset. Green indicates medium dense cloud quality, blue indicates low quality.

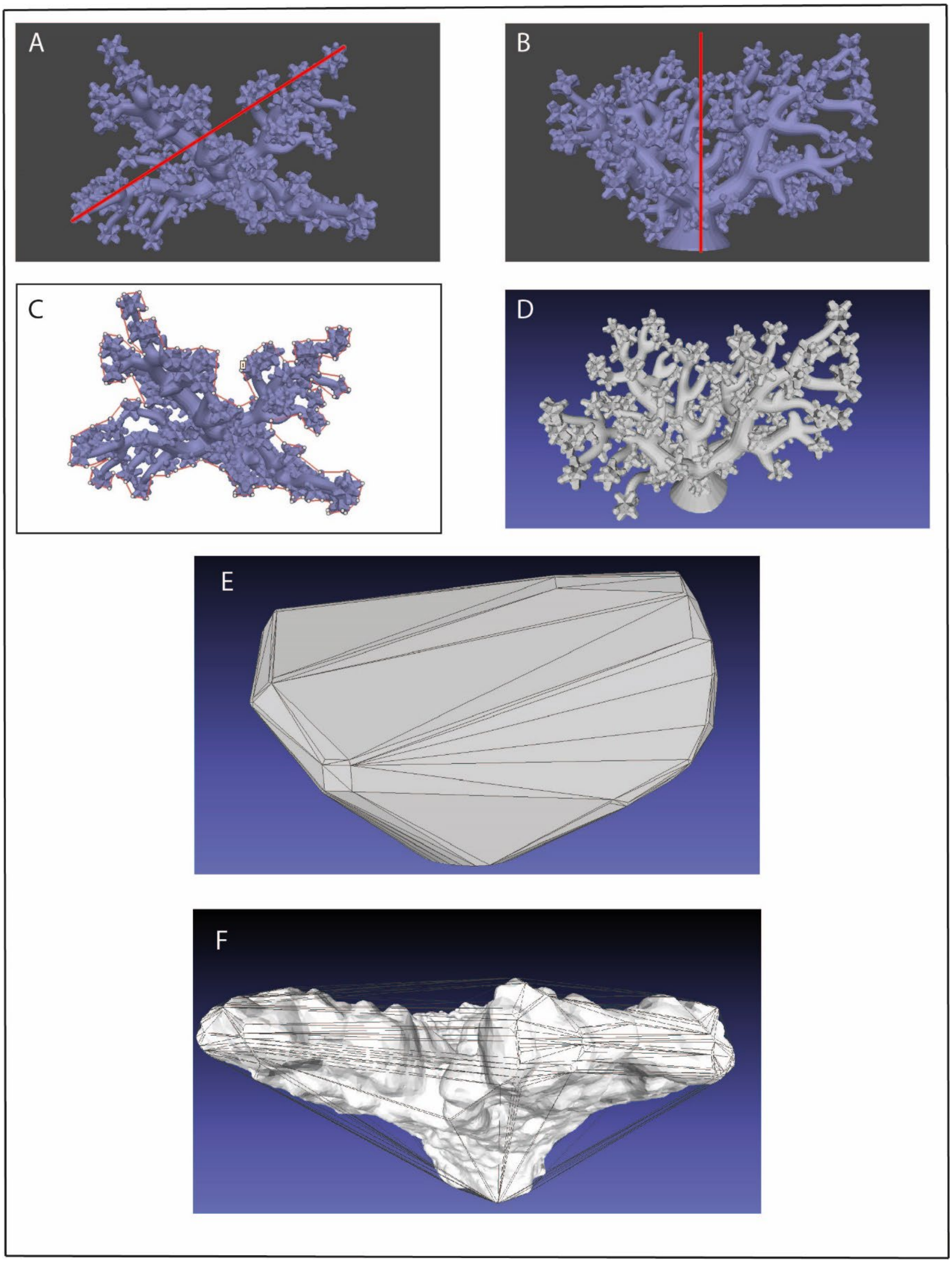

Figure S3.1. Graphical representation of several structural complexity metrics calculated. (A) Colony diameter measures along the widest axis, using the 3D model. (B) Colony height. (C) 2D surface area, measuring the coral footprint using the ruler tool. (D) 3D model used to calculate volume and 3D surface area of the colony. (E)

Minimum bounding convex hull encompassing the colony. (F) Wireframe of convex hull overlaid over a tabular colony to show the area of overhang captured in estimates.

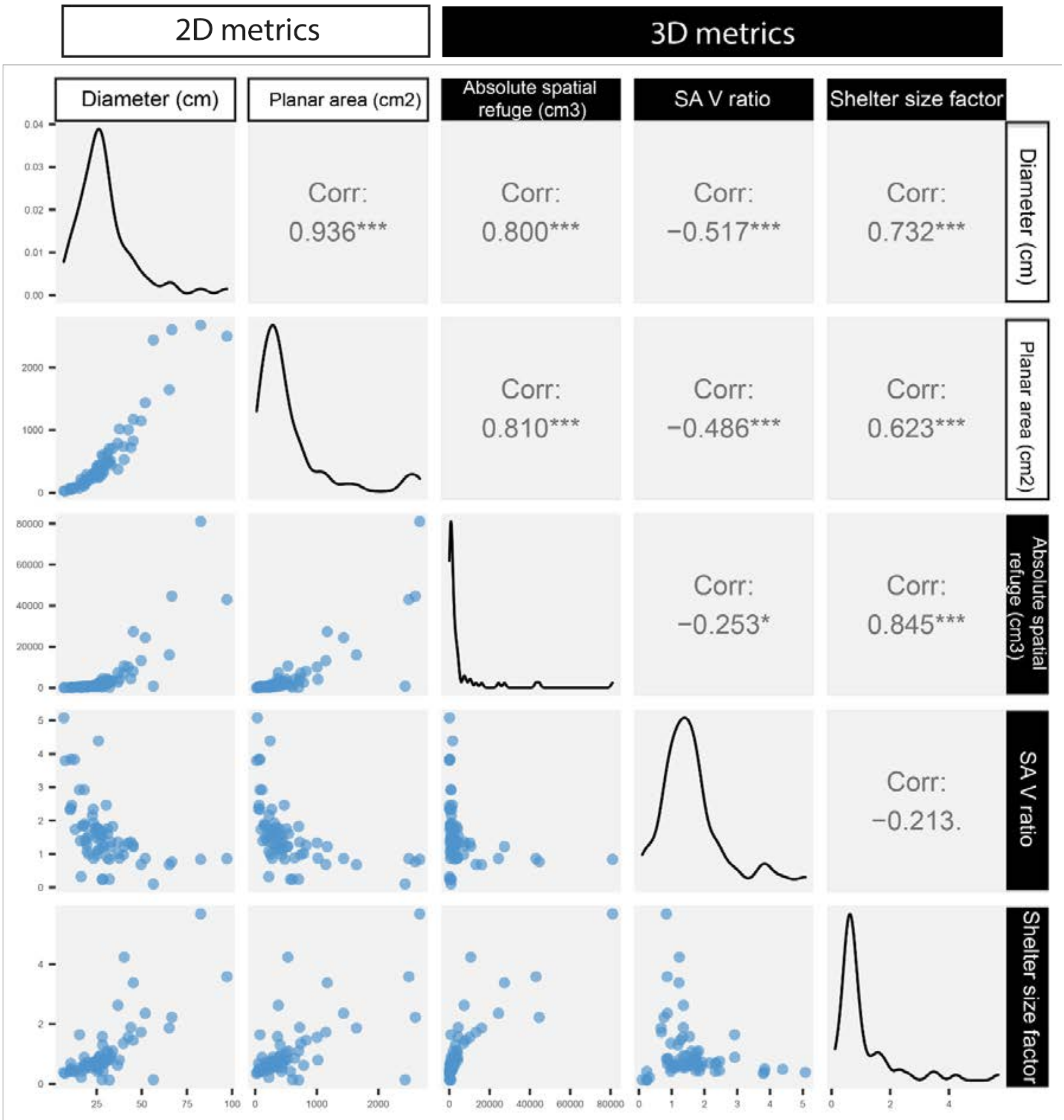

Figure S3.2. Pairwise correlations between 2D and 3D variables (raw data). Blue circles are individual coral colonies. Pearson correlation coefficients are available in the upper right panels for each pair of variables. Significance of relationships is denoted by asterisks (*** = p<0.01). Variable distribution is available on the diagonal.

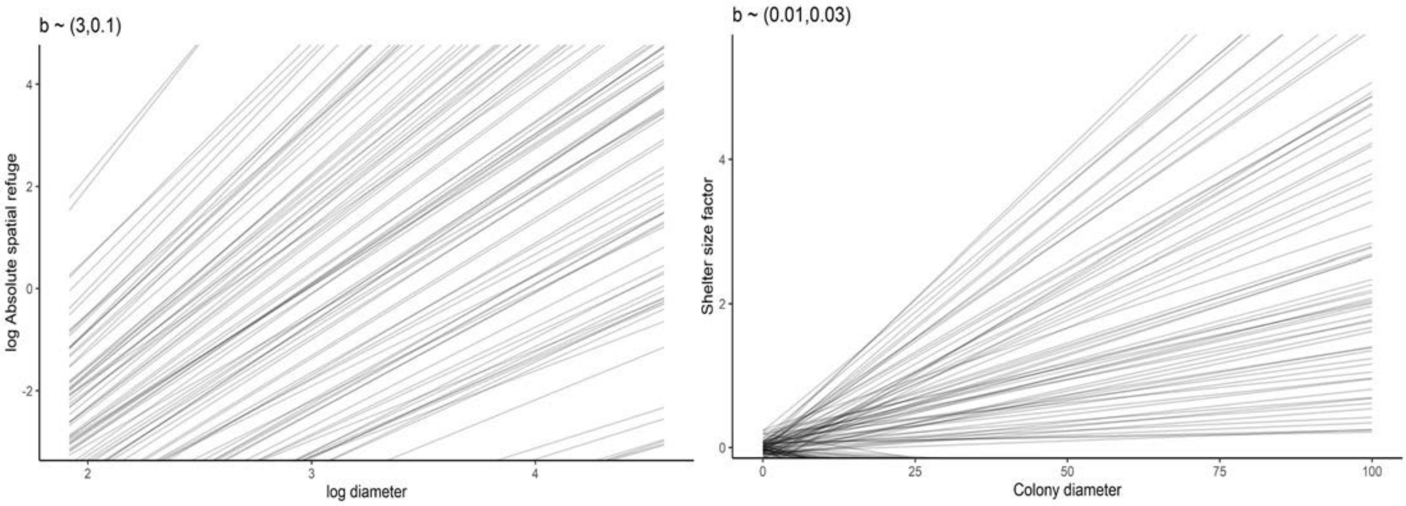

Figure S3.3: (left) 100 randomly sampled lines from prior predictive distribution simulations for linear regression model predicting log absolute refuge using log colony diameter. Prior values for the intercept and slope were chosen based on Urbina-Barreto et al. (2020), since I performed identical data transformations. The intercept prior was not very informative here sinceI wanted to allow the data to drive differences in the data. (right) 100 randomly sampled lines from prior predictive distribution simulations for linear regression model predicting shelter size factor from planar area from colony diameter (cm). Prior values were more relaxed for this model since I had no knowledge of how shelter size factor was likely to change with increasing colony size. However, a colony of zero diameter would necessarily have a shelter size factor of 0, I set the intercept close to 0 and allowed only slight variation.

Table S3.1: Posterior estimates for mean parameters for interaction model predicting absolute spatial refuge with increasing colony diameter. 95% estimates are for compatibility intervals. Rhat values of 1 indicate that the within and between-chain estimates are in agreement, and that the chains have mixed well. Bulk and Tail ESS (effective sample size) values measure sampling efficiency in the bulk and the tails of the of the distribution. These should be at least 100 per markov chain (in this case, 4 chains were used).

	Estimate	Est. error	Lower 95% CI	Upper 95% CI	Rhat	Bulk-ESS	Tail ESS
α Acropora Corymbose	-9.13	0.43	-9.98	-8.28	1.00	36873	28862
α Acropora Digitate	-8.49	0.36	-9.21	-7.79	1.00	37353	29497
α Acropora Tabular	-8.95	0.45	-9.83	-8.08	1.00	36171	29330
α Isopora Branching	-8.80	0.48	-9.74	-7.86	1.00	38337	28892
α Pocillopora Branching	-8.90	0.38	-9.65	-8.15	1.00	36811	28286
α Porites Branching	-8.97	-0.46	-9.87	-8.07	1.00	38289	27950
α massive	-8.87	0.46	-9.78	-7.96	1.00	37375	28438
β Acropora Corymbose	2.94	0.14	2.65	3.21	1.00	36899	28917
β Acropora Digitate	2.73	0.12	2.49	2.97	1.00	37242	28101
β Acropora Tabular	2.80	0.13	2.54	3.06	1.00	36033	29009
β Isopora Branching	2.93	0.12	2.69	3.17	1.00	38811	28345
β Pocillopora Branching	2.94	0.12	2.71	3.18	1.00	36414	29743
β Porites Branching	3.14	0.14	2.86	3.42	1.00	38018	29233
β massive	2.30	0.14	2.02	2.58	1.00	37537	28800
sigma	0.39	0.04	0.32	0.47	1.00	37458	29653

Table S3.2. Results of pareto-smoothed importance sampling leave-one-out (PSIS-LOO) cross validation between the model predicting absolute spatial refuge using diameter with (Model1) and without (Model1.1) the indicator variable for morphotaxa. Note that all of the model weighting is given to the one including the indicator variable.

	elpd_diff	s.e_diff	elpd_loo	s.e_elpd_loo	p_loo	se_p_loo	looic	se_looic	Model weights
Model1	0.0	0.0	-39.0	8.4	11.8	3.4	77.9	16.9	1
Model1.1	-123	9	-162	5.5	68.8	2.5	323	11	0

Table S3.3. Posterior estimates for mean parameters for interaction model predicting shelter size factor with increasing colony planar area. 95% estimates are for compatibility intervals. Rhat values of 1 indicate that the within and between-chain estimates are in agreement, and that the chains have mixed well. Bulk and Tail ESS (effective sample size) values measure sampling efficiency in the bulk and the tails of the of the distribution. These should be at least 100 per markov chain (in this case, 4 chains were used)

	Estimate	**Est. error**	**Lower 95% CI**	**Upper 95% CI**	**Rhat**	**Bulk-ESS**	**Tail ESS**
α Acropora Corymbose	-0.06	0.24	-0.52	0.41	1.00	34163	27316
α Acropora Digitate	0.05	0.21	-0.36	0.46	1.00	35385	28942
α Acropora Tabular	-0.10	0.27	-0.63	0.42	1.00	35975	26087
α Isopora Branching	1.14	0.40	0.34	1.91	1.00	34278	28823
α Pocillopora Branching	-0.05	0.20	-0.44	0.34	1.00	34946	28344
α Porites Branching	0.37	034	-0.30	1.03	1.00	35784	29284
α massive	-0.08	0.31	-0.69	0.53	1.00	34474	30039
β Acropora Corymbose	3.58	0.93	1.74	5.41	1.00	35957	30551
β Acropora Digitate	2.66	0.79	1.10	4.22	1.00	33785	28701
β Acropora Tabular	3.25	0.77	1.74	4.76	1.00	36834	29297
β Isopora Branching	3.88	0.59	2.76	5.07	1.00	33321	29401
β Pocillopora Branching	3.27	0.65	1.99	4.55	1.00	33074	30450
β Porites Branching	5.98	1.05	3.94	8.03	1.00	35364	29430
β massive	0.93	0.93	-0.90	2.77	1.00	34343	29761
sigma	0.40	0.04	0.33	0.09	1.00	36336	30396

Table S3.4. Results of pareto-smoothed importance sampling leave-one-out (PSIS-LOO) cross validation between the model predicting shelter size factor using diameter with (Model2) and without (Model2.1) the indicator variable for morphotaxa. Note that all of the model weighting is given to the one including the indicator variable.

	elpd_diff	**s.e_diff**	**elpd_loo**	**s.e_elpd_loo**	**p_loo**	**se_p_loo**	**looic**	**se_looic**	**Model weights**
Model2	0.0	0.0	-52.2	19.2	26.2	11.5	104.5	38.3	1
Model2.1	-22.9	13.4	-75.1	13.9	7.8	3.9	150.2	27.9	0

Instructions for using python scripts to serially process models and use scripts

NOTE: Version control has been updated and checked for Python 3.10 and pymeshlab 2021.01 (As of Feb 2022 the most up-to-date version of both packages). Installation instructions are reflective of this.

Integration of MeshLab with python to compute several geometric measures of individual coral colonies. This is split in to two parts - processing of photographs in Metashape to turn these in to 3D reconstructions, as well as extracting complexity metrics. These scripts are easy to implement and follow assuming some knowledge of both using metashape and using a python interpreter / installing modules from the command line.

Part I: Metashape processing

This script is a downloadable .py file that is run directly from the metashape GUI (graphical user interface). For every chunk present in the project, it performs end-to-end digitisation of a coral colony according to some user-input values. Fortunately, these are pop-up boxes that have attached instructions. The only manual step required of the user is detecting markers and scaling models.

Requirements: Active license for metashape.

All you need to do is download the script "Metashape_Processing.py" and run it from inside Metashape. The process is interactive at the beginning then applies the chosen settings to all chunks in the project. To set it up correctly, just populate the document with photos of colonies, each one of these added as a separate chunk.

To run the script, simply navigate to Tools > Run Script in the metashape software and locate the downloaded script.

Defaults (and recommended values) for processing are as follows:

Photo quality threshold: <0.35

Alignment quality: High (1)

Dense cloud quality: Medium (4)

Face count for model: High.

Part II: Automated metrics extraction

This code automates the extraction of 10 3D complexity metrics from an obj. file. It loops the function over every file in a specified folder, saving hours/days/weeks of clicking through pesky menus. The most efficient way of running this script is to put the .obj file of each coral in to a single folder, which you refer to in the script. (instructions are embedded)

Requirements: Python interpreter (we recommend PyCharm), installation of PyMeshlab using pip.

INSTRUCTIONS:

Install python (ver 3.6 or above will work but we assume a fresh installation of 3.10 at the time of writing). Do so directly from the Python website (https://www.python.org/downloads/)

When installing, ensure to check the box entitled "Add Python 3.XX to PATH" or nothing will work without manual intervention. 'pip' (the package responsible for installing other packages) comes installed by default.

We will use this to install the dependencies for the script. Open the command prompt terminal (press windows key, then type cmd to find it).

paste the following to install pymeshlab:

pip install pymeshlab

To run the code, a python interpreter is needed. We recommend the use of PyCharm, a freely available integrated development engine (IDE) capable of running the code. This software comes with installation and setup instructions for first time users which may vary between systems so we do not provide instructions on how to install here. Note that any interpreter can be used by those familiar with python.

TO MAKE THE CODE WORK: Create a new project in PyCharm (File > New Project) in your desired location, ensuring the "inherit global site packages" is checked, and that the base interpreter is your installed version of python. On creation, an empty project will automatically open.

Download all of the files in this repository. Then, cut and paste the downloaded files from the zipped folder to the location of the new project file that you just created in PyCharm. Once this is done, open the script "geometric_measures.py" in the project. You should see also in the project tab that the other files are present. The two used in this are the .mlx files - these must both be present in the project file for the code to work.

There is only one thing for you to do to make this code run properly. the directory needs to be changed to direct python to the folder where all your .obj files are stored. This folder can include other file types, it won't break the script - the loop will just ignore all non-.obj files. It should look something like "C:/Documents/Project/objs/". Importantly you must use forward slashes and not backslashes (which are windows defaults). This is line 1 of the script and is marked "INPUT NEEDED".

Table S4.1 | Sampling design detailing how many plots were present within each reef, habitat zone and depth. These numbers refer to all the plots included in analyses, following removal of models with inadequate quality.

Reef	Habitat	Depth	n
Auckane	Shaltered Slope	Shallow	8
	Moderately Exposed Slope	Shallow	4
	Explosed Slope	Deep	4
		Shallow	8
Chicken	Shaltered Slope	Shallow	8
	Moderately Exposed Slope	Shallow	3
	Explosed Slope	Shallow	1
Davies	Shaltered Slope	Deep	7
		Shallow	8
	Moderately Exposed Slope	Deep	4
		Shallow	4
	Explosed Slope	Deep	6
		Shallow	8
	Lagoon	Shallow	8
Dungeness	Shaltered Slope	Shallow	12
	Explosed Slope	Shallow	8
	Lagoon	Shallow	4
Heron Island	Shaltered Slope	Deep	8
		Shallow	8
	Moderately Exposed Slope	Shallow	4
	Explosed Slope	Deep	8
		Shallow	8
	Lagoon	Shallow	3
Keppel Islands	Shaltered Slope	Deep	3
		Shallow	16
	Moderately Exposed Slope	Shallow	4
Lady Musgrave	Shaltered Slope	Shallow	8
	Moderately Exposed Slope	Shallow	8
	Lagoon	Shallow	4
Little Broadhurst	Shaltered Slope	Shallow	3
	Moderately Exposed Slope	Shallow	4
	Lagoon	Shallow	4
Lizard Island	Shaltered Slope	Deep	2
		Shallow	4
	Moderately Exposed Slope	Shallow	4
	Explosed Slope	Shallow	7
	Lagoon	Shallow	4
Masig	Shaltered Slope	Deep	8
		Shallow	8

	Moderately Exposed Slope	Shallow	4
	Explosed Slope	Deep	8
		Shallow	6
	Lagoon	Shallow	4
Moore Reef	Shaltered Slope	Deep	12
		Shallow	4
	Moderately Exposed Slope	Deep	3
		Shallow	4
	Explosed Slope	Deep	9
		Shallow	7
	Lagoon	Deep	4
		Shallow	4
Palm Islands	Shaltered Slope	Deep	7
		Shallow	7
	Moderately Exposed Slope	Deep	2
		Shallow	2
	Explosed Slope	Deep	4
		Shallow	4

Table S4.2 | Model specifications for each of the six generalised linear mixed models fit to the data. Since not all reefs had paired deep and shallow sites, some data were precluded from use depending on the specification of the model. Model specification is:

Response ~ Explanatory variable 1 * Explanatory variable 2 + (Random Slopes | Random effects)

Model specification	Testing criteria	Data distribution / Data used
Rugosity ~ Sector + (1 | Reef / Habitat) FD ~ Sector (1 | Reef / Habitat)	Inter-regional Cross-shelf	Gaussian / All habitats and reefs, shallow sites only
Rugosity ~ Habitat + (1 | Reef) FD ~ Habitat + (1 | Reef)	Inter-habitat	Gaussian / All habitats and reefs, shallow sites only
Rugosity ~ Habitat*Depth + (Depth | Reef) FD ~ Habitat * Depth + (Depth | Reef)	Depth	Gaussian / Reefs with paired deep and shallow sites, lagoon excluded

Table S5.1 | Trophic groupings for the 99 species of fish observed across all sampling sites.

Species Name	Trophic grouping	Species Name	Trophic grouping
Abudefduf sexfasciatus	planktivore	*Labroides bicolor*	carnivore
Abudefduf whitleyi	planktivore	*Labroides dimidiatus*	carnivore
Acanthochromis polyacanthus	omnivore	*Labropsis australis*	corallivore
Amblyglyphidodon curacao	omnivore	*Macropharyngodon meleagris*	invertivore
Amblyglyphidodon leucogaster	omnivore	*Monotaxis grandoculis*	invertivore
		Neoglyphidodon melas	omnivore

Amblyglyphidodon ternatensis	omnivore	*Neoglyphidodon nigroris*	omnivore
Amphiprion akindynos	omnivore	*Neoglyphidodon polyacanthus*	planktivore
Amphiprion chrysopterus	omnivore	*Neopomacentrus azysron*	planktivore
Amphiprion clarkii	omnivore	*Neopomacentrus cyanomos*	planktivore
Amphiprion melanopus	omnivore	*Plectroglyphidodon johnstonianus*	corallivore
Amphiprion perideraion	omnivore	*Plectroglyphidodon lacrymatus*	herbivore
Anampses neoguinaicus	invertivore	*Plectroglyphidodon leucozonus*	herbivore
Assessor macneilli	invertivore	*Pomacanthus spp*	omnivore
Bodianus mesothorax	carnivore	*Pomacentrus adelus*	herbivore
Bodianus spp	carnivore	*Pomacentrus amboinensis*	omnivore
Cheilodipterus quinquelineatus	carnivore	*Pomacentrus australis*	omnivore
Chromis amboinensis	planktivore	*Pomacentrus bankanensis*	omnivore
Chromis atripectoralis	planktivore	*Pomacentrus brachialis*	omnivore
Chromis atripes	planktivore	*Pomacentrus chrysurus*	herbivore
Chromis chrysura	planktivore	*Pomacentrus coelestis*	planktivore
Chromis lepidolepis	planktivore	*Pomacentrus grammorhynchus*	herbivore
Chromis margaritifer	planktivore	*Pomacentrus imitator*	planktivore
Chromis nitida	planktivore	*Pomacentrus lepidogenys*	planktivore
Chromis ternatensis	planktivore	*Pomacentrus moluccensis*	omnivore
Chromis viridis	planktivore	*Pomacentrus nagasakiensis*	omnivore
Chromis weberi	planktivore	*Pomacentrus philippinus*	planktivore
Chromis xanthura	planktivore	*Pomacentrus spp*	planktivore
Chrysiptera brownriggii	omnivore	*Pomacentrus vaiuli*	omnivore
Chrysiptera flavipinnis	planktivore	*Pomacentrus wardi*	herbivore
Chrysiptera rex	omnivore	*Premnas biaculeatus*	omnivore
Chrysiptera rollandi	planktivore	*Pseudanthias squamipinnis*	planktivore
Chrysiptera talboti	planktivore	*Pseudochromis fuscus*	carnivore
Cirrhilabrus exquisitus	planktivore	*Pseudochromis novaehollandiae*	invertivore
Cirrhilabrus punctatus	planktivore	*Pseudochromis paccagnellae*	invertivore
Coris batuensis	invertivore	*Pseudochromis queenslandiae*	invertivore
Dascyllus reticulatus	planktivore	*Pseudolabrus guentheri*	invertivore
Dascyllus trimaculatus	planktivore	*Stegastes apicalis*	herbivore
Dischistodus melanotus	herbivore	*Stegastes fasciolatus*	herbivore
Dischistodus prosopotaenia	herbivore	*Stegastes nigricans*	herbivore
Dischistodus pseudochrysopoecilus	herbivore	*Stegastes spp*	herbivore
Ecsenius bicolor	herbivore	*Stethojulis bandanensis*	invertivore
Halichoeres biocellatus	invertivore	*Stethojulis interrupta*	invertivore
Halichoeres chloropterus	invertivore	*Stethojulis strigiventer*	invertivore
Halichoeres marginatus	invertivore	*Thalassoma amblycephalum*	planktivore
Halichoeres melanurus	invertivore	*Thalassoma hardwicke*	invertivore
Halichoeres nebulosus	invertivore		
Halichoeres prosopeion	invertivore		
Halichoeres richmondi	invertivore		
Halichoeres spp	invertivore		

Labrichthys unilineatus	corallivore	*Thalassoma lunare*	invertivore
		Thalassoma lutescens	invertivore